Award Number: DAMD17-98-1-8223

TITLE: Developing Strategies to Block Beta-Catenin Action in Signaling and Cell Adhesion during Carcinogenesis

PRINCIPAL INVESTIGATOR: Mark A. Peifer, Ph.D.

CONTRACTING ORGANIZATION: University of North Carolina at Chapel Hill
Chapel Hill, North Carolina 27599-1350

REPORT DATE: July 2003

TYPE OF REPORT: Final Addendum

PREPARED FOR: U.S. Army Medical Research and Materiel Command
Fort Detrick, Maryland 21702-5012

REPORT DOCUMENTATION PAGE

Form Approved
OMB No. 074-0188

1. AGENCY USE ONLY (Leave blank)	2. REPORT DATE	3. REPORT TYPE AND DATES COVERED
	July 2003	Final Addendum (1 Jul 02 - 30 Jun 03)

4. TITLE AND SUBTITLE
Developing Strategies to Block Beta-Catenin Action in Signaling and Cell Adhesion during Carcinogenesis

5. FUNDING NUMBERS
DAMD17-98-1-8223

6. AUTHOR(S)
Mark A. Peifer, Ph.D.

7. PERFORMING ORGANIZATION NAME(S) AND ADDRESS(ES)
University of North Carolina at
Chapel Hill
Chapel Hill, North Carolina 27599-1350
E-Mail: peifer@unc.edu

8. PERFORMING ORGANIZATION REPORT NUMBER

9. SPONSORING / MONITORING AGENCY NAME(S) AND ADDRESS(ES)
U.S. Army Medical Research and Materiel Command
Fort Detrick, Maryland 21702-5012

10. SPONSORING / MONITORING AGENCY REPORT NUMBER

11. SUPPLEMENTARY NOTES
Original contains color plates: All DTIC reproductions will be in black and white.

12a. DISTRIBUTION / AVAILABILITY STATEMENT
Approved for Public Release; Distribution Unlimited

12b. DISTRIBUTION CODE

13. ABSTRACT (Maximum 200 Words)

To understand cancer, we must first understand normal cell behavior. *Drosophila* Armadillo (Arm) and its human homolog ß-catenin are key players in adhesive junctions and in transduction of Wingless (Wg)/Wnt signals. Our working hypotheses are: 1) Several protein partners compete to bind Arm, and 2) Arm:dTCF activates Wg-responsive genes, while dTCF alone represses the same genes. Aim 1 is to understand how different partners compete with one another for binding Arm. Aim 2 focuses on how Arm and dTCF positively and negatively regulate Wg-responsive genes. In our Final Report last year, we reported significant progress on both Aims. Here we describe additional work we have accomplished during a final one-year no cost-extension. In this period, we have examined interaction of Wnt and JNK pathways and the role of the MAPK phosphates Puckered in this interaction.

14. SUBJECT TERMS	15. NUMBER OF PAGES
Breast Cancer	52
	16. PRICE CODE

17. SECURITY CLASSIFICATION OF REPORT	18. SECURITY CLASSIFICATION OF THIS PAGE	19. SECURITY CLASSIFICATION OF ABSTRACT	20. LIMITATION OF ABSTRACT
Unclassified	Unclassified	Unclassified	Unlimited

FOREWORD

Opinions, interpretations, conclusions and recommendations are those of the author and are not necessarily endorsed by the U.S. Army.

X Where copyrighted material is quoted, permission has been obtained to use such material.

N/A Where material from documents designated for limited distribution is quoted, permission has been obtained to use the material.

N/A Citations of commercial organizations and trade names in this report do not constitute an official Department of Army endorsement or approval of the products or services of these organizations.

N/A In conducting research using animals, the investigator(s) adhered to the "Guide for the Care and Use of Laboratory Animals," prepared by the Committee on Care and use of Laboratory Animals of the Institute of Laboratory Resources, national Research Council (NIH Publication No. 86-23, Revised 1985).

X For the protection of human subjects, the investigator(s) adhered to policies of applicable Federal Law 45 CFR 46.

_ In conducting research utilizing recombinant DNA technology, the investigator(s) adhered to current guidelines promulgated by the National Institutes of Health.

_ In the conduct of research utilizing recombinant DNA, the investigator(s) adhered to the NIH Guidelines for Research Involving Recombinant DNA Molecules.

N/A In the conduct of research involving hazardous organisms, the investigator(s) adhered to the CDC-NIH Guide for Biosafety in Microbiological and Biomedical Laboratories.

Mark Gal 7/07/03

PI - Signature Date

Table of Contents

(5) Introduction:

To understand abnormal cell behavior in cancer, we must first understand normal cell behavior. We focus on *Drosophila* Armadillo (Arm); Arm and its human homolog ß-catenin are critical for normal embryonic development. Both are key players in two separable biological processes: 1) They are components of cell-cell adhesive junctions, and 2) they act in transduction of Wingless/Wnt (Wg/Wnt) family cell-cell signals (reviewed in Moon et al., 2002). Mutations in ß-catenin or its regulators are early steps in colon cancer and melanoma. We use the fruit fly as our model, combining classical and molecular genetics with cell biology and biochemistry. We take advantage of the speed and ease of the fly system and of its synergy with vertebrate cell biology. As one avenue to reveal Arm's roles in adherens junctions and transduction of Wg signal, we are identifying and examining the function of proteins with which Arm physically and/or functionally interacts. Our goal is to precisely define Arm/ß-catenin's dual roles, ultimately allowing the design of drugs inhibiting oncogenic ß-catenin. Our working hypotheses are: 1) Several protein partners compete to bind to the same site on Arm; the affinity of Arm for different partners is adjusted via phosphorylation of these partners, and 2) The Arm:dTCF complex activates Wg-responsive genes; dTCF represses the same genes in the absence of Arm. We will integrate approaches at all levels from combinatorial chemistry to studying gene function in intact animals, using fruit flies to carry out a functional genomics approach to understanding Arm function, and then transferring this knowledge directly to the mammalian system. Our first Aim was to understand how different partners interact with and compete with one another for binding Arm, and how phosphorylation regulates this. Our second Aim focused on how the Arm and its partner dTCF positively and negatively regulate Wg responsive genes. During our one-year no cost extension, we have broadened this goal, as addressed in our revised SOW, to examine interaction of Wnt and Jun N-terminal kinase (JNK) pathways and the role of the MAPK phosphatase Puckered in this interaction.

(6) Body:

This award was a combined IDEA Award and Career Development Award. The IDEA component of the Award originally was scheduled to send on 30 June 2001,, while the Career Development Award continued through 30 June 2002. We initially obtained a one-year, no-cost extension on the IDEA components until 30 June 2002. Last year, I wrote a Final report describing the significant progress we made on both of our Specific Aims. I have not repeated that discussion here, as it was summarized in last year's report. However, on 30 June 2002 , positive balances remained in both accounts. After discussions with Dr. Patricia Modrow, we requested an additional one-year no cost extension of both components, and also requested that the SOW be modified to add an additional area of research which we would pursue in this last year. This extension and revision were approved by the agency. I summarize below the work during this additional year of funding.

The addendum to our SOW was as follows:

During no cost extension

Examine interaction of Wnt and Jun N-terminal kinase (JNK) pathways and the role of the MAPK phosphatase Puckered in this interaction (D. McEwen)

IDEA Award

Signal transduction pathways orchestrate the differentiation of cell fates as well as maintenance of cellular homeostasis. These same pathways are often commandeered during oncogenic transformation. To gain new insights into neoplastic transformation and to identify potential therapeutic targets, one must first understand the mechanistic events that regulate a cell's decision to proliferate, differentiate, and/or die. To date, both the Wnt and JNK signaling cascades have been shown to influence the development of numerous cell types and tissues. As much of

our current understanding about how these pathways influence cell behavior comes from studies of their invertebrate orthologs, *Drosophila melanogaster* has emerged as a powerful model system for studying clinically relevant biology. To this end, we have used *Drosophila* to characterize Puckered, a MAP-kinase phosphatase that modulates the Wnt and JNK pathways (reviewed in Peifer and McEwen, 2002.

In our earlier published work (McEwen et al., 2000), we examined the interaction between the Wnt and JNK pathways during *Drsoophila* embryogenesis. Elaboration of the *Drosophila* body plan depends on a series of cell-identity decisions and morphogenetic movements regulated by intercellular signals. For example, Jun N-terminal kinase signaling regulates cell fate decisions and morphogenesis during dorsal closure, (reviewed in Noselli and Agnes, 1999) while signaling by the fly Wnt Wingless (Wg) regulates segmental patterning of the larval cuticle via Armadillo (Arm; reviewed in Moon et al., 2002). *wg* or *arm* mutant embryos secrete a lawn of ventral denticles; *arm* mutants also exhibit dorsal closure defects. We found that mutations in *puc*, a phosphatase that antagonizes Jun N-terminal kinase, suppress in a dose-sensitive manner both the dorsal and ventral *arm* cuticle defects. Furthermore, we found that activation of the Jun N-terminal kinase signaling pathway suppresses *arm*-associated defects. Jun N-terminal kinase signaling promotes dorsal closure, in part, by regulating *decapentaplegic* expression in the dorsal epidermis. We demonstrate that Wingless signaling is also required to activate *decapentaplegic* expression and to coordinate cell shape changes during dorsal closure. Together, these results demonstrate that MAP-Kinase and Wingless signaling cooperate in both the dorsal and ventral epidermis, and suggest that Wingless may activate both the Wingless and the Jun N-terminal kinase signaling cascades.

In this earlier work, we examined embryos zygotically mutant for *puc* During *Drosophila* development, the mother contributes some RNA and/or protein products to the developing embryo. Often, these maternal contributions bypass or ameliorate early developmental requirements for certain gene products. To assess whether maternally contributed stores of Puc are required prior to the previously published role for Puc during dorsal closure, we utilized site-specific recombination to generate embryos that lack both maternal and zygotic Puc function. Females whose germline cells are mutant for a weak allele of *puc* produced very few eggs, while those carrying a null allele produced no eggs. Examination of the few cuticles derived from the weak *puc* germline clone embryos suggests that a severe reduction of Puc phosphatase activity results in excessive programmed cell death (PCD), as evidenced by ectopic TUNEL staining through the developing embryos and the severe fragmentation of the resulting cuticle. These results demonstrate that Puc function is required during embryonic development and we hypothesize that inactivation of Puc lowers the threshold of JNK signaling required to induce apoptosis. This is consistent with our earlier work. We have previously found that Wg acts as a survival signal in the embryonic epidermis, such that in its absence cells undergo apoptosis (Cox et a., 2000). Embryos double mutant for *wg* and *puc* exhibit massive apoptosis (McEwen et al., 2000), consistent with the two interacting synergistically to regulate this process. Further, we have found we can mimic the *puc* zygotic phenotype by inducing apoptosis in the cells of the posterior compartment, that normally receive high levels of Wg signal.

To assess whether loss of Puc function promotes apoptosis in other epithelial tissues, we utilized the EGUF/hid and MARCM techniques to generate organisms whose eyes or imaginal discs, respectively, are composed of *puc* mutant tissue. Whereas no ectopic cell death was seen in wild-type controls, creating clones of cells that are homozygous for mutations in *puc* led to loss of the mutant tissues presumably due to ectopic PCD. As a control, mutant clones were rescued via mis-expression of a transgene encoding active Puc protein; thus, demonstrating the at the loss of viable mutant clones results from a loss of Puc and not is not the effect of other incidental mutations on the same chromosome. Previously, changes in JNK signaling have been shown to affect PCP signaling in the developing eye; however, our results suggest that a complete failure to

limit JNK signaling results in the induction of apoptosis in a cell autonomous manner (i.e. independent of exogenously expressed proteins).

To further examine what role Puc may play during the induction of programmed cell death, we assessed what affects other stimuli normally known to induce apoptosis had upon JNK activity. By monitoring Puc expression, which serves as a reporter for JNK activation, we have been able to demonstrate that doses of □amma-radiation capable of inducing wide-spread apoptosis also induce JNK activation. Such activation can be blocked by exogenously expressed Puc. Perhaps most striking, overexpression of Puc can block radiation-induced apoptosis, suggesting that JNK activation is essential for this process. To further test whether JNK activation was instrumental in inducing programmed cell death or just a secondary consequence of caspase activation, we asked whether the anti-apoptotic baculovirus p35 protein could block *puc* induction in response to □amma-radiation. To do this, we utilized the Gal4-UAS system to mis-express p35 in the posterior half of the developing wing disc. Larvae of the appropriate genotype were then subjected to 4000 rads, aged four hours, and *puc* expression assessed. Mis-expression of p35 had no effect on the induction of *puc* expression by radiation; yet, it was able to block apoptosis. These results demonstrate that JNK activation occurs upstream of or in parallel to caspase activation.

We are currently assessing whether JNK activation is upstream of, downstream of, or in parallel to activation of p53 during the response to irradiation. We are also attempting to look at the regulation of the expression of the apoptotic activators Reaper and Hid by Wnt and JNK signaling, to further understand how these two pathways my interact in normal development.

Career Development Award

The Career Development Award component of this grant paid a portion of my salary (of the PI, Mark Peifer). This substantially reduced the amount of time I had to devote to teaching and service, and thus allowed me to focus on research, both that funded by the Army and other research ongoing in my lab. I have thus acknowledged this support in additional publications produced during the last year, which are listed in Section 8, and included reprints for new additions to this list (where available) in the Appendix.

(7) Key research accomplishments for the last year.

a) Removal of both maternal and zygotic Puc function leads to massive apoptosis.
b) The puc zygotic phenotype can also be mimicked by triggering apoptosis in cells that normally receive high levels of Wg signal, suggesting that cells measure the relative levels of Wnt and JNK signaling in choosing fates, and that apoptosis is one of these fates.
c) Removal of Puc function from other epithelial tissues including the eye and the imaginal discs also triggers apoptosis.
d) Puc expression and thus presumably JNK activation is triggered by gamma-irradiation.
e) Puc overexpression can block gamma-irradiation induced apoptosis.
f) Caspase activation is not essential for radiation-induction of *pc* expression.

(8) Reportable outcomes for the past year.

<u>Additional publications acknowledging partial salary support for Mark Peifer via the CDA:</u>

Myster, S.H.,, Cavallo, R., Anderson, C.T., Fox, D.T.. and Peifer, M. (2003). Drosophila p120catenin plays a supporting role in cell adhesion but is not an essential adherens junction component. Journal of Cell Biology160, 433-449 (reprint included in the Appendix).

<u>Publications from the previous year acknowledging partial salary support for Mark Peifer via the CDA for which reprints are now included:</u>

Akong, K., McCartney, B.M., and Peifer, M. (2002). *Drosophila* APC2 and APC1 have overlapping roles in the larval brain despite their distinct intracellular localizations. Developmental Biology 250, 71-90. (reprint included in the Appendix)

Akong, K., Grevengoed, E.E., Price, M.H., McCartney, B.M., Hayden, M.A., DeNofrio, J.C., and

Peifer, M. (2002). *Drosophila* APC2 and APC1 play overlapping roles in Wingless signaling in the embryo and imaginal discs. Developmental Biology 250, 91-100. (reprint included in the Appendix)

Presentations by Mark Peifer discussing work funded in part by the DOD.

"Cell adhesion, signal transduction and cancer: the Armadillo Connection.", "Santa Cruz Developmental Biology Conference, Santa Cruz CA, August 2002.

Cell adhesion, signal transduction, and cancer: the Armadillo Connection." Division of Developmental Biology, Childrens Hospital Medical Center, Cincinnati OH September 2002

"A model system to study the tumor suppressor APC." Department of Genetics, Cell and Developmental Biology, University of Minnesota, Minneapolis MN, September 2002

"Cell adhesion, signal transduction and cancer: the Armadillo Connection.", Netherlands Royal Academy of Science Colloquium on "Wnt signaling in development and cancer", Amsterdam, the NETHERLANDS, October 2002.

"Cell adhesion, signal transduction, and cancer: the Armadillo Connection." Department of Genetics, University of Georgia, Athens GA October 2002

"Cell adhesion, signal transduction, and cancer: the Armadillo Connection." Department of Cell Biology, University of Virginia, Charlottesville VA March 2003

"Cell adhesion, signal transduction, and cancer: the Armadillo Connection." Department of Molecular, Cell and Developmental Biology, Yale University of Virginia, New Haven CT April 2003

"Cell adhesion, signal transduction, and cancer: the Armadillo Connection." Department of Molecular and Cell Biology, University of California at Berkeley, Berkeley CA May 2003

"Cell adhesion, signal transduction, and cancer: the Armadillo Connection." Gordon Conference on "Cell Contact and Adhesion", Andover NH June 2003

List of personnel supported in part by this grant in the past year

Mark Peifer
Don McEwen

(9) Conclusions.

We made significant progress on our modified statement of work. We have extended our analysis of the role of Wnt and JNK signaling, and the role that the JNK-phosphatase plays in this process. Our data point to an important role for JNK signaling and Puc as regulators of apoptosis in a wide-variety of situations, and these data suggest that different levels of JJNK and Wg signals may set thresholds for cell fate choice, below or above which apoptosis may occur.

(10) References.

Cox, R.T., McEwen, D.G., Myster, D.G., Duronio, R.J., Loureiro, J., and Peifer, M. (2000). A screen for mutations that suppress the phenotype of *Drosophila armadillo*, the ß-catenin homolog. Genetics 155, 1725-1740.

McEwen, D.G., Cox, R.T., and Peifer, M. (2000). The canonical Wg and JNK signaling cascades collaborate to promote both dorsal closure and ventral patterning. Development 127, 3607-3617.

Moon RT, Bowerman B, Boutros M, and Perrimon, N. (2002). The promise and perils of Wnt signaling through beta-catenin. Science 296:1644-6.

Noselli S, and Agnes F. (1999) Roles of the JNK signaling pathway in Drosophila morphogenesis. Curr Opin Genet Dev.9:466-72.

Peifer, M., and McEwen, D.G. (2002). The ballet of morphogenesis: Identifying the hidden choreographers. Cell 109: 271-274.

Appendix —Reprints of publications in the past year supported in part by this grant

Myster, S.H.,, Cavallo, R., Anderson, C.T., Fox, D.T.. and Peifer, M. (2003). Drosophila p120catenin plays a supporting role in cell adhesion but is not an essential adherens junction component. Journal of Cell Biology160, 433-449 (reprint included in the Appendix).

Akong, K., McCartney, B.M., and Peifer, M. (2002). *Drosophila* APC2 and APC1 have overlapping roles in the larval brain despite their distinct intracellular localizations. Developmental Biology 250, 71-90. (reprint included in the Appendix)

Akong, K., Grevengoed, E.E., Price, M.H., McCartney, B.M., Hayden, M.A., DeNofrio, J.C., and Peifer, M. (2002). *Drosophila* APC2 and APC1 play overlapping roles in Wingless signaling in the embryo and imaginal discs. Developmental Biology 250, 91-100. (reprint included in the Appendix)

JCB Article

Abelson kinase regulates epithelial morphogenesis in *Drosophila*

Elizabeth E. Grevengoed,[1] Joseph J. Loureiro,[2] Traci L. Jesse,[3] and Mark Peifer[1,2,3]

[1]Curriculum in Genetics and Molecular Biology, [2]Department of Biology, and [3]Lineberger Comprehensive Cancer Center, University of North Carolina at Chapel Hill, Chapel Hill, NC 27599

Activation of the nonreceptor tyrosine kinase Abelson (Abl) contributes to the development of leukemia, but the complex roles of Abl in normal development are not fully understood. *Drosophila* Abl links neural axon guidance receptors to the cytoskeleton. Here we report a novel role for *Drosophila* Abl in epithelial cells, where it is critical for morphogenesis. Embryos completely lacking both maternal and zygotic Abl die with defects in several morphogenetic processes requiring cell shape changes and cell migration. We describe the cellular defects that underlie these problems, focusing on dorsal closure as an example. Further, we show that the Abl target Enabled (Ena), a modulator of actin dynamics, is involved with Abl in morphogenesis. We find that Ena localizes to adherens junctions of most epithelial cells, and that it genetically interacts with the adherens junction protein Armadillo (Arm) during morphogenesis. The defects of *abl* mutants are strongly enhanced by heterozygosity for *shotgun*, which encodes DE-cadherin. Finally, loss of Abl reduces Arm and α-catenin accumulation in adherens junctions, while having little or no effect on other components of the cytoskeleton or cell polarity machinery. We discuss possible models for Abl function during epithelial morphogenesis in light of these data.

Introduction

The nonreceptor tyrosine-kinase Abl is the cellular homologue of *v-abl*, the transforming gene of Abelson (Abl)* murine leukemia virus (for review see Zou and Calame, 1999; Mauro and Druker, 2001). Bcr-Abl, an activated, chimeric form of Abl resulting from a chromosomal translocation, plays a causative role in human chronic myelogenous and acute lymphocytic leukemia. Bcr-Abl has deregulated tyrosine kinase activity, and an inhibitor of this kinase has shown promise in treating leukemia. Multiple substrates for oncogenic Abl kinase in diverse signaling pathways have been identified, revealing complex effects of Abl misregulation.

Abl's normal role has remained more elusive. Abl homologues are found in all animals. All share conserved NH_2-terminal SH3, SH2, and tyrosine kinase domains, as well as distinct COOH-terminal F- and G-actin binding domains (for review see Lanier and Gertler, 2000). Mammalian Abl, unlike its fly homologue, also contains nuclear import and export signals and a COOH-terminal DNA binding domain, and thus it localizes to both nuclei and the cytoplasm. In nuclei, it is thought to regulate the cell cycle and the response to DNA damage (for review see Van Etten, 1999). Cytoplasmic Abl predominantly associates with the actin cytoskeleton (e.g., van Etten et al., 1994) and can be found at cell–matrix junctions in cultured cells (Lewis et al., 1996). The different subcellular pools of Abl may perform distinct functions, though Abl can translocate to nuclei in response to cytoplasmic cues (Lewis et al., 1996). Bcr-Abl exclusively localizes to the cytoplasm, suggesting that its role in oncogenesis involves cytoplasmic targets.

In *Drosophila*, Abl localizes to the axons of the central nervous system (CNS) (Bennett and Hoffmann, 1992). In epithelial cells, Abl's localization varies with stage of development and tissue, but it is often concentrated near the apical cortex. Abl localizes to apical cell junctions soon after cells form and to the apical cytoplasm during gastrulation and in imaginal discs. In contrast, it is diffusely cytoplasmic in extended germband embryos.

Genetic analyses in mice and flies have begun to shed light on Abl's biological function. *abl* mutant mice are embryonic-viable but runted and exhibit defects in develop-

The online version of this paper contains supplemental material.

Address correspondence to Mark Peifer, CB#3280, Department of Biology, Coker Hall, University of North Carolina at Chapel Hill, Chapel Hill, NC 27599-3280. Tel.: (919) 962-2271. Fax: (919) 962-1625. E-mail:peifer@unc.edu

Elizabeth E. Grevengoed and Joseph J. Loureiro contributed equally to this paper.

*Abbreviations used in this paper: Abl, Abelson; abl^{MZ}, *abl* maternal/zygotic; Arm, Armadillo; CNS, central nervous system; dab, disabled; Ena, Enabled; GFP, green fluorescent protein; scb, scab; shg, shotgun.

Key words: Abelson kinase; Armadillo; adherens junctions; enabled; *Drosophila*

ment of the bones, immune system, and sperm. A null mutation and a COOH-terminal truncation removing the actin binding domains have similar phenotypes, suggesting that the interaction with actin is functionally important (for review see Van Etten, 1999). Analysis of Abl function in mice is complicated by the presence of the related kinase Arg; mice lacking both *abl* and *arg* die as embryos with defects in neurulation that may reflect problems in actin organization (Koleske et al., 1998).

In *Drosophila*, analysis of the single Abl homologue primarily revealed roles in neural development. *abl* mutants are pupal lethal with defects in retinal development (Henkemeyer et al., 1987); they also have subtle CNS defects in which certain axons stop short of innervating their target muscles (Wills et al., 1999b). Much more severe CNS defects are seen in *abl* mutants that are also heterozygous or homozygous for the neural cell adhesion molecule *fasciclin*, the receptor tyrosine phosphatase *dLAR*, the axon guidance receptor *robo*, the adaptor *disabled (dab)*, the Rho-family GEF *trio*, or the actin regulator *profilin* (for review see Lanier and Gertler, 2000). These data led to a model in which Abl transduces signals from neural cell surface receptors, influencing actin dynamics in growth cones.

In doing so, Abl is thought to act via one of its substrates, Enabled (Ena; Comer et al., 1998). Originally identified as a suppressor of *abl; dab/+* mutants (Gertler et al., 1990), Ena is a member of the Ena/VASP family (for review see Lanier and Gertler, 2000), which modulate actin dynamics (Gertler et al., 1996). *Drosophila ena* mutants are embryonic lethal with defects in the CNS and its peripheral projections (Gertler et al., 1990; Wills et al., 1999a). The effects of *ena* mutations are opposite to those of *abl;* axons go past their muscle targets rather than stopping short, consistent with the idea that Abl negatively regulates Ena. Like Abl, Ena is thought to act downstream of the axon guidance receptors Robo (Bashaw et al., 2000) and dLAR (Wills et al., 1999a), mediating cytoskeletal events.

Our interest in *abl* emerged from its genetic interactions with the adherens junction protein Armadillo (Arm; Loureiro and Peifer, 1998). We investigate morphogenesis, the process by which animals create their complex body plans by organized cell shape changes and rearrangements. Epithelial cells must remain in intimate contact throughout morphogenesis, and in order to change shape or move must coordinate their actin cytoskeletons. Cells accomplish these tasks via cell–cell adherens junctions, which form a continuous adhesive belt around the apex of each cell that anchors a contractile ring of actin filaments (for review see Tepass et al., 2000). Junctions are organized around transmembrane cadherins. Human E-cadherin mediates cell–cell adhesion and organizes a multiprotein complex of catenins bound to its cytoplasmic tail, binding directly to β-catenin, which in turn anchors actin via interactions with α-catenin. *Drosophila* E-cadherin, Arm (the β-catenin homologue), and α-catenin function similarly.

Cadherin-catenin–mediated adhesion must be dynamic, allowing cell movement during morphogenesis (for review see Tepass et al., 2000). We used a genetic approach in *Drosophila* to identify regulators of epithelial morphogenesis. *abl* mutations substantially enhance the CNS defects of *arm* mutants. Further, *abl* genetically interacts with *arm* in the epidermis (Loureiro and Peifer, 1998). This suggested that Abl acts in epidermal cells during morphogenesis. Thus, we investigated whether Abl regulates epithelial development in *Drosophila*. Previous studies of Abl function relied on zygotic mutations, and thus the maternal contribution of Abl may have masked roles in other developmental processes. We removed this maternal contribution, analyzing *abl* maternal/zygotic mutants. This revealed a requirement for Abl in epithelial morphogenesis. Here we report the characterization of this role.

Results

Abelson is essential for embryonic morphogenesis

Previous studies identified a role for Abl in the CNS. Zygotic *abl* mutants have subtle CNS defects, that are enhanced in double mutant combinations (for review see Lanier and Gertler, 2000). We found previously that *abl* interacts with *arm* in its role as a catenin during CNS development (Loureiro and Peifer, 1998), where Arm works with N-cadherin (Iwai et al., 1997). We also observed genetic interactions between *abl* and *arm* in the epidermis. Thus, we hypothesized that Abl might also act in epithelial cells, and that this role might be masked by maternally contributed Abl. To test this, we removed maternal and zygotic Abl using the FLP dominant female sterile technique (Chou and Perrimon, 1996) to generate *abl* heterozygous females whose germ lines are homozygous *abl* mutant. These females contribute no wild-type Abl to their progeny. When crossed to

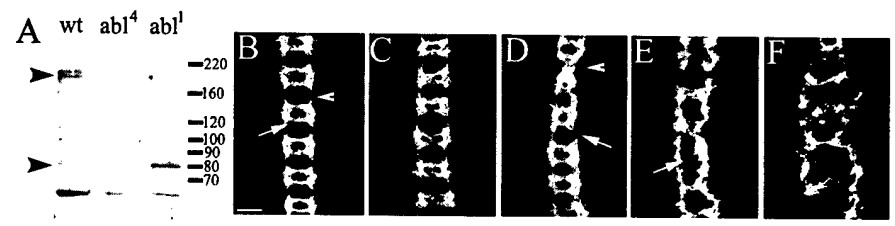

Figure 1. **Complete loss of Abl disrupts CNS development.** (A) Cell extracts from 3-h-old wild-type embryos or embryonic progeny of females with *abl* mutant germlines, immunoblotted with anti-Abl antibody. Wild-type Abl is ~180 kD (top arrow). abl^4 does not produce a protein recognized by this antibody. abl^1 produces a truncated protein product of ~80 kD (bottom arrow). (B–F) Embryos (anterior up) labeled with mAb BP102, which labels all axons. (B) Wild-type CNS, with a scaffold of longitudinal (arrowhead) and commissural (arrow) axons. (C and D) Maternally *abl* mutant but zygotically-rescued embryos have relatively wild-type CNS development, with occasional collapsed longitudinal axons (D, arrowhead) and gaps in axon bundles (D, arrow). (E and F) abl^{MZ} mutants exhibit severe disruptions in CNS development. Most exhibit loss of commissural axons (arrow, E) and some have defects in both longitudinal and commissural axons (F). Bar, 25 μm.

Table I. **Embryonic viability of *abl* maternal and zygotic mutants**

Genotype	Percentage hatched	*n*
abl^1 glc x +/+	92.9	878
abl^4 glc x +/+	89	365
abl^4 glc x shg^2/+	39.5	283[a]
abl^1 glc x shg^2/+	71.1	669[a]
abl^4 glc x shg^{R69}/+	70.4	409[a]
abl^1 glc x scb^2/+	92.3	339[a]
abl^1 glc x abl^1/+	41.0	751[b]
abl^4 glc x abl^4/+	35.6	1149[b]
abl^4 glc; TnAblWT or + x abl^4/+	76	290[c]
abl^4 glc; TnAblK-N or + x abl^4/+	40	299[c]
abl^4 glc; *ena* or +/+ x abl^4/+	61	142[c]
abl^4 glc x shg^2/+; abl^4/+	35.4	398
abl^4 glc x shg^{R69}/+; abl^4/+	38	522

glc, germline clone; TnAblWT, wild-type Abl transgene; TnAblK-N, a kinase-dead Abl trangene (Henkemeyer et al., 1990).
[a]These *shg* or *scb* mutants were balanced with *CyO*.
[b]These *abl* mutants were balanced with TM3.
[c]Only half of the mothers carried the indicated Abl transgene or were heterozygous for *ena*.

abl heterozygous males, half the progeny are maternally and zygotically *abl* mutant, while the other half receive a wild-type copy of *abl* paternally. We used two *abl* alleles: abl^1 produces a truncated protein, and abl^4 is a protein null (Bennett and Hoffmann, 1992; Fig. 1 A). The results were essentially identical with both alleles, and, where tested, were identical when embryos were transheterozygotes.

Embryos lacking both maternal and zygotic Abl (below referred to as abl^{MZ}) die at the end of embryogenesis, while those that receive wild-type paternal Abl survive and go on to adulthood (Table I and unpublished data). Since Abl's role was first defined in the CNS, we examined axon outgrowth using the antibody BP102, which labels all axons of the ventral nerve cord. Zygotic *abl* mutant embryos have subtle defects in CNS development (Wills et al., 1999b). We found that in *abl* maternal mutants that are paternally rescued (identified using a green fluorescent protein [GFP]-marked chromosome), the CNS is normal or has subtle defects (Fig. 1, C and D) which resemble those of *abl dab*/*abl*+ embryos (Gertler et al., 1989). In contrast, maternal/zygotic *abl* mutants have severe defects in CNS development (Fig. 1, E and F). One common feature was a reduction in the commissures which cross the midline. This phenotype resembles that of *abl dab* double mutants (Gertler et al., 1989) and is consistent with previous analysis of the effects of Abl overexpression, which had the opposite effect: enhanced midline crossing (Bashaw et al., 2000). Thus, maternal Abl obscures a role for Abl in CNS axon outgrowth.

We then examined whether Abl plays a role in epithelial development that is obscured by maternally contributed Abl. We first looked at the cuticle, secreted by the epidermal epithelium. abl^{MZ} mutants exhibit defects in three morphogenetic processes, all of which require orchestrated cell shape changes and cell migration: germband retraction, head involution, and dorsal closure (Table II). Approximately 7% of abl^{MZ} mutants completely fail to germband retract or complete head involution (Fig. 2 B), whereas ~14% exhibit partial germband retraction and dorsal closure defects (Fig. 2 C). Approximately 67% of abl^{MZ} mutants have more subtle defects in dorsal closure (Fig. 2, D and F), whereas ~12% are wild-type in appearance or have minor head involution defects. In contrast, *abl* maternal mutants that inherit a paternal wild-type *abl* gene are rescued to normal embryogenesis and adulthood; most hatching larvae are wild-type whereas 5% have slight defects in germband retraction and dorsal patterning. Previous work revealed that certain Abl functions require kinase activity, whereas others do not (Henkemeyer et al., 1990). We found that maternal Abl's role in morphogenesis requires kinase activity, as both the embryonic phenotype and adult viability are rescued by a kinase-active Abl transgene but not by a kinase-dead version (Table I; unpublished data).

One important clue to Abl's function may come from its intracellular localization. Previous work (Bennett and Hoffmann, 1992) documented that *Drosophila* Abl is found in axons of the CNS. Abl is also expressed in epithelial cells, with enrichment in the apical cortical cytoplasm during cellularization, early gastrulation, and in the epithelial cells of the imaginal discs. In later embryos, it is diffuse in the cytoplasm. The original Abl antibody from the Hoffmann lab is no longer available. We attempted to extend this work by generating an anti-Abl polyclonal antibody. This works well on

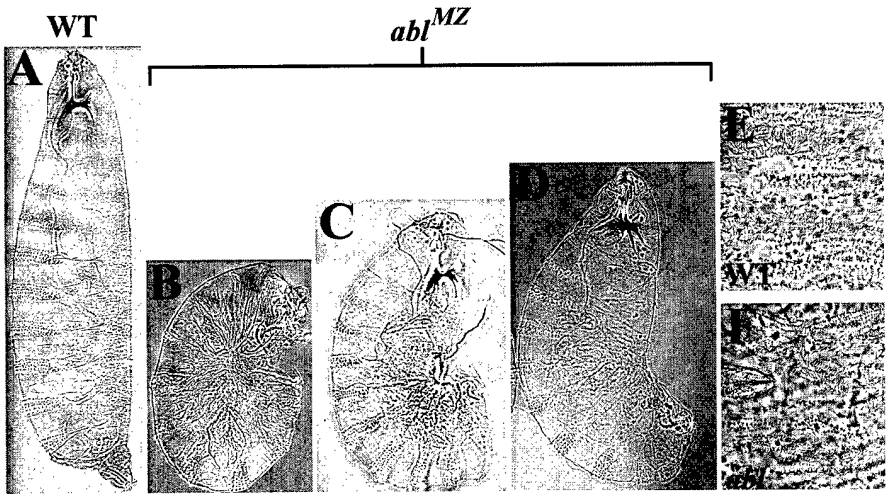

Figure 2. **abl^{MZ} mutants have defects in epithelial morphogenesis.** Cuticle preparations, anterior up. In A–D, dorsal is to the right. (A) Wild-type. (B–D) The range of phenotypes in abl^4 maternal/zygotic mutants, a similar range is observed in abl^1. (B) Approximately 7% of abl^{MZ} mutants have head involution defects and completely fail to germband retract. (C) ~14% of abl^{MZ} mutants partially fail to germband retract and have variable dorsal closure defects. Note the dorsal hole (arrow). (D) Approximately 67% of abl^{MZ} mutants have dorsal closure defects. (E) Wild-type dorsal hair pattern. (F) Misaligned dorsal hairs in abl^{MZ} mutant.

Table II. **Percentage of dead embryos which have the following defects**

Genotype	U-shaped[a]	Tail-up[b]	Dorsal defects[c]	Wild-type	Dorsal and head defects[d]	*n*
	%	%	%	%	%	
abl^4 glc x +/+			Not applicable as almost all hatch			
abl^4 glc x shg^2/+	7	2	45	6	40	298
abl^4 glc x shg^{R69}/+	10	2	54	2	32	121
abl^4 glc x abl^4/+	7	14	67	6	6	388
abl^4 glc x shg^2/+; abl^4/+	2	5	13	10	70	141
abl^4 glc x shg^{R69}/+; abl^4/+	3	1	60	4	38	307
abl^1 glc x abl^1/+	1	13	67	17	1	91
abl^1 glc x scb^2/+; abl^1/+	3	8	75	10	5	63

[a]Embryos in this class exhibited a complete failure in germband retraction.
[b]Embryos in this class exhibited strong defects in germband retraction and also often had defects in dorsal closure.
[c]Embryos in this class exhibited defects in dorsal closure ranging from dorsal holes to defects in the dorsal pattern.
[d]Embryos in this class exhibited severe defect in head involution; most also showed defects in dorsal closure and/or germband retraction.

immunoblots (Fig. 1 A), but does not show specific staining in situ, as assessed using embryos maternally and zygotically mutant for the protein-null abl^4 (unpublished data).

Loss of Abl disrupts cell migration and cell shape changes during dorsal closure

Previous studies supported a role for Abl in signaling from cell surface receptors to the actin cytoskeleton during axon outgrowth (Wills et al., 1999a; Bashaw et al., 2000). Having identified a role for Abl in epithelial tissues, we hypothesized that Abl might act there by a similar mechanism. One place to address this is during dorsal closure, when lateral epidermal epithelial sheets migrate toward the dorsal midline, enclosing the embryo in epidermis. Dorsal closure involves dynamic actin reorganization to form an acto-myosin purse string in cells at the leading edge of the sheet (Young et al., 1993), as well as orchestrated cell shape changes and cell migration (Kiehart et al., 2000). Since Abl plays a role in dorsal closure, we wondered whether Abl modulates these cellular events.

To compare cell shape changes and cell migration in wild-type and abl^{MZ} mutants, we examined embryos during dorsal closure, using antiphosphotyrosine to label both adherens junctions and the leading edge actin cable. As wild-type dorsal closure initiates, leading edge cells elongate uniformly along the dorsal-ventral axis, perpendicular to the leading edge (Fig. 3 A, arrow). As closure proceeds, successive rows of cells lateral to the leading edge also uniformly elongate (Fig. 3, B and C, arrow). The lateral epithelial sheets eventually meet at the dorsal midline, and cells intercalate with one another, making the dorsal surface a continuous epithelial sheet with little midline discontinuity (Figs. 3, D and E, arrow).

abl^{MZ} mutants have striking defects in the cellular events of dorsal closure. Cells fail to change shape in a coordinated fashion (Fig. 3, F–J). As leading edge cells begin to elongate, cells do not elongate uniformly in comparison to their neighbors (Fig. 3, F and G, arrows), and groups of cells have overly broad or narrowed leading edges (arrowheads). As cell shape is likely maintained against tension along the leading edge from the actin cable, altered cell shapes may result from alterations in the polymerization or anchoring of actin (see below). We also observed groups of cells that completely fail to change shape (Fig. 3, G–I, asterisks). As closure proceeds, the cell shape defects persist as cells behind the leading edge begin to elongate (Fig. 3, G–I). Not all abl^{MZ} mutants close dorsally, but those that do show a variety of defects at the cellular level. Some embryos maintain groups of cells that have never elongated (Fig. 3 I, asterisks). Other embryos fail to properly align the opposing epithelial sheets at the midline upon completion of closure (Fig. 3 J, arrow), likely contributing to the altered dorsal hair patterning evident in the cuticles (Fig. 2 F). A subset of the abl^{MZ} mutants fail to complete germband retraction (Figs. 2 C and 3, K and L). In these embryos, cells along the leading edge exhibit the same cell shape abnormalities during dorsal closure as mutants that complete germband retraction (Fig. 3 L, arrows). A fraction of the cells in abl^{MZ} mutants become multinucleate due to defects in cellularization (unpublished data). We verified that cell shape and migration defects during dorsal closure are independent of cell shape disruption due to polyploidy (Fig. 3 O).

The failure to initiate uniform cell shape changes in abl^{MZ} mutants is similar to the phenotype we observed in *arm* zygotic mutants (McEwen et al., 2000). These embryos have only maternal Arm, and thus their levels of wild-type Arm are substantially reduced. While *arm* mutants are more severely compromised in their ability to complete dorsal closure than are abl^{MZ} mutants, leading edge cells of both *arm* (Fig. 3, M and N) and abl^{MZ} mutants fail to elongate uniformly as closure is initiated.

The defects in cell morphology during dorsal closure in abl^{MZ} mutants led us to examine localization of actin and of the Abl target Ena, an actin regulator during this process. In the initial stages of dorsal closure, as cells along the leading edge begin to elongate, Ena surrounds the cell membrane but is enriched at vertices of cell–cell contact and at adherens junctions of leading edge cells (Fig. 4 A, left, red). Actin localizes around the entire cell and begins to accumulate at the leading edge at this stage (Fig. 4 A, middle, green; Young et al., 1993). As closure proceeds, Ena accumulates at uniformly high levels in adherens junctions of leading edge cells (Fig. 4 C, left, red), while actin forms a uniform and tightly localized band along the leading edge (Fig. 4 D middle, green).

The localization of both Ena and actin is altered during dorsal closure in abl^{MZ} mutants, and these changes parallel the changes in cell shape. As closure initiates, Ena is enriched at adherens junctions, but the level of Ena is not

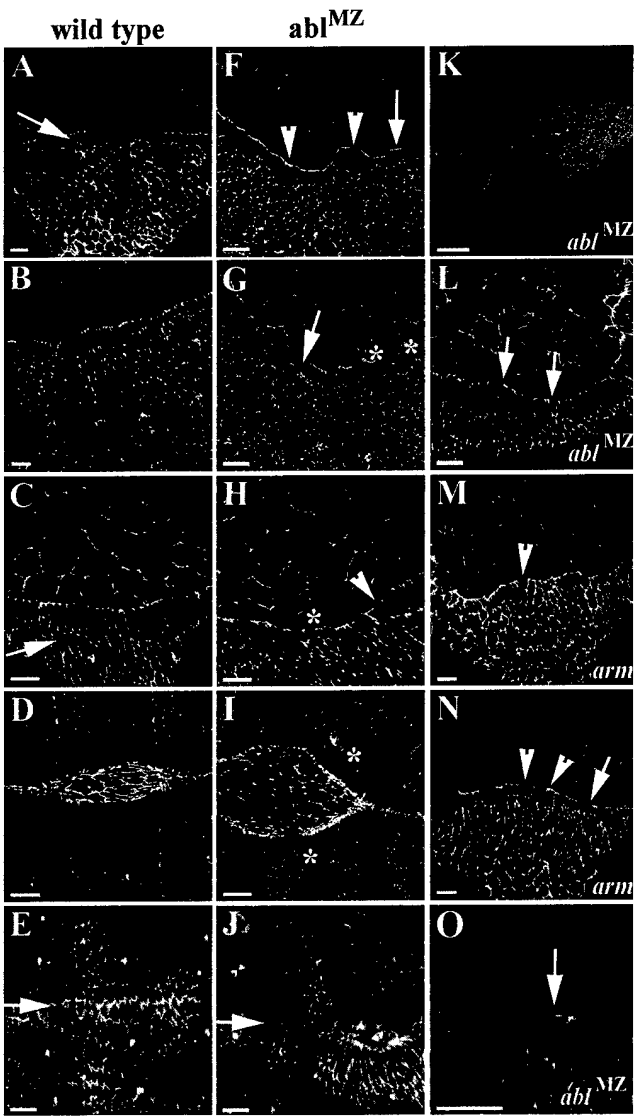

Figure 3. ***abl*^{MZ} mutants fail to undergo coordinated changes in cell shape during dorsal closure.** Embryos labeled with antiphosphotyrosine. Anterior is to the left. (A–E) Wild-type at progressively later stages of dorsal closure. (A–C) Lateral views. (D and E) Dorsal views. (A) Leading edge cells have begun to uniformly elongate (arrow). (B and C) Successive lateral cell rows uniformly elongate (arrow). (D) Lateral epithelial sheets zip together. (E) Closure is complete, with lateral epithelial cells evenly matched at the midline (arrow). (F–J) *abl*^{MZ} mutants at progressively later stages of dorsal closure. (F–H) Lateral and (I–J) dorsal views. (F) Leading edge cells do not elongate uniformly (arrow). Some cells have broadened or constricted leading edges (arrowheads). (G and H) Lateral cells have begun to elongate, but do so nonuniformly (arrow). Some cells have broadened or narrowed leading edges (arrowheads). Other groups of cells completely fail to elongate (asterisks). (I) *abl*^{MZ} mutants that proceeded through dorsal closure. Small groups of cells have still completely failed to change shape (asterisks). (J) *abl*^{MZ} mutant that completed closure. Epithelial sheets often fail to align properly at the midline (arrow). (K and L) Some *abl*^{MZ} mutants initiate dorsal closure even though they have not completed germband retraction. Cell shape defects are also seen in these embryos (arrows). (M and N) *arm*^{XP33} mutants have cell shape defects similar to *abl*^{MZ} mutants. Cells fail to elongate uniformly (arrow) and have broadened or narrowed leading edges (arrowheads). (O) Cell shape defects in *abl*^{MZ} mutants are not caused by multinucleate cells. *abl*^{MZ}, double-labeled with antiphosphotyrosine and with propidium iodide, labeling nuclei. Mononucleate cells have defects in shape (arrow). Bars: (A–J and L–O) 10 μm; (K) 50 μm.

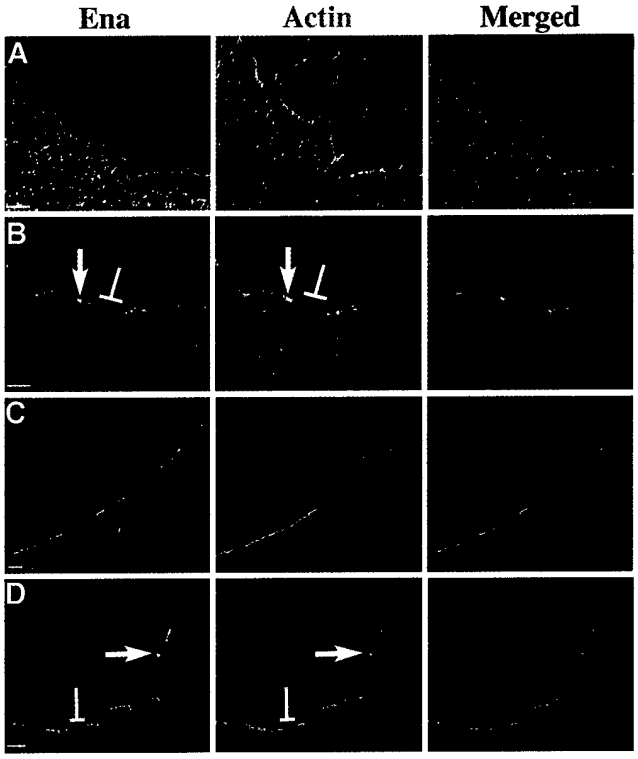

Figure 4. **Complete loss of Abl alters Ena and actin localization during dorsal closure.** Lateral view. Embryos double-labeled with anti-Ena (red) and phalloidin (green), labeling F-actin. (A) Stage 13 wild-type embryo with leading edge cells initiating elongation. Ena (left, red) is enriched at vertices of cell–cell contact. Actin (middle, green) outlines all cell membranes and is beginning to accumulate at the leading edge. Actin and Ena colocalize at cell junctions. (B) Stage 13 *abl*^{MZ} mutant. Ena (left, red) and Actin (middle, green) enrichment is not uniform at the leading edge. Both are enriched in some cells (arrows) and depleted in others (brackets). (C) Stage 14 wild-type embryo. More lateral cells have undergone uniform elongation. Ena is uniformly enriched at adherens junctions of leading edge cells (left, red). Actin forms a tight cable along the leading edge (middle, green). Ena and actin colocalize at adherens junctions as actin expands along the entire leading edge. (D) Stage 14 *abl*^{MZ} mutant. Nonuniform localization of Ena and Actin persists. Cells with excess Ena (left, arrow) often accumulate excess Actin (middle, arrow), whereas cells with diminished Ena levels (left, bracket) have diminished levels of Actin (middle, bracket) Bars, 10 μm.

uniform in different cells (Fig. 4 B, arrow vs. bracket). The actin cable is also not uniform; levels of actin often change in parallel to Ena (Fig. 4 B). This uneven distribution of Ena and actin persists throughout dorsal closure (Fig. 4 D). Changes in Ena and actin levels often correlate with defects in cell shape. Cells with constricted leading edges tend to accumulate abnormally high levels of both proteins, whereas cells with broadened leading edges tend to have lower levels of Ena in junctions and lower levels of leading edge actin. This correlation may be explained by the fact that the leading edge is under tension, presumably due to the contractile actin cable (Kiehart et al., 2000). Defects in actin cable assembly or anchoring within individual cells could lead those cells to splay open at the leading edge; adjacent cells might then hypercontract due to the release of the tension normally exerted by their neighbors.

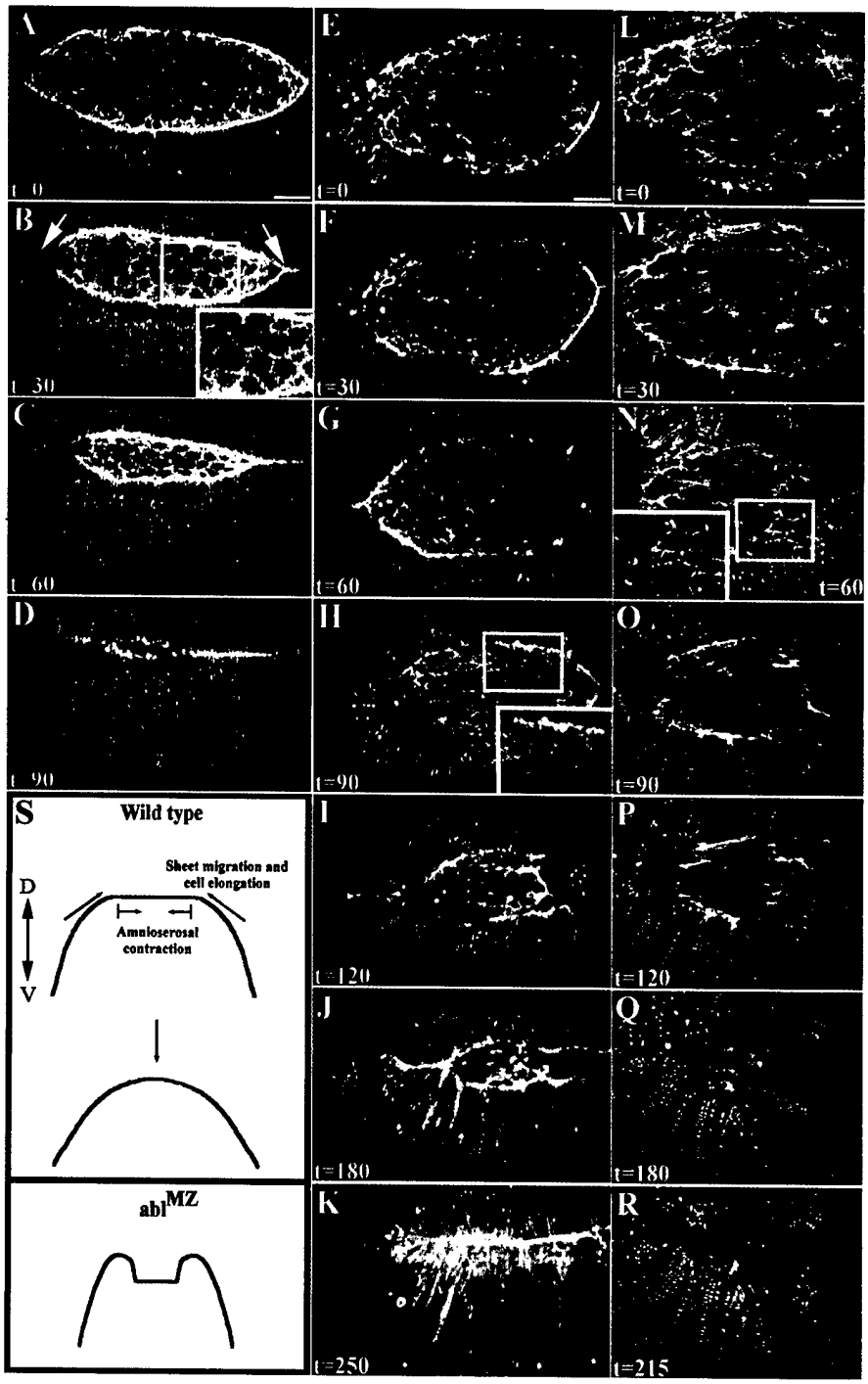

Figure 5. **Dorsal closure is substantially slowed in *abl*^{MZ} mutants.** Dorsal view of embryos expressing moesin-GFP, anterior to the right. Time is in minutes. Insets in (B, H, and N) display actin-rich filopodia extending from amnioserosa or leading edge cells. (A–D) Wild-type embryo at 30 min intervals during dorsal closure. (A) The leading edge of the dorsal closure front is uniformly enriched in actin. Lateral epithelial sheets elongate uniformly. (B) 30 min. Amnioserosa cells are undergoing apical constriction and the embryo is zipping together at the anterior and posterior ends (arrows). (C) 60 min. Amnioserosa cells have constricted apically and remain in the same plane of focus as the lateral epithelial sheets. (D) 90 min. Dorsal closure is complete. (E–K) *abl*^{MZ} mutant. The amnioserosa cells in E are comparable in surface area to the wild-type in A. (F–H) As closure progresses, amnioserosa cells constrict and lateral epithelial cells elongate, but dorsal closure is delayed relative to wild-type (compare D and H). If one matches embryos based on the length of the leading edge (compare A and G), closure is still delayed. This embryo took >4 h to complete closure (K). (L–R) A different *abl*^{MZ} mutant at higher magnification, illustrating the folding-under of the leading edge and failure to complete closure. (S) Cross-section diagram depicting one interpretation of the defects of *abl*^{MZ} mutants. In wild-type embryos, the rate at which lateral cells elongate, the sheets migrate, and amnioserosa cells constrict are tightly coordinated. In *abl*^{MZ} mutants, the leading edge folds under the more lateral epidermis, perhaps because leading edge cells migrate too slowly or amnioserosa cell constriction is slowed (these events are likely coupled), forcing the sheet to fold under. Time-lapse videos supplementing this figure are available at http://www.jcb.org/cgi/content/full/jcb.200105102/DC1. Bars, 25 μm.

Dorsal closure is slowed in *abl* mutants

Multiple forces drive dorsal closure, including forces generated by cell shape changes, contraction of the leading edge actin-myosin cable, and pulling forces exerted by amnioserosa cells. These forces act combinatorially, so disruption of one force slows but does not prevent closure (Kiehart et al., 2000). *abl*^{MZ} mutants display defects in both cell shape and in the actin cable, yet many embryos complete closure, albeit imperfectly. To analyze how *abl*^{MZ} mutants compensate for disruptions in cell shape and the actin cable, we performed time-lapse confocal microscopy on embryos undergoing closure (see videos available at http://www.jcb.org/cgi/content/full/jcb.200105102/DC1). We analyzed transgenic flies expressing the actin binding domain of Moesin fused to GFP (Kiehart et al., 2000), allowing us to visualize actin dynamics in real time.

During dorsal closure in living wild-type embryos, the leading edge becomes uniformly enriched in actin as leading edge cells elongate (Fig. 5 A). Amnioserosa cells, the large squamous cells exposed on the dorsal surface of the embryo, undergo apical constriction (Kiehart et al., 2000), decreasing in surface area throughout closure (Fig. 5, A–D). Finally, as the lateral epithelial sheets migrate toward one another, closure is initiated at the anterior and posterior ends of the opening (Fig. 5 B, arrows) and the sheets zip together from the ends (Fig. 5, A–D) (Jacinto et al., 2000). Once the cells

initiate elongation and the front is enriched in actin, dorsal closure is completed in a little over 1.5 h.

Dorsal closure is substantially slowed in abl^{MZ} mutants. It is not simple to define an equivalent starting point for abl^{MZ} and wild-type embryos, as the dorsal/ventral extent of the amnioserosa is larger in abl^{MZ} mutants, both in cell number and distance (compare Fig. 5 A to E). This may be due to defects in cell rearrangements during germband retraction. However, regardless of whether we compared embryos with equivalent amnioserosa surface areas (Fig. 5 A vs. E) or with roughly equivalent length leading edges (Fig. 5 A vs. G), closure is substantially delayed in abl^{MZ} mutants, taking two to three times longer than normal. At the cellular level, lateral cells elongate on schedule in the mutants (despite defects in cell shape) and amnioserosa cells apically constrict, though more slowly than in wild-type.

Time-lapse imaging also revealed defects that were not apparent in our fixed images. As closure proceeds, the leading edge of the lateral epidermis folds under the more lateral cells that follow it (Fig. 5, J, Q, and R). This suggests that while lateral epithelial cells continue to elongate and migrate, driving sheet extension, leading edge cells do not migrate toward one another at an appropriate rate (diagram in Fig. 5 S). Our movies also suggest that filopodial extensions from the leading edge might aid in the eventual closure, as they do in wild-type (Jacinto et al., 2000), actively zipping the epidermal sheets together. Filopodial extensions from epidermal and amnioserosa cells are present in both wild-type and abl^{MZ} mutants, and even appear more fre-

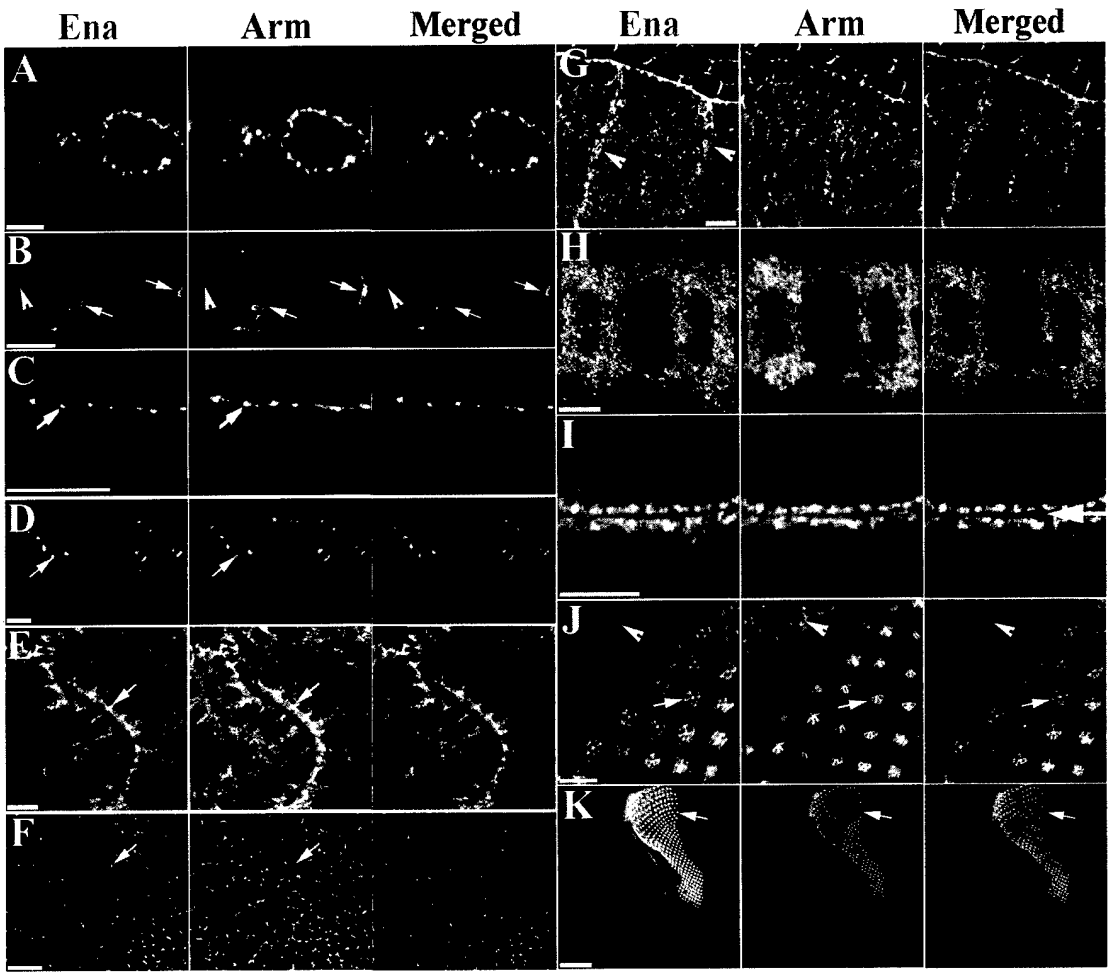

Figure 6. **Ena and Arm colocalize at adherens junctions throughout development.** All images (except I) are anterior to the right. Ena is green and Arm is red in merged images. (A) Stage 3 egg chamber. Ena and Arm are enriched in apical adherens junctions of follicle cells. (B and C) Stage 10 egg chamber. Levels of Ena and Arm drop, but both remain at adherens junctions. Anterior (border cells) and posterior polar follicle cells are enriched in both Ena and Arm (B, arrows). Ena and Arm also colocalize to nurse cell membranes (B, arrowhead). (D–G) During embryogenesis Ena and Arm colocalize to adherens junctions of epithelial tissues. (D) Cross-section, stage 9 embryo. Ectodermal adherens junctions (arrow). (E) Adherens junctions of polarized cells of the invaginating hindgut (arrow). (F) Apical view, stage 9 embryo. Ena is enriched at vertices of cell–cell contact (arrow), whereas Arm is more uniform. (G) During dorsal closure Ena is enriched at adherens junctions of leading edge cells, but it is also found in the cytoplasm of cells at the segment boundary (arrowheads). (H) Ena and Arm both localize to axons. (I–K) Imaginal discs. (I) Apical surfaces of two epithelial sheets opposed to one another in the wing imaginal disc (arrow). Ena and Arm colocalize to apical adherens junctions, and are also found at the apical surface. (J and K) In eye imaginal discs cell differentiation occurs after the morphogenetic furrow passes. In undifferentiated cells, Ena and Arm colocalize to cell boundaries (J, arrowhead). As groups of cells begin differentiating as photoreceptors (J, arrow), Ena localizes uniformly to all cells of the precluster. Arm, in contrast, accumulates at high levels in a subset of these cells. Later, Ena and Arm colocalize in photoreceptor rhabdomeres (K, arrow). Bars: (A–J) 10 μm; (K) 50 μm.

quent in late-stage mutants (Fig. 5, B, H, and N, insets). We suspect epithelial sheet migration is compromised in *abl* mutants due to the discontinuity of the leading edge actin cable and the cell shape defects. In this situation, filopodia may be needed to locate the opposing epidermis and eventually zip up the embryo.

ena suppresses the *abl* phenotype and localizes to adherens junctions

The best characterized substrate of *Drosophila* Abl is Ena. Mutations in *ena* suppress the effects of *abl dab* mutations (Gertler et al., 1995). We thus examined whether *ena* might act with Abl in epithelial morphogenesis. Data from the Hoffmann lab supported this possibility: they found that females homozygous for *abl* mutations, which are normally sterile, become fertile when they are also heterozygous for *ena* (Bennett and Hoffmann, 1992). We thus generated homozygous *abl* germline clones in females that were heterozygous for *ena* (for experimental reasons only 50% of the females generated in the experiment are *ena* heterozygotes) and crossed them to *abl* heterozygous males. *ena* heterozygosity significantly rescued the abl^{MZ} embryonic lethality (Table I).

These data suggest that Ena misregulation contributes to the defects in morphogenesis we observed in abl^{MZ} mutants. We thus examined Ena localization in epithelial tissues, as this might reveal, at least in part, where Abl is acting. We used two different anti-Ena antibodies (Gertler et al., 1995; Bashaw et al., 2000) with similar results. We found that Ena colocalizes with Arm at adherens junctions throughout most stages of development. During early oogenesis, Ena and Arm are strongly enriched at adherens junctions of follicle cells surrounding the germline (Fig. 6 A; Baum and Perrimon, 2001) and remain enriched at junctions, though at lower levels as oogenesis proceeds (Figs. 6, B and C). During embryogenesis, Ena begins to accumulate in adherens junctions at the onset of gastrulation (unpublished data) and colocalizes with Arm at adherens junctions in germband-extended embryos (Fig. 6 D, arrow) and in fully polarized cells, such as the invaginating hindgut (Fig. 6 E, arrow). Arm localizes uniformly around cells (Fig. 6 F), whereas Ena, though present all around the plasma membrane, is enriched at vertices of cell–cell contact (Fig. 6 F, arrow). Ena is strongly enriched in adherens junctions of leading edge cells during dorsal closure (Figs. 4 C and 6 G), and also localizes to the cytoplasm in a stripe of epidermal cells at the segmental boundary (Fig. 6 G, arrowheads). Ena and Arm also localize to CNS axons (Gertler et al., 1990; Fig. 6 H). During larval development, Ena and Arm are strongly enriched at adherens junctions of the highly polarized imaginal disc epithelia, precursors of the adult epidermis (Figs. 6 I, arrow), as well as in the specialized junctions of the photoreceptor rhabdomeres (Fig. 6, J and K). Thus, Arm and Ena colocalize in adherens junctions in most epithelial cells.

ena and *arm* genetically interact during dorsal closure

Our genetic experiments suggest that Ena misregulation plays a role in the defects in morphogenesis of abl^{MZ} mutants (Table I). As Ena localizes to adherens junctions, we wondered whether it might work with adherens junction components during morphogenesis. We thus looked for genetic interactions between *ena* and *arm*. We crossed females heterozygous for mutations in both *arm* and *ena* to males heterozygous for *ena*. Both *arm* and *ena* are embryonic lethal; as *arm* is on the X-chromosome, we expect 43% of the dead progeny to be *arm* mutant, 43% to be *ena* mutant, and 14% to be *arm; ena* double mutants. Null alleles of Arm have dorsal closure defects, due to a combination of affects on cell adhesion and Wg signaling (McEwen et al., 2000), whereas weaker *arm* alleles do not have dorsal closure defects. We first tested the weakest allele of *arm*, $arm^{H8.6}$, in which dorsal closure is normal, although segment polarity is affected (Fig. 7 B). Although *ena* homozygotes are embryonic lethal, most of the dead embryos only have mild defects in head involution (Gertler et al., 1990; Fig. 7 C). A small fraction (~5%) have dorsal pattern defects indicative of mild problems in dorsal closure. When we generated $arm^{H8.6}$; ena^{GC1} double mutants, we found strong synergistic defects in both head involution and dorsal closure (Fig. 7 D; Table III). Mutations in *ena* also enhance the dorsal closure defects of the stronger *arm* mutants arm^{XM19}, arm^{XP33} (unpublished data), and arm^{YD35} (Fig. 7, E and F; Table III), though it is difficult to rule out the possibility that these interactions are simply additive.

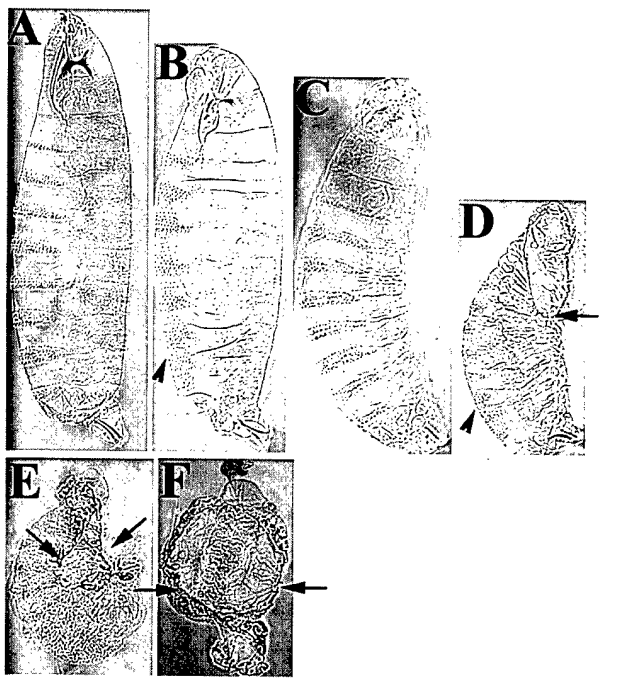

Figure 7. **Mutations in *ena* enhance *arm*'s dorsal closure defects.** Cuticle preparations, anterior up. (A) Wild-type. (B) $arm^{H8.6}$ mutants have segment polarity defects due to defects in Wingless signaling (arrowhead), but head involution and dorsal closure are normal. (C) ena^{210}/ena^{GC1}. (D) $arm^{H8.6}/Y$; ena^{GC1}/ena^{GC1}. Note strong defects in dorsal closure and head involution (arrow), with no change in the segment polarity phenotype (arrowhead). (E) arm^{YD35} mutants have a dorsal hole (arrows), as well strong segment polarity defects. (F) The dorsal side of arm^{YD35}; ena^{210}/ena^{210} embryos is completely open (arrows).

Table III. ***arm*** **and** ***ena*** **genetically interact**

Cross	Percentage of dead embryos with: *arm* ø-type	*ena* ø-type	*arm; ena*	*n*
$arm^{H8.6}$/+; ena^{GC1}/+ × +/Y; ena^{GC1}/+	34	53	13	218
arm^{YD35}/+; ena^{GC1}/+ × +/Y; ena^{GC1}/+	51	35	14	635
Predicted by Mendelian ratios	43	43	14	

Mutations in DE-cadherin enhance the *abl* phenotype

The genetic interactions between *arm* and *abl* in the CNS and epidermis (Loureiro and Peifer, 1998) and the localization of Ena to adherens junctions suggest that Abl might act in part at adherens junctions. In cultured mammalian cells Abl localizes to cell–matrix junctions (Lewis et al., 1996). As one test of the possible sites of Abl action during morphogenesis, we looked for dose-sensitive genetic interactions between *abl* and genes encoding proteins involved in epithelial adhesion: DE-cadherin (encoded by *shotgun* (*shg*); Tepass et al., 1996; Uemura et al., 1996), which mediates cell–cell adhesion, and *scab* (*scb*), an integrin α-chain which mediates cell-matrix adhesion during dorsal closure (Stark et al., 1997).

We saw strong genetic interactions of *abl* with the cadherin *shg*, but not with the integrin *scb*. We crossed females with *abl* mutant germlines to males heterozygous for *shg* or *scb*. All progeny lack maternal Abl and are zygotically *abl* heterozygous, receiving a wild-type copy paternally. Zygotic wild-type Abl normally rescues all of these embryos to viability (Table I). However, shg^2 heterozygosity led to lethality of *abl*/+ embryos (Table I). Only 40% of the progeny hatch, and the dead embryos have dorsal closure and germband retraction defects similar to abl^{MZ} mutants. Many also have severe defects in head involution (Fig. 8 B, arrow). Similar, though somewhat less penetrant, results were seen with the *shg* null allele, shg^{R69} (Table I). In contrast, we saw no effects on the survival of *abl*/+ embryos of removing one copy of *scb* (Table I). To increase the sensitivity of this genetic interaction assay, we crossed females with *abl* mutant germ lines to *abl*/+; *shg*/+ or *abl*/+; *scb*/+ males. Half of the progeny lack both maternal and zygotic Abl, and half of those are also heterozygous for either *shg* or *scb*. Heterozygosity for shg^2 substantially enhanced the abl^{MZ} phenotype (Fig. 8 D; Table II). Approximately half of the dead embryos (presumably those that were *abl*/*abl*; shg^2/+) had a prominent dorsal anterior hole not seen in abl^{MZ} mutants (Fig. 8 D); these embryos also had the typical spectrum of dorsal closure and germband retraction defects. We saw similar phenotypic enhancement in abl^{MZ} embryos heterozygous for the *shg* null allele, shg^{R69}. (Fig. 8 E; Table II). In contrast, this sensitized assay did not uncover a significant genetic interaction between *abl* and *scb* (Table II).

Loss of Abl decreases the amount of junctional arm and α-catenin

The genetic interactions between *abl* and *shg* suggested that some of the morphogenesis defects observed could result from effects of Abl at adherens junctions. Alternately, they might result from more nonspecific effects on cell polarity or the cytoskeleton. We thus examined the subcellular localization of adherens junction proteins and other markers of cell polarity in abl^{MZ} mutants. To control for variability between experiments, we analyzed mixed populations of wild-type and mutant embryos that had undergone simultaneous fixation, staining, and microscopy. We used a wild-type strain carrying a GFP transgene, allowing us to unambiguously discriminate between wild-type and mutant embryos. The mutant embryos had fathers which were heterozygous for *abl* and a different GFP-transgene, to differentiate abl^{MZ} from paternally rescued embryos.

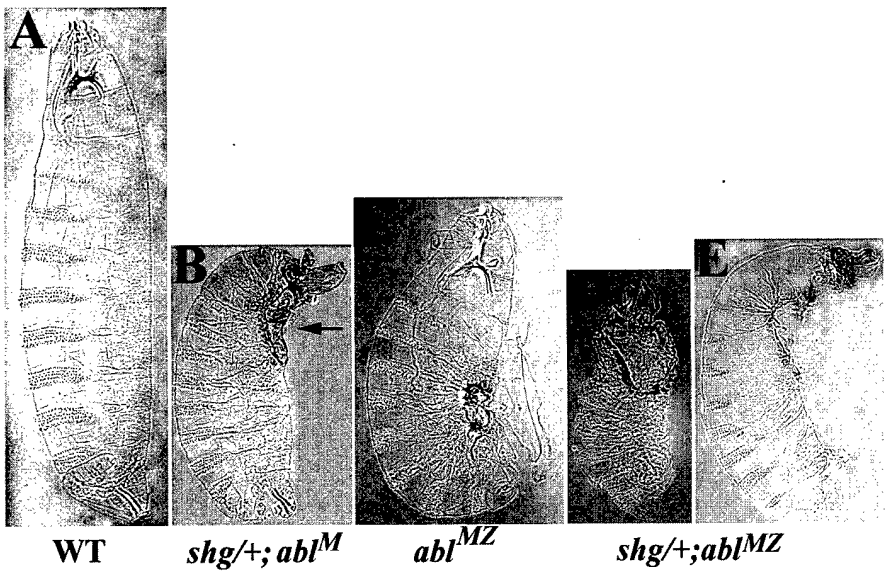

Figure 8. **DE-cadherin (*shg*) genetically interacts with Abl.** Cuticle preparations, anterior up. (A) Wild-type. (B) abl^4/abl^4 × shg^2/*CyO*. abl^4 maternal mutants are zygotically rescued, with all hatching as larvae and most appearing wild-type. *shg* heterozygosity prevents zygotic rescue of *abl* maternal mutants and leads to morphogenesis defects. Note defects in dorsal closure and head involution (arrow). (C) abl^{MZ} mutants die during embryogenesis with defects in epithelial morphogenesis. (D and E) *shg* heterozygosity enhances the abl^{MZ} phenotype. (D) 70% of lethal progeny of abl^4/abl^4 × shg^2/+; abl^4/+ have cuticles that are reduced in size with a large dorsal-anterior hole. (E) 30% of the lethal progeny of abl^4/abl^4 × shg^{R69}/+; abl^4/+ have a prominent dorsal-anterior hole.

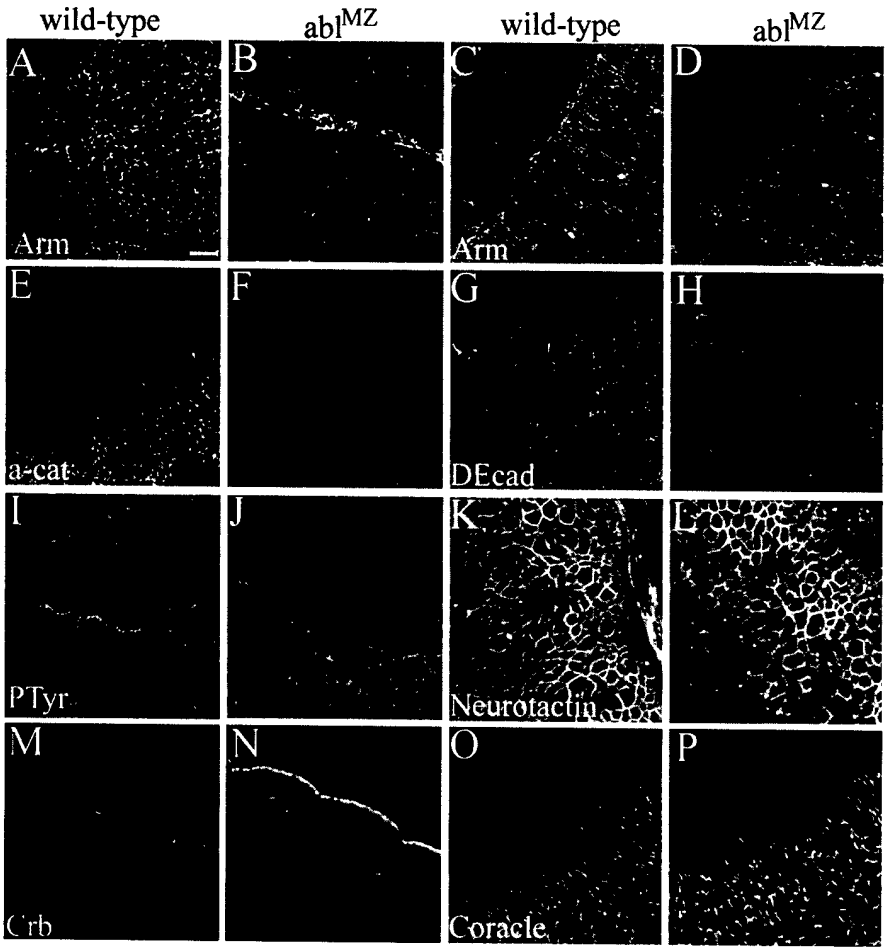

Figure 9. **Levels of junctional Arm and α-catenin are reduced in *abl*^{MZ} mutants.** Embryos labeled with anti-Arm (A–D), anti–α-catenin (E and F), anti–DE-cadherin (G and H), antiphosphotyrosine (I and J), anti-Neurotactin (K and L), anti-Crumbs (M and N), and anti-Coracle (O-P). (A and B) Stage 8. (C and D) Stage 14. (A and C) Wild-type. Arm localizes to adherens junctions. (B and D) *abl*^{MZ} mutants. Arm accumulates at reduced levels in adherens junctions. (E and F) Stage 13. (E) Wild-type. α-catenin localizes to adherens junctions. (F) *abl*^{MZ} mutant. α-catenin accumulates at reduced levels in adherens junctions. (G–J) Stage 13. DE-cadherin localizes to adherens junctions, without striking differences in localization or levels between wild-type (G) and *abl*^{MZ} mutants (H). Phosphotyrosine localizes to adherens junctions, without noticeable differences between wild-type (I) and *abl*^{MZ} mutants (J). (K and L) Stage 11. Neurotactin localizes to the baso-lateral membrane without noticeable differences between wild-type (K) and *abl*^{MZ} mutants (L). (M and N) Cross-sectional views, Stage 11. Crumbs localizes to the apical membrane of epithelial cells without striking differences between wild-type (M) and *abl*^{MZ} mutants (N). (O and P) Stage 13. Coracle localizes to septate junctions with no striking difference in levels between wild-type (O) and *abl*^{MZ} mutants (P). Bar, 10 μm.

abl^{MZ} mutants had reduced levels of Arm in adherens junctions. This was first noticeable in germband-extended embryos (Fig. 9, A and B) and became more pronounced during dorsal closure in wild-type (Fig. 9, C and D). Cross-sectional views suggest that the decrease in Arm at adherens junctions is not due to mislocalization of Arm to a different place in the cell (unpublished data), and we also think it is unlikely to be solely due to the alterations in cell shape in the mutant. Given these effects on Arm, we analyzed other adherens junction components. α-catenin, a protein that links Arm to the actin cytoskeleton, also showed reduced accumulation in adherens junctions (Fig. 9, E and F). The localization of both Arm and α-catenin was more variable in paternally rescued embryos, with reduction in some individuals but not others (unpublished data). The accumulation of DE-cadherin at junctions also may be slightly reduced in *abl*^{MZ} mutants (Figs. 9, G and H), but this effect was less pronounced than that on Arm or α-catenin. We also examined several other cortical or membrane markers. The accumulation of phosphotyrosine in adherens junctions (Fig. 9, I and J), Coracle at septate junctions (Fig. 9, O and P), Neurotactin at the basolateral membrane (Fig. 9, K and L), and Crumbs at the apical membrane (Fig. 9, M and N) were only slightly reduced or unaffected. In doing these experiments, we also observed that the defects in cell shape in *abl*^{MZ} mutants are not restricted to dorsal closure. We observed defects in the uniform apical constrictions that occur in cells along the ventral midline (Fig. 9, A and B). Defects in cell shape changes and cell migration could also explain the observed defects in germband retraction.

To complement these immunofluorescence assays, we examined total protein levels of Arm and other proteins in the progeny of *abl*^{1} germline mutant females crossed to *abl* heterozygous males. Half of these embryos are *abl*^{MZ} and the other half are zygotically rescued. To ensure that embryos were similarly aged and to remove unfertilized eggs from the samples, we selected living embryos at the cellular blastoderm stage and then let them develop for given amounts of time. Total levels of Arm protein are significantly reduced throughout development compared with wild-type (Fig. 10, A–C). Similar reductions in Arm protein were observed in *abl*^{1} (unpublished data). In contrast to Arm, the levels of two unrelated control proteins, Pnut and BicD, were unaffected by loss of Abl function (Fig. 10, A–C). We next examined the levels of other adherens junction proteins. Reduction in Abl function also led to reduction in α-catenin protein levels (Fig. 10 A). In contrast, levels of DE-cadherin are not altered in *abl* mutants (Fig. 10, A–C). We then assessed whether these effects were specific for adherens junction proteins, by examining the levels of other markers of cell polarity or the cytoskeleton. We saw either subtle reduction or no effect of *abl* mutations on the levels of actin, the septate junction protein Coracle, and the apical marker Crumbs (Fig. 10, B and C).

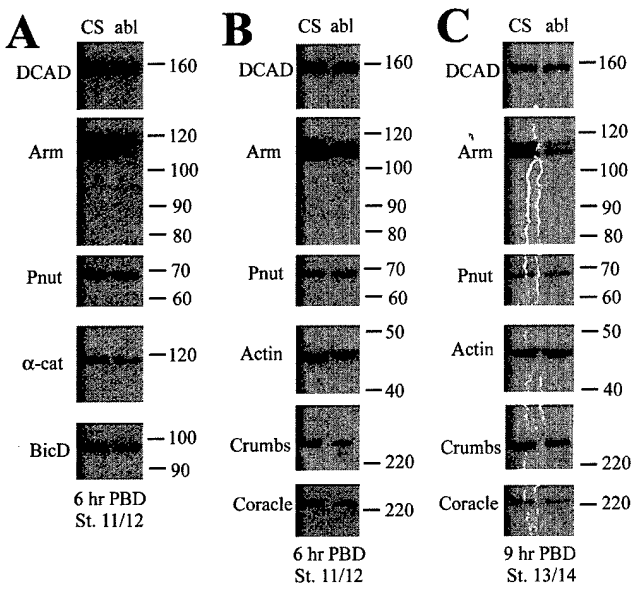

Figure 10. **Total levels of Arm and α-catenin are reduced in *abl* mutants.** *abl* germline mutant females were mated to *abl* heterozygous males and progeny were picked at the cellular blastoderm stage and aged for the indicated time postblastoderm (PBD). Wild-type embryos (Canton S [CS]) served as a control. Cell extracts were fractionated by SDS-PAGE and immunoblotted with the indicated antibodies. Molecular weight markers are to the right. Bicaudal D (BicD) or Peanut (Pnut) are loading controls. Each vertical set of samples represents sequential reprobing of the same blot. (A and B) Stage 11/12 embryos (6 h postblastoderm). (C) Stage 13/14 embryos (9 h postblastoderm).

Discussion

Activation of Abl tyrosine kinase plays a key role in the development of certain human leukemias (for review see Zou and Calame, 1999). Despite the attention paid to its role in oncogenesis, the complex roles Abl plays in normal cells are not as well understood. Here we report a novel role for Abl in epithelial cells, in which it regulates cell shape changes and cell migration during epithelial morphogenesis in vivo. These data may have broader implications, providing insights into the possible underlying cause of some of the defects seen in the mouse *abl* mutants and *abl; arg* double mutants, and may also provide insight into the role Bcr-Abl plays in leukemic cells. Further, these data provide in vivo evidence for a role for a tyrosine kinase in epithelial morphogenesis. This has been suspected from the actions of activated kinases in cultured cells (for review see Daniel and Reynolds, 1997), but our experiments test this in the intact animal.

It is useful to compare what we observed in the epidermis with Abl's role in axon outgrowth, where it is thought to modulate communication between at least two transmembrane axon guidance receptors, Robo and dLAR, and the actin cytoskeleton (for review see Lanier and Gertler, 2000). Abl is thought to antagonize Ena in this process. The *ena* and *abl* phenotypes were surprising in one respect. Ena/VASP proteins had been thought to enhance actin polymerization based on promotion of intracellular motility of the bacteria *Listeria*. However, while promoting actin polymerization might be expected to drive growth cone extension and axon outgrowth, Ena promotes growth cone repulsion and axon stalling (Bashaw et al., 2000; Wills et al., 1999a,b), whereas Abl has opposite effects. Work in cultured fibroblasts led to similar conclusions: Ena/VASP proteins inhibit cell migration (Bear et al., 2000).

Building on this model, Abl and Ena might play analogous roles in epithelial cells, translating extracellular signals into changes in the actin cytoskeleton. This sort of cytoskeletal modulation plays a key role in cell migration and cell shape changes during epithelial morphogenesis. One model consistent with our data is that Abl acts at adherens junctions during morphogenesis. Cadherins and catenins play important roles in morphogenesis in all animals. Severe reduction in *Drosophila* Arm (Cox et al., 1996) or DE-cadherin (Tepass et al., 1996) function leads to early loss of epithelial integrity. Less severe reduction in cadherin/catenin function affects head involution, dorsal closure, and other morphogenetic processes (Tepass et al., 1996; Uemura et al., 1996; McEwen et al., 2000). In fact, many epithelial defects of *DE-cadherin* mutants are blocked by blocking morphogenetic movements (Tepass et al., 1996), suggesting that modulating adhesion is critical to morphogenesis.

Several lines of evidence support the possibility that the morphogenetic defects of abl^{MZ} mutants result, at least in part, from Abl action at adherens junctions. First, the effects on dorsal closure, germband retraction, and head involution are strongly enhanced by reducing the dose of DE-cadherin. Second, the defects in cell shape during dorsal closure resemble, in part, those of *arm* mutants. Third, the defects in morphogenesis are suppressed by mutations in *ena*, which is primarily found at adherens junctions. Finally, we observed a reduction in junctional Arm and α-catenin in abl^{MZ} mutants. It is important to note, however, that any role for Abl at adherens junctions would be a modulatory one. It is not absolutely essential for adherens junction assembly or function. Of course, it remains possible that other tyrosine kinases may act redundantly with Abl. The relationship between the cadherin-catenin system, Abl, and Ena that may occur in epithelial cells could also exist in the CNS. Arm and DN-cadherin play roles in axon outgrowth in *Drosophila*, and in this role *arm* interacts genetically with *abl* (Iwai et al., 1997; Loureiro and Peifer, 1998).

One target of Abl might be Ena, which could regulate actin dynamics in the actin belt underlying the adherens junction. Just as local modulation of actin dynamics likely regulates growth cone extension or stalling, the cell shape changes and cell migration characteristic of morphogenesis will require modulation of actin dynamics and junctional linkage. The idea that Ena may regulate cell–cell adhesion recently received strong support from work in cultured mammalian keratinocytes, where inhibiting Ena/VASP function prevented actin rearrangement upon cell–cell adhesion (Vasioukhin et al., 2000). This model was further supported by work published while our paper was under review, which demonstrated that both Abl and Ena regulate actin polymerization at the adherens junctions of ovarian follicle cells in *Drosophila* (Baum and Perrimon, 2001).

Other models are also consistent with our data. Abl may act directly on the actin cytoskeleton, with its effects on

junctions a more indirect consequence. Junctional linkage to actin is critical for effective cell adhesion (Hirano et al., 1992) and alterations in actin polymerization could affect the ability to assemble stable cadherin–catenin complexes, as was observed in cultured mammalian cells (Quinlan and Hyatt, 1999), resulting in the observed loss of Arm from junctions. Abl could also play a more general role in the establishment and maintenance of cell polarity. Finally, studies of cultured mammalian cells also suggest that Abl acts at cell-matrix junctions to modulate responses to integrin-mediated adhesion by associating with and phosphorylating focal adhesion proteins like paxillin and Crkl (for review see Van Etten, 1999). In doing so, it may influence both tethering to actin and signal transduction. *Drosophila* integrins play important roles in morphogenetic processes such as dorsal closure and germband retraction (for review see Brown et al., 2000). We did not detect genetic interactions between *abl* and *scab*, the integrin α-chain that plays a role in dorsal closure (Stark et al., 1997). However, this does not rule out interplay between integrins and Abl in morphogenesis. It is now important to test these different models by investigating the mechanism by which Abl and Ena act during morphogenesis.

Materials and methods

Fly stocks and phenotypic analysis

All mutations are described in Flybase (http://flybase.bio.indiana.edu/). abl^1 and abl^4 germ line clones were generated by the FLP dominant female sterile technique (Chou and Perrimon, 1996). 48–72-h-old *hsflp:abl FRT 79D-F/ovo*^{D1} *FRT 79D-F* larvae were heat shocked for 3 h at 37°C. Only homozygous *abl* mutant germ cells develop in these females. Stocks to generate *abl* germ line clones, *hsflp;Dr*^{MIO}*/TM3*, *FRT3L79D-F/TM3*, and *ovo*^{D1} *FRT3L79D-F/TM3*, were from the Bloomington *Drosophila* Stock Center. *abl* and *ena* alleles were from M. Hoffmann (University of Wisconsin, Madison, WI). The wild-type was Canton-S. Transgenic lines expressing *histone-GFP*, the actin binding domain of Moesin fused to GFP (Kiehart et al., 2000), or *UAS-GFP* under the control of *sim-GAL4* were provided by R. Saint (University of Adelaide, South Australia, Australia), D. Kiehart (Duke University, Durham, NC), and S. Crews (University of North Carolina, Chapel Hill, NC), respectively. Cuticle preparations were as in Wieschaus and Nüsslein-Volhard (1986).

Immunolocalization and immunoblotting

Embryos were bleach dechorionated and fixed for 20 min in 1:1 4% formaldehyde/0.1 M Pipes/2 mM $MgSO_4$/1 mM EGTA/0.1% NP-40:heptane. For DE-cadherin localization, embryos were fixed for 1 h in the same fix with 0.3% Triton X-100 added. Vitelline membranes were removed with methanol. For actin visualization, embryos were fixed for 5 min in 1:1 37% formaldehyde:heptane and their vitelline membranes were removed manually. Larval tissues were dissected in insect media and fixed in 4% paraformaldehyde in PBS for 20 min. Ovaries were dissected and fixed as in Peifer et al. (1993). All tissues were blocked and stained in PBS/1% goat serum/0.1% TritonX-100 (PBS/2% BSA/0.3% Triton X-100 was used for DE-cadherin staining). Antibodies used were mouse monoclonals antiphosphotyrosine (Upstate Biotechnology; 1:1,000), anti-Arm N27A1 (DSHB, 1:200), anti-Ena (1:500; Bashaw et al., 2000), BP102 (DSHB, 1:200), anti-Crumbs (DSHB; 1:2), anti-Coracle (9C and 16B, R. Fehon; 1:500 each), and anti-Neurotactin (DSHB; 1:5); rabbit polyclonals anti-Arm N2 (1:200) and anti-Ena (1:500) (Gertler et al., 1995); and rat monoclonals anti–α-catenin (1:250) (Oda et al., 1993) and anti–DE-cadherin (1:250) (Oda et al., 1994). Actin was visualized using Alexa 488 phalloidin (Molecular Probes). For DNA visualization, embryos were treated with 300 μg/ml RNase for 30 min at room temperature and stained for 20 min with 10 μg/ml propidium iodide. A ZEISS 410 laser scanning confocal microscope was used. For biochemical experiments, embryos were placed in halocarbon oil to allow staging under the dissecting microscope, picked at the cellular blastoderm stage, and aged defined periods of time. Extract preparation and cell fractionation were as in Peifer et al. (1993). Samples were analyzed by 6% SDS-PAGE, transferred to nitrocellulose and immunoblotted with mouse anti-Arm N27A1 (1:500), anti-Bicaudal D (B. Suter, McGill University, Montreal, Canada; 1:500), anti-pnut at (DSHB;1:30), antiactin (Chemicon; 1:250), rat anti–DE-cadherin1 (1:100), anti–α-catenin, anticoracle (both 1:500), and anticrumbs (1:50).

Time lapse microscopy

Wild-type embryos imaged were homozygous for Moesin-GFP (Kiehart et al., 2000), whereas *abl* mutant embryos imaged were derived from abl^4 germ line clone females crossed to abl^4, *FRT 79D-F*, moesin-GFP/*TM3* males; thus, the only GFP fluorescent embryos in this collection are those that are *abl* maternal/zygotic mutants. Embryos were bleach dechorionated and mounted in halocarbon oil (series 700; Halocarbon Products Corporation) between a coverslip and a gas permeable membrane (Petriperm; Sartorius Corporation). Images were captured every 30 s using a PerkinElmer Wallac Ultraview Confocal Imaging System, and image analysis was performed using NIH Image 1.62.

Online supplemental material

Time-lapse videos are available to supplement Fig. 5. Images were captured every 25 s and the videos are played at a rate of 10 frames/s. Videos are available at http://www.jcb.org/cgi/content/full/jcb.200105102/DC1.

We are grateful to E. Crafton and Z. Ozsoy for help with genetic interaction assays; to M. Hoffmann, G. Bashaw, R. Fehon, F. Fogerty, D. Kiehart, R. Saint, T. Uemura, U. Tepass, N. Brown, B. Suter, S. Crews, the Bloomington *Drosophila* Stock Center, and the Developmental Studies Hybridoma Bank for stocks or antibodies; to S. Whitfield for assistance with the figures; and to B. Duronio, B. McCartney, and the reviewers for helpful comments.

This work was supported by National Institutes of Health (NIH) grant R01 GM47857 to M. Peifer. E.E. Grevengoed was supported by NIH 5T32GM07092 and 1T32CA72319. T.L. Jesse was supported by NIH 5T3CA09156 and 1F32GM20797. M. Peifer was supported in part by the U.S. Army Breast Cancer Research Program.

Submitted: 22 May 2001
Revised: 5 November 2001
Accepted: 6 November 2001

References

Bashaw, G.J., T. Kidd, D. Murray, T. Pawson, and C.S. Goodman. 2000. Repulsive axon guidance: Abelson and Enabled play opposing roles downstream of the roundabout receptor. *Cell.* 101:703–715.

Baum, B., and N. Perrimon. 2001. Spatial control of the actin cytoskeleton in *Drosophila* epithelial cells. *Nat. Cell Biol.* 3:883–890.

Bear, J.E., J.J. Loureiro, I. Libova, R. Fassler, J. Wehland, and F.B. Gertler. 2000. Negative regulation of fibroblast motility by Ena/VASP proteins. *Cell.* 101: 717–728.

Bennett, R.L., and F.M. Hoffmann. 1992. Increased levels of the *Drosophila* Abelson tyrosine kinase in nerves and muscles: Subcellular localization and mutant phenotypes imply a role in cell-cell interactions. *Development.* 116:953–966.

Brown, N.H., S.L. Gregory, and M.D. Martin-Bermudo. 2000. Integrins as mediators of morphogenesis in *Drosophila*. *Dev. Biol.* 223:1–16.

Chou, T.B., and N. Perrimon. 1996. The autosomal FLP-DFS technique for generating germline mosaics in *Drosophila* melanogaster. *Genetics.* 144:1673–1679.

Comer, A.R., S.M. Ahern-Djamali, J.-L. Juang, P.D. Jackson, and F.M. Hoffmann. 1998. Phosphorylation of Enabled by the *Drosophila* Abelson tyrosine kinase regulates the in vivo function and protein-protein interactions of Enabled. *Mol. Cell. Biol.* 18:152–160.

Cox, R.T., C. Kirkpatrick, and M. Peifer. 1996. Armadillo is required for adherens junction assembly, cell polarity, and morphogenesis during *Drosophila* embryogenesis. *J. Cell Biol.* 134:133–148.

Daniel, J.M., and A.B. Reynolds. 1997. Tyrosine phosphorylation and cadherin/catenin function. *Bioessays.* 19:883–891.

Gertler, F., R. Bennett, M. Clark, and F. Hoffmann. 1989. *Drosophila* abl tyrosine kinase in embryonic CNS axons: a role in axonogenesis is revealed through dosage-sensitive interactions with disabled. *Cell.* 58:103–113.

Gertler, F., J. Doctor, and F. Hoffman. 1990. Genetic suppression of mutations in the *Drosophila abl* proto-oncogene homolog. *Science.* 248:857–860.

Gertler, F.B., A.R. Comer, J. Juang, S.M. Ahern, M.J. Clark, E.C. Liebl, and F.M.

Hoffmann. 1995. *enabled*, a dosage-sensitive suppressor of mutations in the *Drosophila* Abl tyrosine kinase, encodes an Abl substrate with SH3 domain-binding properties. *Genes Dev.* 9:521–533.

Gertler, F.B., K. Niebuhr, M. Reinhard, J. Wehland, and P. Soriano. 1996. Mena, a relative of VASP and *Drosophila* Enabled, is implicated in the control of microfilament dynamics. *Cell.* 87:227–239.

Henkemeyer, M., F. Gertler, W. Goodman, and F. Hoffmann. 1987. The *Drosophila* Abelson proto-oncogene homolog: identification of mutant alleles that have pleiotropic effects late in development. *Cell.* 51:821–828.

Henkemeyer, M., S. West, F. Gertler, and F. Hoffmann. 1990. A novel tyrosine kinase-independent function of *Drosophila* abl correlates with proper subcellular localization. *Cell.* 63:949–960.

Hirano, S., N. Kimoto, Y. Shimoyama, S. Hirohashi, and M. Takeichi. 1992. Identification of a neural α-catenin as a key regulator of cadherin function and multicellular organization. *Cell.* 70:293–301.

Iwai, Y., T. Usui, S. Hirano, R. Steward, M. Takeichi, and T. Uemura. 1997. Axon patterning requires DN-Cadherin, a novel neuronal adhesion receptor, in the *Drosophila* embryonic CNS. *Neuron.* 19:77–89.

Jacinto, A., W. Wood, T. Balayo, M. Turmaine, A. Martinez-Arias, and P. Martin. 2000. Dynamic actin-based epithelial adhesion and cell matching during *Drosophila* dorsal closure. *Curr. Biol.* 10:1420–1426.

Kiehart, D.P., C.G. Galbraith, K.A. Edwards, W.L. Rickoll, and R.A. Montague. 2000. Multiple forces contribute to cell sheet morphogenesis for dorsal closure in *Drosophila*. *J. Cell Biol.* 149:471–490.

Koleske, A.J., A.M. Gifford, M.L. Scott, M. Nee, R.T. Bronson, K.A. Miczek, and D. Baltimore. 1998. Essential roles for the Abl and Arg tyrosine kinases in neurulation. *Neuron.* 21:1259–1272.

Lanier, L.M., and F.B. Gertler. 2000. From Abl to actin: Abl tyrosine kinase and associated proteins in growth cone motility. *Curr. Opin. Neurobiol.* 10:80–87.

Lewis, J.M., R. Baskaran, S. Taagepera, M.A. Schwartz, and J.Y. Wang. 1996. Integrin regulation of c-Abl tyrosine kinase activity and cytoplasmic-nuclear transport. *Proc. Nat. Acad. Sci. USA.* 93:15174–15179.

Loureiro, J., and M. Peifer. 1998. Roles of Armadillo, a *Drosophila* catenin, during central nervous system development. *Curr. Biol.* 8:622–632.

Mauro, M.J., and B.J. Druker. 2001. Chronic myelogenous leukemia. *Curr. Opin. Oncol.* 13:3–7.

McEwen, D.G., R.T. Cox, and M. Peifer. 2000. The canonical Wg and JNK signaling cascades collaborate to promote both dorsal closure and ventral patterning. *Development.* 127:3607–3617.

Oda, H., T. Uemura, Y. Harada, Y. Iwai, and M. Takeichi. 1994. A *Drosophila* homolog of cadherin associated with Armadillo and essential for embryonic cell-cell adhesion. *Dev. Biol.* 165:716–726.

Oda, H., T. Uemura, K. Shiomi, A. Nagafuchi, S. Tsukita, and M. Takeichi. 1993. Identification of a *Drosophila* homologue of α-catenin and its association with *armadillo* protein. *J. Cell Biol.* 121:1133–1140.

Peifer, M., S. Orsulic, D. Sweeton, and E. Wieschaus. 1993. A role for the *Drosophila* segment polarity gene *armadillo* in cell adhesion and cytoskeletal integrity during oogenesis. *Development.* 118:1191–1207.

Quinlan, M.P., and J.L. Hyatt. 1999. Establishment of the circumferential actin filament network is a prerequisite for localization of the cadherin-catenin complex in epithelial cells. *Cell Growth Differ.* 10:839–854.

Stark, K.A., G.H. Yee, C.E. Roote, E.L. Williams, S. Zusman, and R.O. Hynes. 1997. A novel alpha integrin subunit associates with betaPS and functions in tissue morphogenesis and movement during *Drosophila* development. *Development.* 124:4583–4594.

Tepass, U., E. Gruszynski-DeFeo, T.A. Haag, L. Omatyar, T. Török, and V. Hartenstein. 1996. *shotgun* encodes *Drosophila* E-cadherin and is preferentially required during cell rearrangement in the neurectoderm and other morphogenetically active epithelia. *Genes Dev.* 10:672–685.

Tepass, U., K. Truong, D. Godt, M. Ikura, and M. Peifer. 2000. Cadherins in embryonic and neural morphogenesis. *Nat. Rev. Mol. Cell. Biol.* 1:91–100.

Uemura, T., H. Oda, R. Kraut, S. Hayashi, Y. Kotaoka, and M. Takeichi. 1996. Zygotic *Drosophila* E-cadherin expression is required for processes of dynamic epithelial cell rearrangement in the *Drosophila* embryo. *Genes Dev.* 10:659–671.

Van Etten, R.A. 1999. Cycling, stressed-out and nervous: cellular functions of c-Abl. *Trends Cell Biol.* 9:179–186.

van Etten, R.A., P.K. Jackson, D. Baltimore, M.C. Sanders, P.T. Matsudeira, and P. Janmey. 1994. The COOH terminus of the c-Abl tyrosine kinase contains distinct F- and G-actin binding domains with bundling activity. *J. Cell Biol.* 124:325–340.

Vasioukhin, V., C. Bauer, M. Yin, and E. Fuchs. 2000. Directed actin polymerization is the driving force for epithelial cell-cell adhesion. *Cell.* 100:209–219.

Wieschaus, E., and C. Nüsslein-Volhard. 1986. Looking at embryos. *In Drosophila*, A Practical Approach. D.B. Roberts, editor. IRL Press, Oxford, England. 199–228.

Wills, Z., J. Bateman, C.A. Korey, A. Comer, and D. Van Vactor. 1999a. The tyrosine kinase Abl and its substrate enabled collaborate with the receptor phosphatase Dlar to control motor axon guidance. *Neuron.* 22:301–312.

Wills, Z., L. Marr, K. Zinn, C.S. Goodman, and D. Van Vactor. 1999b. Profilin and the Abl tyrosine kinase are required for motor axon outgrowth in the *Drosophila* embryo. *Neuron.* 22:291–299.

Young, P.E., A.M. Richman, A.S. Ketchum, and D.P. Kiehart. 1993. Morphogenesis in *Drosophila* requires nonmuscle myosin heavy chain function. *Genes Dev.* 7:29–41.

Zou, X., and K. Calame. 1999. Signaling pathways activated by oncogenic forms of Abl tyrosine kinase. *J. Biol. Chem.* 274:18141–18144.

Developmental Biology 250, 91–100 (2002)
doi:10.1006/dbio.2002.0776

Drosophila APC2 and APC1 Play Overlapping Roles in Wingless Signaling in the Embryo and Imaginal Discs

Kathryn Akong,* Elizabeth E. Grevengoed,* Meredith H. Price,† Brooke M. McCartney,†‡ Melissa A. Hayden,* Jan C. DeNofrio,* and Mark Peifer*,†,‡,[1]

**Curriculum in Genetics and Molecular Biology, †Department of Biology, and ‡Lineberger Comprehensive Cancer Center, University of North Carolina, Chapel Hill, North Carolina 27599-3280*

The regulation of signal transduction plays a key role in cell fate choices, and its disregulation contributes to oncogenesis. This duality is exemplified by the tumor suppressor APC. Originally identified for its role in colon tumors, APC family members were subsequently shown to negatively regulate Wnt signaling in both development and disease. The analysis of the normal roles of APC proteins is complicated by the presence of two APC family members in flies and mice. Previous work demonstrated that, in some tissues, single mutations in each gene have no effect, raising the question of whether there is functional overlap between the two APCs or whether APC-independent mechanisms of Wnt regulation exist. We addressed this by eliminating the function of both *Drosophila* APC genes simultaneously. We find that APC1 and APC2 play overlapping roles in regulating Wingless signaling in the embryonic epidermis and the imaginal discs. Surprisingly, APC1 function in embryos occurs at levels of expression nearly too low to detect. Further, the overlapping functions exist despite striking differences in the intracellular localization of the two APC family members.

Key Words: **APC; β-catenin; Armadillo; Wnt; Wingless; *Drosophila*; tumor suppressor.**

INTRODUCTION

Signal transduction plays a key role in setting cell fates in embryogenesis. When inappropriately activated by mutation, however, signal transduction pathways often help trigger oncogenesis. The Wnt pathway provides an excellent example of this. Wnt signaling regulates diverse developmental decisions in all animals studied, and inappropriate activation of Wnt signaling leads to colon and other cancers. The most common mechanism by which Wnt signaling is activated in tumors is by loss-of-function mutations in the tumor suppressor APC (reviewed in Polakis, 2000).

Transduction of Wnt signals occurs via regulation of the levels of cytoplasmic Arm/βcat (the pool not assembled into cell–cell adhesive junctions; reviewed in Polakis, 2000). In the absence of signal, cytoplasmic Arm/βcat is rapidly targeted for destruction in a two-step process. Arm/βcat is first captured by a multiprotein complex that includes APC and a second scaffolding protein Axin. This complex targets Arm/βcat for phosphorylation by Zeste-white3 (Zw3)/glycogen synthase kinase-3 (GSK3). Phosphorylated Arm/βcat is a substrate for a ubiquitin ligase, targeting it for proteasomal destruction. Wnt signaling turns off the APC/Axin/GSK3 complex by an unknown mechanism. This triggers the accumulation of Arm/βcat, which enters the nucleus and works with DNA-binding proteins of the TCF/LEF family to activate Wnt target genes. These data helped explain APC's tumor suppressor role. In the colon, the absence of functional APC allows βcat levels to rise, activating Wnt target genes such as *cyclinD1* and *c-myc*, promoting cell proliferation. This model fits the data well, though questions remain. For example, since APC is expressed in most tissues, why is the colon the primary tissue in which tumors arise in *APC* heterozygous people or mice?

APC's role in tumors led to the hypothesis that it is a key

[1] To whom correspondence should be addressed. Fax: (919) 962-1625. E-mail: peifer@unc.edu.

0012-1606/02 $35.00

negative regulator of Wnt signaling in other contexts (APC family proteins also play Wnt-independent cytoskeletal roles; see accompanying paper for details). Supporting a key role in Wnt regulation, mammalian APC is broadly expressed, and mice homozygous for loss-of-function mutations in *APC* die as early embryos (Fodde *et al.*, 1994; Moser *et al.*, 1995). This hypothesis was further tested in *Drosophila*, where a firm connection to Wnt signaling was established. Loss-of-function mutations in fly *APC1* activate Wnt signaling in the photoreceptors of the eye, triggering their apoptosis (Ahmed *et al.*, 1998). Unlike mammalian APC, however, mutations in fly *APC1* are not lethal, and its protein product is not ubiquitous. In embryos, high level expression is limited to CNS axons and developing germ cells (Hayashi *et al.*, 1997), suggesting that APC1 is absent from many tissues where Wnt signaling is required.

One possible explanation for the limited effect of mutations in fly *APC1* as well as the limited tissue-spectrum of tumors resulting from mutations in mammalian *APC* was functional redundancy with other, as yet undiscovered APC family members. This led several labs to identify second *APC* relatives in both mammals (APC2 or APC-L; (Nakagawa *et al.*, 1998; van Es *et al.*, 1999) and flies (APC2 or E-APC; Hamada *et al.*, 1999; McCartney *et al.*, 1999; Yu *et al.*, 1999). Fly APC2 is broadly expressed in embryonic and postembryonic development, consistent with the redundancy hypothesis (McCartney *et al.*, 1999; Yu *et al.*, 1999). To test this further, mutations in *APC2* were characterized. Animals maternally and zygotically mutant for *APC2* die as embryos with inappropriate stabilization of Arm and activation of Wg signaling in the embryonic epidermis (McCartney *et al.*, 1999), supporting the idea that different APC family members function in different tissues.

However, there are many tissues where neither single mutant has an effect (Ahmed *et al.*, 1998; McCartney *et al.*, 1999). Most striking are the larval imaginal discs, precursors of the adult epidermis, which are affected by neither single mutant. Two hypotheses might explain this. First, APC proteins may not be essential for all Wnt regulation—in cultured cells, Axin overexpression partially compensates for loss of APC (von Kries *et al.*, 2000). Alternatively, in some *Drosophila* tissues, APC1 and APC2 may play redundant roles, and thus mutation in one would not disrupt function. We have tested these hypotheses by creating situations where animals or tissues are double mutant for both *APC* genes. These experiments reveal that APC1 and APC2 play redundant roles in both the embryonic epidermis and the larval imaginal discs, where they cooperate to regulate Wg signaling.

MATERIALS AND METHODS

Genetic and Phenotypic Analysis

Alleles used were: $APC2^{\Delta 5}$ (McCartney *et al.*, 1999), $APC2^{d40}$ (McCartney *et al.*, 2001), and $APC1^{Q8}$ (Ahmed *et al.*, 1998). $APC2^{g10}$ was generated in an EMS mutagenesis screen, identified by failure to complement $APC2^{\Delta 5}$ (unpublished data). Double mutant *APC2 APC1* chromosomes were generated by meiotic recombination. All stocks were kept at 25°C. Embryo collections were done at 27°C. Transgenic lines used for misexpression and overexpression studies were UAS-APC2-GFP (R. Rosin-Arbesfeld and M. Bienz), UAS-APC1 (E. Wieschaus). Transgenes were expressed by crossing to Engrailed-GAL4 at 27°C. Canton S was the wild type. To generate germline clones, larvae of genotype $FRT82B\ ovo^{D}/APC2^{d40}APC^{Q8}$ were γ–irradiated with 1000 rads at 32–48 h after egg-laying (AEL) at 25°C. Females were crossed to $APC2^{d40}\ APC^{Q8}/TM3actinGFPSer$ males at 27°C. Embryos produced from this cross were either maternally and zygotically mutant, or paternally rescued; these were distinguished by the presence of GFP. To generate imaginal disc clones, larvae of the genotype $FRT82B\ myc\ Sb^{63}/APC2^{d40}\ APC^{Q8}$ were γ–irradiated with 1100 rads at 24–36 h AEL at 25°C. Clones in the discs of wandering third instar larvae were identified by the absence of APC2 and myc. Adult wings with clones were mounted on slides in Faure's solution.

Immunolocalization

Imaginal discs were fixed in 4% paraformaldehyde for 20 min. Embryos were fixed in 1:1 3.7% formaldehyde in PBS:heptane for 20 min. All were blocked in 1% normal goat serum/0.1% Triton X-100 in PBS for at least 2 h. Primary antibodies were as follows: rat polyclonal anti-APC2 (1:1000), mouse monoclonal anti-Arm N27A1 (DSHB, 1:200), and rabbit polyclonal anti-Armadillo N2 (1:200) and anti-APC1 (1:1000).

RESULTS

APC1 and APC2 Play Overlapping Roles in Regulating Wg Signaling during Embryogenesis

Both APC1 and APC2 (McCartney *et al.*, 1999) have phenotypes that suggest that they act as regulators of Wg signaling, but each only affects a subset of the tissues where Wg signaling regulates development. Further, there are certain tissues, such as the imaginal discs, where neither gene has a phenotype. One possible explanation is partial redundancy between the two genes. We first addressed this issue in the embryo. Embryos maternally and zygotically mutant for *APC2* exhibit Arm stabilization and thus activation of Wg signaling in the epidermis (McCartney *et al.*, 1999; Hamada and Bienz, 2002). However, neither their cuticle phenotype nor the level of Arm accumulation are as drastic as those of *zw3* maternal and zygotic mutants (Peifer *et al.*, 1994; Siegfried *et al.*, 1992). Three hypotheses seemed possible: (1) The *APC2* allele tested retained some function, (2) APC1 might provide some function in the absence of APC2, or (3) APC proteins might not be absolutely essential for Arm destruction.

To test the redundancy hypothesis, we generated embryos that were maternally and zygotically $APC2^{d40}\ APC1^{Q8}$, and thus double mutant for both APCs (Figs. 1E and 1F). Wild-type embryos have a segmentally reiterated pattern of anterior denticles (Fig. 1A, arrow) and posterior naked cuticle (Fig. 1A, arrowhead) on their ventral surfaces. Dorsally, cells secrete different hair types at different posi-

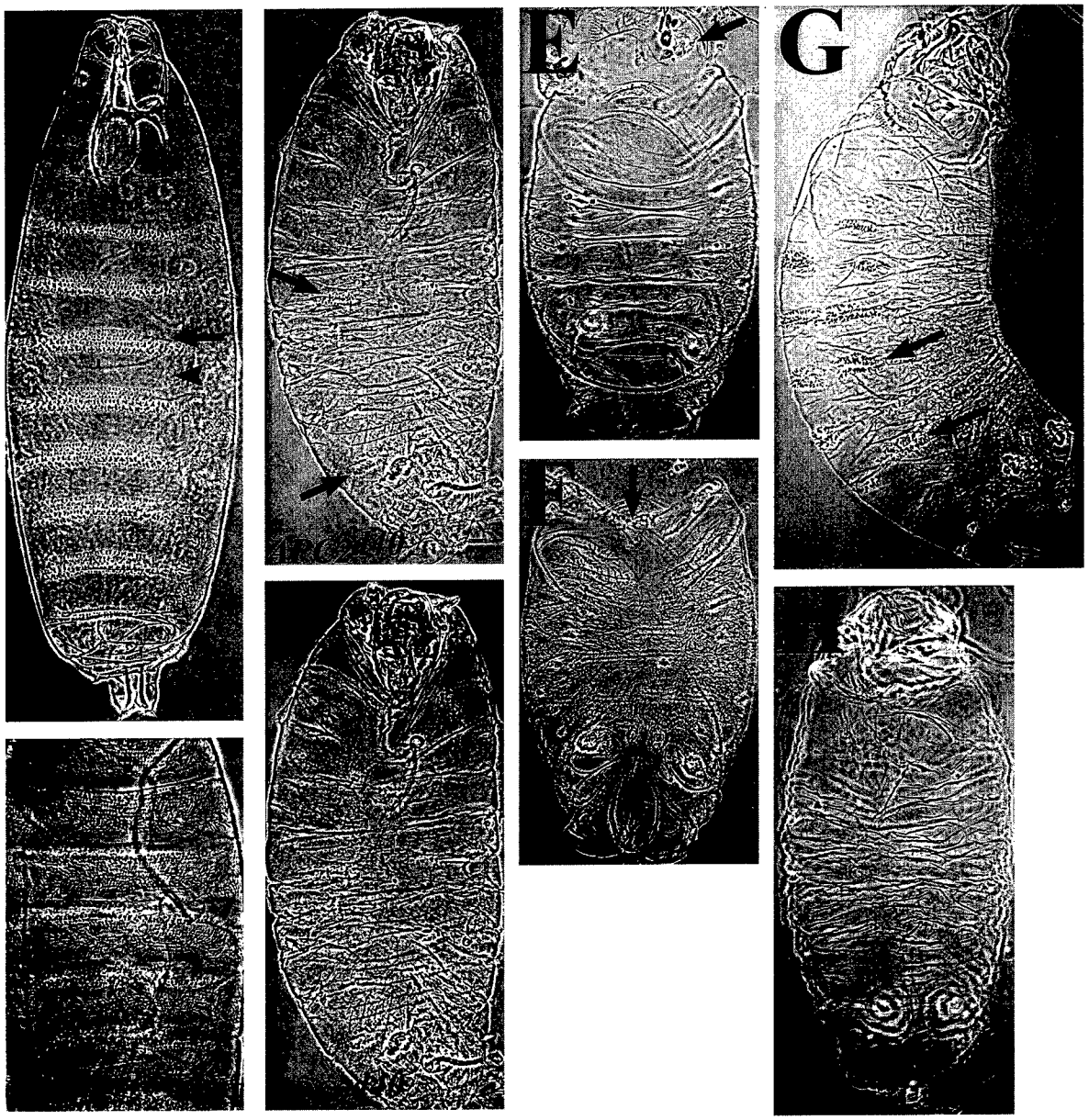

FIG. 1. *APC1* mutations enhance the embryonic phenotype of *APC2*. Cuticle preparations, anterior up. (A, B) Wild-type ventral (A) and dorsal (B) cuticles. Ventrally, note the segmentally reiterated anterior denticle belts (arrow) and posterior naked cuticle (arrowhead). Dorsally, different hair types are secreted at different positions along the anterior–posterior axis. (C, D) $APC2^{d40}$ maternal and zygotic mutant. Ventral (C) and dorsal (D) cuticles. Ventrally, most cells are converted to posterior fates but some cells still secrete denticles (e.g., arrows). (E, F) $APC2^{d40}$ $APC1^{Q8}$maternal and zygotic double mutant. Ventral (E) and dorsal (F) cuticles. Ventrally, all cells secrete naked cuticle, and dorsally, all cells secrete fine hairs characteristic of posterior cells. Head involution is disrupted (E, arrow) and dorsal closure is partially disrupted (F, arrow). (G) $APC2^{\Delta S}$ maternal and zygotic mutant. Ventrally, most cells choose posterior fates but some cells still secrete denticles (arrows). (H) Progeny of $APC2^{\Delta S}$ $APC1^{Q8}/APC2^{\Delta S}$ females and males. All ventral cells secrete naked cuticle.

tions (Fig. 1B). In $APC2^{d40}$ maternal and zygotic single mutants, most cells take on posterior fates and secrete naked cuticle, indicative of excess Wg signaling (Fig. 1C). However, unlike *zw3* maternal and zygotic mutants, some cells still adopt anterior fates and secrete denticles. (e.g., Fig. 1C, arrows), In contrast, $APC2^{d40}$ $APC1^{Q8}$ maternal and zygotic double mutants exhibit a much stronger embryonic cuticle phenotype (Fig. 1E). Maternal and zygotic double mutant cuticles were shorter, and, unlike $APC2^{d40}$ maternal and zygotic single mutants, most embryos completely lack

denticles. Further, maternal and zygotic double mutants exhibit a complete failure of head involution (Fig. 1E, arrow). Dorsally, all cells are transformed to the fate normally adopted by posterior cells, and thus all secrete fine dorsal hairs (Fig. 1F), and maternal and zygotic double mutants exhibit slight abnormalities in dorsal closure not seen in the single mutant (Fig. 1F, arrow). Thus, the cuticle phenotype of the maternal and zygotic double mutant is much more similar to that of embryos maternally and zygotically mutant for *zw3* (Siegfried *et al.*, 1992), suggesting that APC1 partially compensates for loss of APC2 in the embryonic epidermis. Interestingly, embryos receiving paternal wild-type copies of *APC2* and *APC1* are rescued to viability.

We also looked at zygotic *APC2 APC1* double mutants, combining $APC1^{Q8}$ with $APC2^{d40}$, $APC2^{\Delta S}$, and $APC2^{s10}$. All of these zygotic double mutant combinations were embryonic viable and exhibited a wild-type cuticle pattern (data not shown). This suggests that maternally contributed APC1 and APC2 are sufficient for embryonic Wg signaling; this is similar to what we previously observed for *APC2* zygotic single mutants (McCartney *et al.*, 1999). Zygotic *APC2 APC1* double mutants die later as larvae, with defects in brain development (see accompanying paper).

APC1 and APC2 Both Regulate Arm Levels in Embryos

To further test the functional overlap between APC1 and APC2, we examined Arm accumulation in maternal and zygotic double mutants. In wild-type embryos, Arm accumulates at adherens junctions of all cells, but in cells that do not receive Wg signal, Arm levels in the cytoplasm and nucleus are low (Fig. 2I, arrowheads). Wg signal stabilizes cytoplasmic and nuclear Arm (Fig. 2I, arrows). In $APC2^{d40}$ maternal and zygotic single mutants, Arm levels are elevated (Fig. 2D), but do not become uniformly high as is observed in *zw3* maternal and zygotic mutants (Fig. 2G; Peifer *et al.*, 1994); in this, $APC2^{d40}$ resembles $APC2^{\Delta S}$ (McCartney *et al.*, 1999). In contrast, in $APC2^{d40}$ $APC1^{Q8}$ maternal and zygotic double mutants, Arm levels become extremely elevated (Figs. 2B and 2E), thus more precisely matching *zw3* maternal and zygotic mutants.

We next looked more closely at subcellular localization. In $APC2^{d40}$ maternal and zygotic single mutants, the levels of Arm are elevated but one can see further Arm stabilization by Wg signaling (Fig. 2L, arrows). In maternal and zygotic double mutants (when we turned down the brightness to compensate for increased Arm levels), we observed that Arm is highly elevated in both the cytoplasm and nuclei (Fig. 2K), with no differences seen between cells that receive Wg signal and those that do not. Further, in $APC2^{d40}$ $APC1^{Q8}$ maternal and zygotic double mutants, Arm becomes somewhat enriched in nuclei relative to the cytoplasm; this is most evident in cells of the amnioserosa (Figs. 2H and 2K, arrowheads). In this regard, $APC2^{d40}$ $APC1^{Q8}$ maternal and zygotic double mutants are more similar to *Axin* maternal and zygotic mutants (Tolwinski and Wieschaus, 2001) than to *zw3* maternal and zygotic mutants, in which levels of Arm in the cytoplasm and nuclei are equal (Peifer *et al.*, 1994). Tolwinski and Wieschaus (2001) previously suggested that Axin acts as a cytoplasmic anchor for Arm, and that this plays an important role in regulating Wg signaling. Our data suggest that APC proteins may act with Axin to form this cytoplasmic anchor. We also noted that in $APC2^{d40}$ $APC1^{Q8}$ maternally double mutant but zygotically rescued siblings, cells that do not receive Wg signal (Fig. 2J, arrowheads) have slightly elevated Arm levels relative to wild type. This may result from Arm stabilization before the onset of zygotic gene expression, as we previously observed in *zw3* (Peifer *et al.*, 1994).

APC1 Is Expressed at Very Low Levels in the Epidermis during Embryogenesis

These data, along with the lack of an embryonic phenotype of the *APC1* single mutant (Ahmed *et al.*, 1998), suggest that, while APC2 plays an essential role in the embryonic epidermis, APC1 plays an accessory role, ameliorating the *APC2* mutant phenotype. APC2 is uniformly expressed by all cells in the embryonic epidermis, accumulating at the apicolateral cell cortex (McCartney *et al.*, 1999; Figs. 3A and 3B). Previous analysis of APC1 suggested that in the embryo it accumulates to high levels only in the axons and the developing germline (Hayashi *et al.*, 1997), although uniformly expressed maternal mRNA is present. We thus reexamined APC1 expression in the epidermis, using the zygotic double mutant $APC2^{d40}$ $APC1^{Q8}$ as a negative control. While we could easily detect APC1 accumulation in CNS axons (see accompanying paper) and the germline (data not shown), the level of accumulation in the epidermis was relatively low, and it appeared diffusely cytoplasmic. At early stages of embryogenesis, the epidermal staining we observed in wild type and $APC2^{d40}$ $APC1^{Q8}$ was very similar, perhaps reflecting maternally contributed APC1, while in late embryos we could detect expression above background in the wild-type versus the mutant epidermis (Figs. 3C and 3D). Thus, a very low level of APC1 seems to be able to provide some residual function in Arm destruction.

This activity of APC1, despite its low level of expression, prompted us to examine whether there might be dose-sensitive interactions between the two *APC* genes. We thus reduced the dose of *APC1* in embryos mutant for *APC2*, by crossing males and females of the genotype $APC2^{\Delta S}$ $APC1^{Q8}/APC2^{\Delta S}$ $APC1^{+}$. The progeny of this cross (Fig. 1H) had a more severe cuticle phenotype than the progeny mutant only for $APC2^{\Delta S}$ (Fig. 1G). We saw similar dose-sensitive interactions using the $APC2^{d40}$ $APC1^{Q8}/APC2^{d40}$ genotype (data not shown).

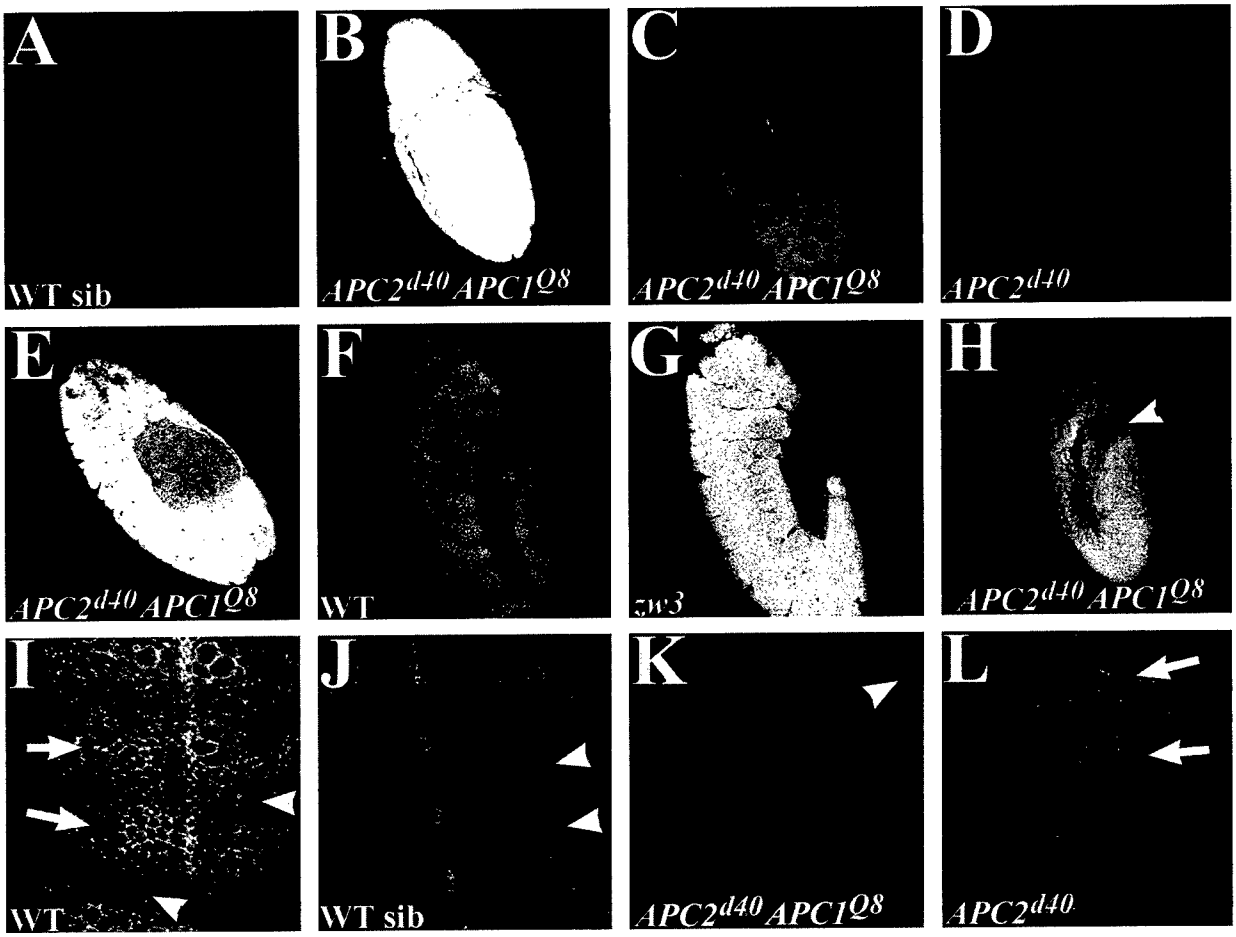

FIG. 2. In *APC2 APC*1 maternal and zygotic double mutant embryos, Arm levels are highly elevated. Embryos stained to reveal Arm. Anterior is up. (A–D) Stage 9. (A, B) Both are progeny of a mother whose germline was $APC2^{d40}$ $APC1^{Q8}$ double mutant. They were prepared for immunofluorescence and imaged together. (A) Zygotically rescued sibling. Stripes of cells in which Wg has stabilized Arm are clearly visible. (B) $APC2^{d40}$ $APC1^{Q8}$ maternal and zygotic double mutant. Arm levels are highly elevated. (C) Same as (B) with brightness reduced to allow visualization of subcellular localization. (D) $APC2^{d40}$ maternal and zygotic single mutant. Levels of Arm are somewhat elevated in all cells. (E) Stage 14 $APC2^{d40}$ $APC1^{Q8}$maternal and zygotic double mutant. (F) Stage 11 wild-type. (G) Stage 11 *zw3* maternal and zygotic mutant. (H) Lateral view of stage 9 $APC2^{d40}$ $APC1^{Q8}$ maternal and zygotic double mutant. Arrowhead, nuclear enrichment in amnioserosa. (I–L) Close-ups, stage 9. Brightness in (K) was reduced to allow visualization of subcellular localization. (I) Wild-type. Arrowheads, cells not receiving Wg– Arm is only in adherens junctions. Arrows, cells that received Wg, have stabilized cytoplasmic and nuclear Arm. (J) $APC2^{d40}$ $APC1^{Q8}$ maternal mutant that was zygotically rescued. Cells that have not received Wg signal accumulate slightly elevated levels of Arm (arrowheads). (K) $APC2^{d40}$ $APC1^{Q8}$maternal and zygotic double mutant. All cells accumulate high levels of Arm; some nuclear enrichment is observed (e.g., arrowhead). (L) $APC2^{d40}$ maternal and zygotic single mutant. While Arm levels are somewhat elevated in all cells, Wg signal still can further stabilize Arm (arrows).

APC1 and APC2 Accumulate at Very Different Intracellular Locations When Mis-Expressed in the Embryonic Epidermis

Endogenous APC2 localizes to the cell cortex in most cells throughout development, including those of the embryonic epidermis during the establishment of segment polarity (McCartney *et al.*, 1999). We thus have suggested that the cell cortex is the likely location of the destruction complex, and that the function of APC2 might be to recruit the destruction complex to this site. In support of this, the mutant proteins encoded by $APC2^{d40}$and $APC2^{\Delta S}$, that lack function in Wg regulation, no longer localize to the cortex (McCartney *et al.*, 1999, 2001).

As the data above suggest that APC1 can contribute to destruction complex function, we suspected that it should localize similarly to APC2. As the endogenous level of expression of APC1 was too low to reliably assess intracellular localization, we mis-expressed both APC1 and APC2-GFP in stripes in the embryonic neurectoderm using en-

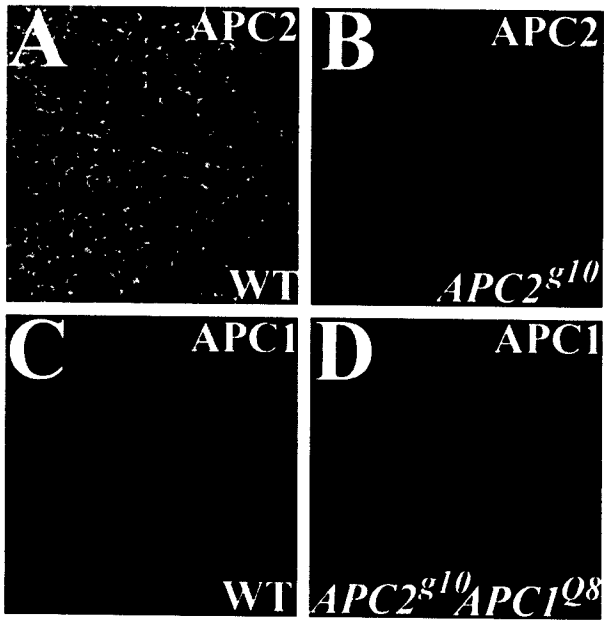

FIG. 3. APC1 and APC2 localization in embryos. (A, B) APC2 expression in the embryonic epidermis of stage 11 wild-type (A) and $APC2^{g10}$ maternal and zygotic mutant (B; negative control) embryos. APC2 is enriched at the apicolateral cell cortex. (C, D) APC1 expression in the epidermis of stage 15 wild-type (C) and $APC2^{g10}APC1^{Q8}$ zygotic double mutant (D; negative control) embryos. APC1 accumulates at low levels diffusely in the cytoplasm.

grailed (en)-GAL4. Expression levels exceeded those of endogenous APC2, as revealed by staining embryos expressing APC2-GFP with anti-APC2, which recognizes both endogenous and exogenous protein. Levels of staining were much higher in the segmental stripes where en-GAL4 is expressed (Fig. 4A). When overexpressed, APC2 localized to the cell cortex (Figs. 4A–4C), resembling endogenous APC2. In contrast, overexpressed APC1 was diffusely cytoplasmic, with strong enrichment at what appear to be centrosomes and associated microtubules of both epidermal cells (Figs. 4D–4G and 4I) and neuroblasts (Figs. 4J and 4K). We saw similar differences in localization of the two proteins in the larval brain (see accompanying paper). These data raise questions about the normal localization of the destruction complex, as the primary location of APC1 upon overexpression is different from that of APC2. We also made one additional observation that may be relevant to this discussion. When we overexpressed APC1 in the embryonic epidermis, we found that endogenous APC2 now became less cortical and more diffusely cytoplasmic (Figs. 4G and 4H, white bracket vs red bracket). We also observed recruitment of endogenous APC2 to centrosomes (Figs. 4G–4L, white arrowheads) in epidermal cells and neuroblasts overexpressing APC1. This suggests that the two APCs may each be able to recruit the other to new locations; this is further supported by similar observations after mis-expression in the larval brain (see accompanying paper).

APC1 and APC2 Play Redundant Roles during Imaginal Disc Development

The overlapping functions of APC1 and APC2 in the embryo raised the possibility that redundancy might help explain why neither *APC1* (Ahmed *et al.*, 1998) nor *APC2* (McCartney *et al.*, 1999) single mutants have defects in patterning of the imaginal discs, precursors of the adult epidermis. To test this, we induced mitotic recombination to produce clones of double mutant cells in animals heterozygous for a wild-type and a double mutant chromosome. In animals in which we induced clones, we found alterations of imaginal disc patterning consistent with activation of Wg signaling (Fig. 5). In the wing, one function of Wg is to specify the wing margin. Activation of Wg signaling by removing *zw3* function was previously observed to transform cells from a wing blade to a wing margin fate, leading to patches of margin bristles in the blade (Blair, 1992). We observed similar patches of bristles in the wing blades of animals in which $APC2^{d40}$ $APC1^{Q8}$ double mutant clones were induced (Figs. 5B, 5C, 5E, and 5F); they varied in size from tens to hundreds of cells. We also saw regions of the notum where too many cells adopted bristle fates (Fig. 5H, arrow); this was also previously observed in clones mutant for *zw3* (Simpson and Cateret, 1989).

These data suggest that loss of both APC family members activates Wg signaling in imaginal discs, presumably via Arm stabilization. To test this hypothesis, we examined the effect of clonal loss of both *APC* genes on Arm levels. We generated clones of cells that were homozygous $APC2^{d40}$ $APC1^{Q8}$ double mutant in an $APC2^{d40}$ $APC1^{Q8}$/+ heterozygous background. In doing so, one generates adjacent "twin spots"—clones of homozygous wild-type cells. We detected mutant clones by the absence of APC2 staining; both mutant clones (Fig. 5J, arrows) and their homozygous wild-type twin spots (with elevated APC2; Fig. 5J, arrowheads) could be easily distinguished from their heterozygous neighbors. In $APC2^{d40}$ $APC1^{Q8}$ double mutant clones, we saw elevated Arm accumulation. Thus, loss-of-function of both APC family members is sufficient to deregulate Arm accumulation in the imaginal discs.

DISCUSSION

APC is a tumor suppressor that negatively regulates Wnt signaling, functioning in a multiprotein complex that targets the Wnt effector Arm/β-cat for proteolytic destruction (reviewed in Polakis, 2000). This model of APC function was strongly supported by genetic analysis of the roles of APC proteins during *Drosophila* development (Ahmed *et al.*, 1998; McCartney *et al.*, 1999). However, this relatively simple picture recently became more complex. There are two APC family members in both flies and mammals, with both conserved and divergent structural elements, raising questions about their overlapping or divergent functions in both cell biological and biological events.

A Complex Functional Relationship between APC1 and APC2

Our data reveal a complex pattern of overlapping functions between APC1 and APC2. When we began, we knew that, in certain tissues, individual APCs play critical roles: APC1 is essential in photoreceptors (Ahmed *et al.*, 1998), while APC2 plays critical roles in syncytial embryos and the embryonic epidermis (McCartney *et al.*, 1999, 2001). This functional partition is paralleled by distinct embryonic expression patterns, with APC1 on at high levels in axons (Hayashi *et al.*, 1997) and APC2 on at high levels in the ectoderm (McCartney *et al.*, 1999). In other tissues, such as imaginal discs, neither APC family member is essential, even though both Wg signaling and regulation of Arm stability are critical there. This raised the question of whether the two proteins are redundant in these tissues or whether APC-independent means of regulating Arm stability exist.

Our data suggest a complex picture in which some tissues depend exclusively on one APC family member (photoreceptors), others depend primarily on one family member (the embryonic ectoderm), while in some, either family member provides sufficient function (the larval brain or imaginal discs). The embryonic ectoderm provides a striking example of this complexity. APC2 plays an important role there, with the Wg pathway activated in *APC2* mutants (McCartney *et al.*, 1999). However, certain aspects of the *APC2* phenotype were puzzling; embryos null for another destruction complex component, *zw3*, have a more severe phenotype and more highly elevated Arm levels (Peifer *et al.*, 1994), suggesting that residual destruction complex activity remains in APC2's absence.

We considered several explanations for this. First, the *APC2* allele we used is not a protein null allele. Second, residual destruction complex function might remain in the absence of all APC family members. However, our data support a third possibility: in the absence of APC2, APC1 provides function in the embryonic epidermis that is not sufficient for wild-type pattern, but does allow residual activity of the destruction complex. This is somewhat surprising in view of the expression pattern of APC1 in embryos, which was initially thought to be restricted to axons and primordial germ cells. However, the uniform maternal mRNA (Hayashi *et al.*, 1997) and low levels of APC1 protein (Fig. 3) appear to provide a low level of APC1 function in epidermal cells. While this paper was under review, a similar study of the redundancy of the two fly APC proteins was published (Ahmed *et al.*, 2002). These authors also document redundancy between the *APC1* and *APC2* in both the embryo and the imaginal discs. They further demonstrate that raising the level of expression of *APC1* can rescue the embryonic defects of *APC2*, and that elevated expression of *APC2* can rescue the eye phenotype of *APC1* mutants. These data further underscore the functional overlap between the two proteins.

Together, these two studies raise questions about the possible overlap in function of the mammalian APC proteins in development and oncogenesis and also raise interesting questions about the evolution of small multigene families. The two APC proteins in flies and in mammals appear to have been derived from independent gene duplication events in each lineage. After duplication, the two genes diverged in their patterns of expression and their domain structures (APC2 appears to have lost certain domains, such as the putative microtubule-binding domain). It thus remains to be determined whether there is selective pressure to retain low levels of APC1 in the embryonic ectoderm, or whether residual expression is simply a relict of a time when flies may have had only a single APC. APC family proteins also have Wnt-independent cytoskeletal roles, and may have overlapping roles in these as well; the accompanying paper describes an apparent example of this during brain development.

Overlapping Functions and Divergent Localization

The functional overlap of the two APC family members is even more striking given their distinct structures and intracellular localizations. All APC family proteins share a core structure: a block of highly conserved Arm repeats, which in APC2 is essential for cortical localization and function in the destruction complex, and a set of short repeated sequences that bind Arm/β-cat or Axin, the number and arrangement of which are variable. APC2 contains only this core, which is thus sufficient for both regulating Arm levels as well as for APC2's Wnt-independent role in spindle anchoring. APC1 is longer at its N and C termini, and shares with mammalian APC (at least by sequence similarity) a domain known to bind microtubules. These structural differences confer strikingly different cell biological properties upon the two fly APCs. When overexpressed, APC2 localized almost exclusively to the cell cortex, resembling its endogenous localization. In contrast, overexpressed APC1 localized to the region of the centrosome and to cytoplasmic microtubules, a localization potentially mediated by its putative microtubule-binding domain.

This striking difference in localization raises several interesting issues. We suspect that the localization of APC proteins depends on the availability of and the affinity for different binding partners, as we previously observed for Arm. We hypothesize that the core APC domains are sufficient for cortical localization, but that the additional domain(s) in APC1 redirect it to microtubules. We further hypothesize that if APC1 were detached from microtubules, it would exhibit a default localization to the cortex. This hypothesis is supported by Bienz and colleagues, who showed that one could shift mammalian APC from association with microtubules to actin by disrupting microtubules (Rosin-Arbesfeld *et al.*, 2001).

These data also have implications for the destruction complex. Two mutations that disrupt the localization of APC2 to the cell cortex also disrupt its function in Arm

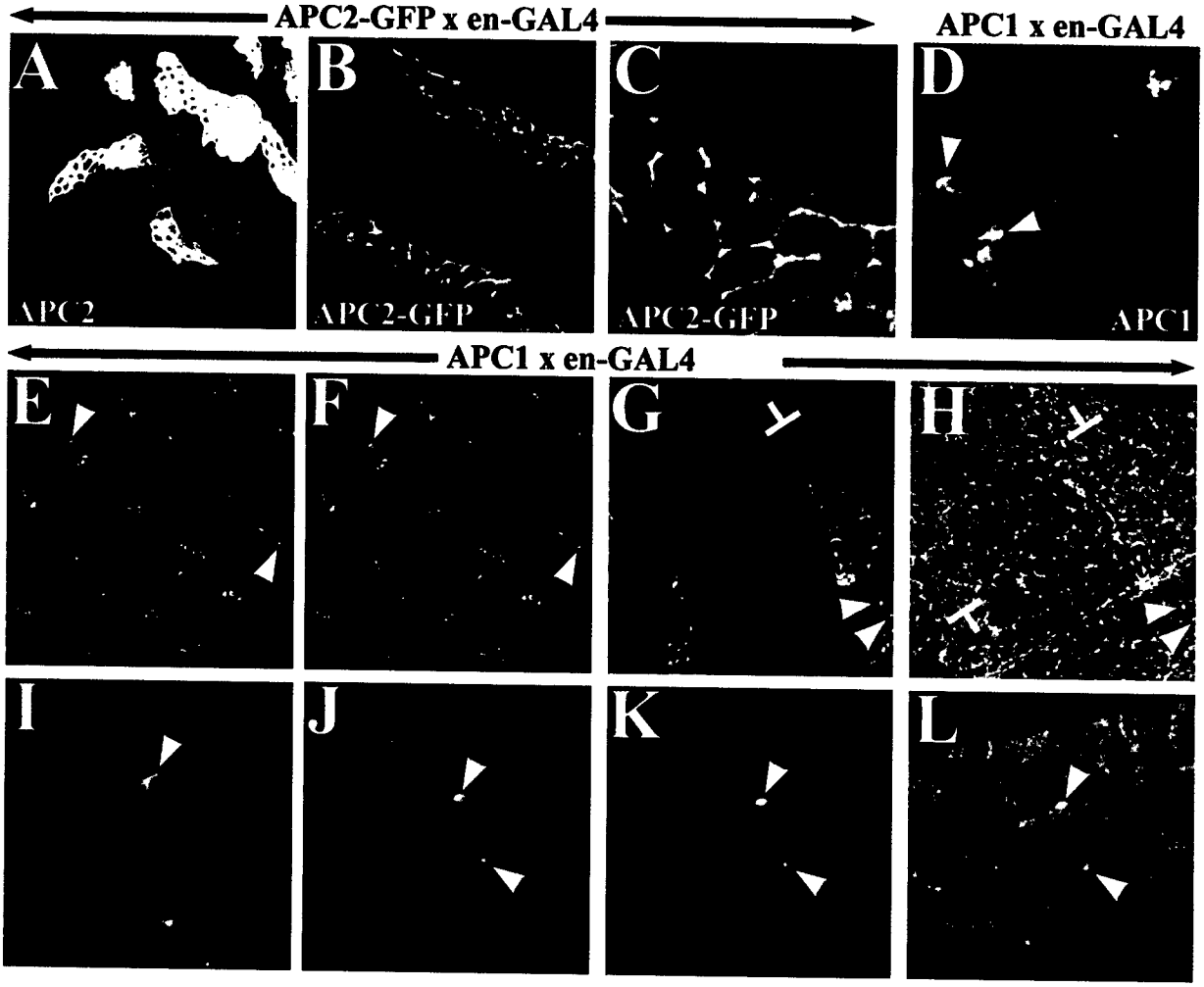

FIG. 4. APC1 and APC2 localize differently when overexpressed in embryos. (A–H) Surface views of extended germ-band embryos. (I–L) Optical cross-sections. (A–C) Embryos expressing APC2-GFP under the control of *en*-GAL4. (A) Anti-APC2 antibody. (B, C) GFP visualized directly. (A) *en*-GAL4-driven APC2-GFP accumulates in segmental stripes, at levels much higher than that of endogenous APC2. (B, C) APC2-GFP localizes to the cell cortex, similar to endogenous APC2. (D–L) Embryos expressing APC1 under the control of *en*-GAL4. (D) Close-up. APC1 localizes to centrosomes and associated microtubules (arrowheads). (E–L) Double-labeled embryos: APC1 (E, G, I, J green, F, K), endogenous APC2 (E, G, I, J purple, H, L). Overexpressed APC1 does not accumulate at the cortex—instead, it accumulates diffusely in the cytoplasm with stronger localization to structures that appear to be centrosomes and microtubules (white arrowheads). (E, F) Green arrowhead, cell with separated centrosomes. (G, H) Green arrowhead, cell in the late stages of mitosis. Endogenous APC2 is normally cortical (G, H, red bracket). In cells expressing APC1, endogenous APC2 becomes diffusely cytoplasmic (G, H, white bracket) and is recruited to presumptive centrosomes with APC1 (white arrowheads). (I) Ectodermal cell, cross-section. APC1 and APC2 colocalize to the apical centrosome and the microtubules radiating from it (white arrowhead). (J–L) Mitotic neuroblast, cross-section. APC1 and APC2 accumulate at the separated centrosomes (white arrowheads).

regulation (McCartney *et al.*, 1999, 2001), suggesting that cortical localization of the destruction complex is important for function. However, the distinctive localization of APC1 raises questions about this conclusion. The simplest interpretation of our data are that APC1 and APC2 localize the destruction complex to distinct places, but that the complex functions at either location. There are several caveats to this interpretation, not least of which is that the predominant localization of APC1 upon overexpression may mask a small amount localized to the cortex; our genetic experiments suggest that nearly undetectable levels of APC1 can confer Arm regulatory activity. It is also possible that both APC2 and APC1 bind to similar partners but with different affinities. Thus, in the absence of APC2 (in *APC2* mutants or in tissues where it is not normally expressed), APC1 may localize to places where APC2 is normally found.

Finally, our data suggest that APC1 and APC2 may

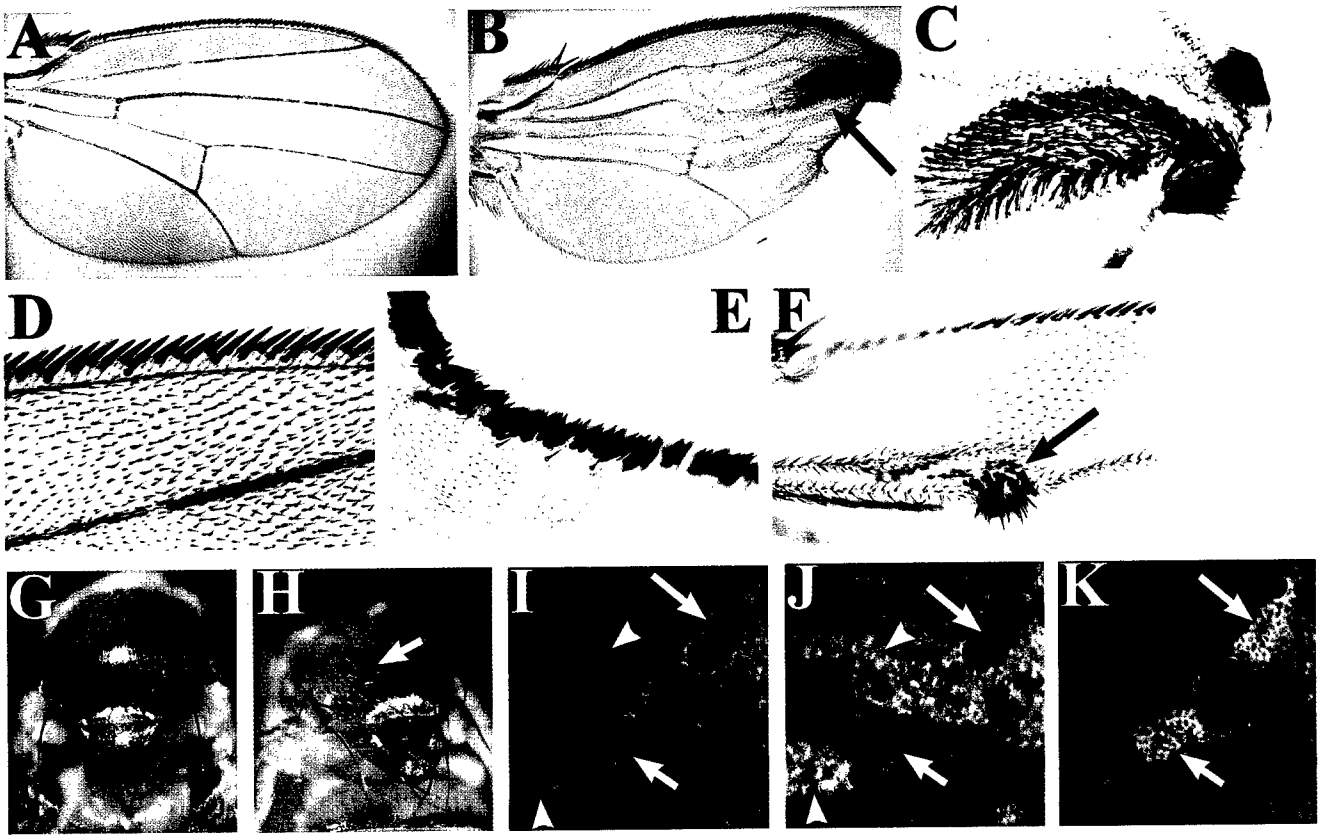

FIG. 5. *APC1* and *APC2* play redundant roles in imaginal disc development. (A–F) Wings from wild-type adults (A, D), or adults in which we induced clones of cells double mutant for $APC2^{d40}$ $APC1^{Q8}$ (B, E, F; C, close up of region in B indicated by arrow). Variable size patches of ectopic wing margin bristles occur in wing blades of animals in which clones were induced (arrows). (D) Wild-type wing margin. (E) Excess cells adopting the wing margin bristle fate. (G, H) Notums. Wild-type (G) and adult in which we induced clones of cells double mutant for $APC2^{d40}$ $APC1^{Q8}$ (H). Note ectopic notal bristles (arrow). (I–K) Wing imaginal disc with clones of cells double mutant for $APC2^{d40}$ $APC1^{Q8}$. Double labeled: APC2 (I purple, J), Arm (I green, K). Double-mutant cells can be identified by reduced APC2 levels (J, arrow); homozygous wild-type twin spots have increased APC2 (J, arrowheads). Double-mutant cells have elevated Arm levels (K, arrows) relative to heterozygous mutant or wild-type cells; this was most evident when one focused below the apical-most plane.

interact. Overexpression of APC1 triggered relocalization of endogenous APC2 from the cortex to centrosomes and microtubules. When both APCs were overexpressed, APC2 recruited APC1 to the cortex (accompanying paper). The mechanism by which this occurs is not clear. Mammalian APC homodimerizes via an N-terminal coiled-coil (Day and Alber, 2000). A clear match to this region is found in mammalian APC2, raising the possibility that mammalian APC and APC2 heterodimerize. However, there is only a weak, partial similarity to this region in fly APC1, and fly APC2 lacks this region entirely. Other mechanisms of oligimerization may exist, or a linker protein or proteins could mediate this putative interaction.

ACKNOWLEDGMENTS

We thank E. Wieschaus and Y. Ahmed for sharing information and reagents before publication, and R. Rosin-Arbesfeld and M. Bienz for sharing the APC2-GFP fusion before publication. We also thank the Bloomington *Drosophila* Stock Center and the Developmental Studies Hybridoma Bank for flies and antibodies, B. Duronio for helpful discussions, and S. Whitfield for help with the figures. This work was supported by a grant to M.P. from the HFSP. B.M. was supported by a Leukemia and Lymphoma Society Senior Fellowship, E.G. by NIH 5T32CA71341, and M.P. in part by a CDA from the U.S. Army Breast Cancer Research Program.

REFERENCES

Ahmed, Y., Hayashi, S., Levine, A., and Wieschaus, E. (1998). Regulation of Armadillo by a *Drosophila* APC inhibits neuronal apoptosis during retinal development. *Cell* **93,** 1171–1182.

Ahmed, Y., Nouri, A., and Wieschaus, E. (2002). Drosophila Apc1 and Apc2 regulate Wingless transduction throughout development. *Development* **129,** 1751–1762.

Blair, S. S. (1992). Shaggy (zeste-white 3) and the formation of supernumerary bristle precursors in the developing wing blade of Drosophila. *Dev. Biol.* **152,** 263–278.

Day, C. L., and Alber, T. (2000). Crystal structure of the amino-terminal coiled-coil domain of the APC tumor suppressor. *J. Mol. Biol.* **301,** 147–156.

Fodde, R., Edelmann, W., Yang, K., van Leeuwen, C., Carlson, C., Renault, B., Breukel, C., Alt, E., Lipkin, M., Khan, P. M., *et al.* (1994). A targeted chain-termination mutation in the mouse Apc gene results in multiple intestinal tumors. *Proc. Natl. Acad. Sci. USA* **91,** 8969–8973.

Hamada, F., Murata, Y., Nishida, A., Fujita, F., Tomoyasu, Y., Nakamura, M., Toyoshima, K., Tabata, T., Ueno, N., and Akiyama, T. (1999). Identification and characterization of E-APC, a novel Drosophila homologue of the tumour suppressor APC. *Genes Cells* **4,** 465–474.

Hamada, F., and Bienz, M. (2002). A Drosophila APC tumour suppressor homologue functions in cellular adhesion. *Nat. Cell Biol.* **4,** 208–213.

Hayashi, S., Rubinfeld, B., Souza, B., Polakis, P., Wieschaus, E., and Levine, A. (1997). A *Drosophila* homolog of the tumor suppressor gene adenomatous polyposis coli down-regulates β-catenin but its zygotic expression is not essential for the regulation of Armadillo. *Proc. Natl. Acad. Sci. USA* **94,** 242–247.

McCartney, B. M., Dierick, H. A., Kirkpatrick, C., Moline, M. M., Baas, A., Peifer, M., and Bejsovec, A. (1999). *Drosophila* APC2 is a cytoskeletally-associated protein that regulates Wingless signaling in the embryonic epidermis. *J. Cell Biol.* **146,** 1303–1318.

McCartney, B. M., McEwen, D. G., Grevengoed, E., Maddox, P., Bejsovec, A., and Peifer, M. (2001). *Drosophila* APC2 and Armadillo participate in tethering mitotic spindles to cortical actin. *Nat. Cell Biol.* **3,** 933–938.

Moser, A. R., Shoemaker, A. R., Connelly, C. S., Clipson, L., Gould, K. A., Luongo, C., Dove, W., Siggers, P. H., and Gardner, R. L. (1995). Homozygosity for the Min allele of Apc results in disruption of mouse development prior to gastrulation. *Dev. Dyn.* **203,** 422–433.

Nakagawa, H., Murata, Y., Koyama, K., Fujiyama, A., Miyoshi, Y., Monden, M., Akiyama, T., and Nakamura, Y. (1998). Identification of a brain-specific APC homologue, APCL, and its interaction with beta-catenin. *Cancer Res.* **58,** 5176–5181.

Peifer, M., Sweeton, D., Casey, M., and Wieschaus, E. (1994). *wingless* signal and Zeste-white 3 kinase trigger opposing changes in the intracellular distribution of Armadillo. *Development* **120,** 369–380.

Polakis, P. (2000). Wnt signaling and cancer. *Genes Dev.* **14,** 1837–1851.

Rosin-Arbesfeld, R., Ihrke, G., and Bienz, M. (2001). Actin-dependent membrane association of the APC tumour suppressor in polarized mammalian epithelial cells. *EMBO J.* **20,** 5929–5939.

Siegfried, E., Chou, T.-B., and Perrimon, N. (1992). *wingless* signaling acts through *zeste-white 3*, the *Drosophila* homolog of *glycogen synthase kinase-3*, to regulate *engrailed* and establish cell fate. *Cell* **71,** 1167–1179.

Simpson, P., and Cateret, C. (1989). A study of *shaggy* reveals spatial domains of expression of *achaete-scute* alleles on the thorax of *Drosophila*. *Development* **106,** 57–66.

Tolwinski, N. S., and Wieschaus, E. (2001). Armadillo nuclear import is regulated by cytoplasmic anchor Axin and nuclear anchor dTCF/Pan. *Development* **128,** 2107–2117.

van Es, J. H., Kirkpatrick, C., van de Wetering, M., Molenaar, M., Miles, A., Kuipers, J., Destrée, O., Peifer, M., and Clevers, H. (1999). Identification of APC2, a homologue of the adenomatous polyposis coli tumour suppressor. *Curr. Biol.* **9,** 105–108.

von Kries, J. P., Winbeck, G., Asbrand, C., Schwarz-Romond, T., Sochnikova, N., Dell'Oro, A., Behrens, J., and Birchmeier, W. (2000). Hot spots in beta-catenin for interactions with LEF-1, conductin and APC. *Nat. Struct. Biol.* **7,** 800–807.

Yu, X., Waltzer, L., and Bienz, M. (1999). A new Drosophila APC homologue associated with adhesive zones of epithelial cells. *Nat. Cell Biol.* **1,** 144–151.

Received for publication March 27, 2002
Revised May 13, 2002
Accepted June 27, 2002
Published online August 26, 2002

Developmental Biology **250**, 71–90 (2002)
doi:10.1006/dbio.2002.0777

Drosophila APC2 and APC1 Have Overlapping Roles in the Larval Brain Despite Their Distinct Intracellular Localizations

Kathryn Akong,* Brooke M. McCartney,†‡ and Mark Peifer*,†,‡,[1]

**Curriculum in Genetics and Molecular Biology, †Lineberger Comprehensive Cancer Center, and ‡Department of Biology, University of North Carolina, Chapel Hill, North Carolina 27599-3280*

The tumor suppressor APC and its homologs, first identified for a role in colon cancer, negatively regulate Wnt signaling in both oncogenesis and normal development, and play Wnt-independent roles in cytoskeletal regulation. Both *Drosophila* and mammals have two APC family members. We further explored the functions of the *Drosophila* APCs using the larval brain as a model. We found that both proteins are expressed in the brain. APC2 has a highly dynamic, asymmetric localization through the larval neuroblast cell cycle relative to known mediators of embryonic neuroblast asymmetric divisions. Adherens junction proteins also are asymmetrically localized in neuroblasts. In addition they accumulate with APC2 and APC1 in nerves formed by axons of the progeny of each neuroblast-ganglion mother cell cluster. APC2 and APC1 localize to very different places when expressed in the larval brain: APC2 localizes to the cell cortex and APC1 to centrosomes and microtubules. Despite this, they play redundant roles in the brain; while each single mutant is normal, the zygotic double mutant has severely reduced numbers of larval neuroblasts. Our experiments suggest that this does not result from misregulation of Wg signaling, and thus may involve the cytoskeletal or adhesive roles of APC proteins. © 2002 Elsevier Science (USA)

Key Words: **APC; β-catenin; Armadillo; brain; Wingless; *Drosophila*; tumor suppressor; neuroblast; cadherin; asymmetric division.**

INTRODUCTION

The tumor suppressor APC is mutated in familial adenomatous polyposis, a genetic predisposition to colon cancer. APC is also mutated in >70% of sporadic cases of colon cancer (reviewed in Polakis, 2000). The initial cloning of APC provided few clues as to its normal cell biological function, as it had no obvious relationship to any known protein. The breakthrough came from experiments that revealed that APC physically associates with β-catenin (βcat). βcat and its fly homolog Armadillo (Arm) were known to play two important roles in normal cells, as components of cell–cell adhesive junctions and as key transducers of Wnt signal transduction.

Further experiments revealed that APC is a negative regulator of Wnt signaling (reviewed in Polakis, 2000). APC is a key component of a multiprotein complex that targets Arm/βcat for phosphorylation by the kinase glycogen synthase kinase 3 (GSK3)/Zeste white 3 (Zw3), leading to its ubiquitination and destruction by the proteasome. Wnt signaling inactivates the destruction complex, allowing Arm/βcat to accumulate and act with its DNA-binding partner TCF/LEF to activate Wnt target genes. In tumors, loss of APC allows constitutive elevation of βcat levels and thus continuous activation of Wnt target genes, which triggers proliferation in that tissue.

In addition to regulating Arm/βcat levels and thus transcriptional activation, APC family members also regulate the cytoskeleton. The first hint of this came from the localization and biochemical properties of human APC. APC binds and bundles microtubules *in vitro*, and when overexpressed, colocalizes with microtubules (Munemitsu *et al.*, 1994; Smith *et al.*, 1994; Zumbrunn *et al.*, 2001). Endogenous APC localizes to the cell cortex, often at sites where bundles of microtubules terminate (Näthke *et al.*,

[1] To whom correspondence should be addressed. Fax: (919) 962-1625. E-mail: peifer@unc.edu.

0012-1606/02 $35.00

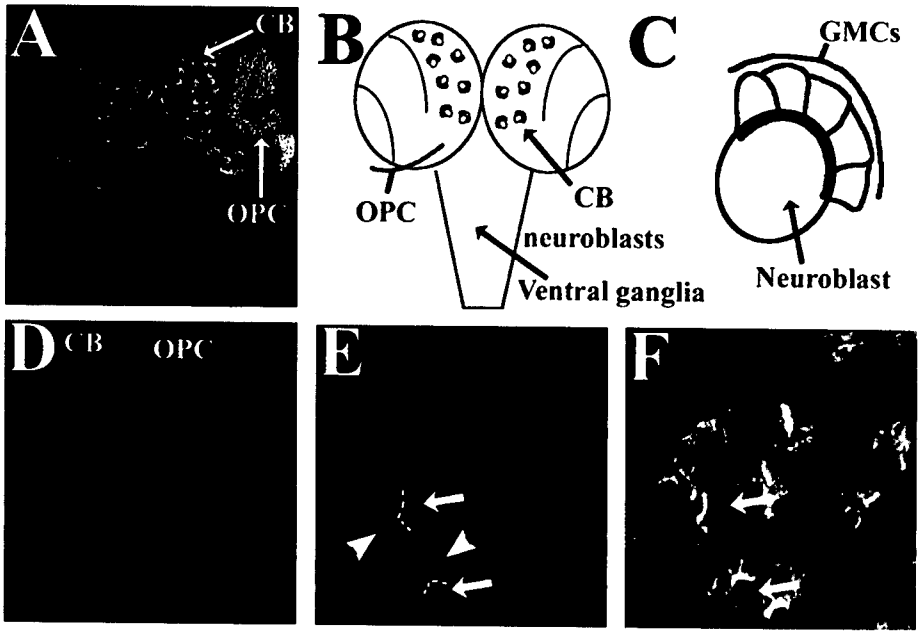

FIG. 1. APC2 accumulates asymmetrically in larval neuroblasts. (A) Double-labeled third instar brain: APC2 (red), Arm (green). (B) Schematic showing the central brain (CB) neuroblasts, outer proliferation center (OPC), and ventral ganglia. (C) Schematic illustrating a neuroblast and its ganglion mother cell (GMC) progeny. The red crescent illustrates the localization of APC2. (D–F) Double-labeled brains: APC2 (D, E, red; F), Pros (D, E, green). (D) Brain lobe. (E, F) Close-up of the CB. APC2 localizes to crescents (dashed lines) where neuroblasts (white arrows) touch GMCs (arrowheads). Pros is found at low levels in GMCs (E, arrowheads) and higher levels in ganglion cells (E, green arrows), but is not found in neuroblast nuclei (E, white arrows).

1996), and an APC–GFP fusion (Mimori-Kiyosue *et al.*, 2000) travels along microtubules to their plus ends and then forms cortical puncta. In contrast, *Drosophila* APC2 colocalizes with cortical actin in a wide variety of tissues (McCartney *et al.*, 1999; Townsley and Bienz, 2000; Yu and Bienz, 1999).

Functional studies subsequently revealed roles for APC family members as Wnt-independent cytoskeletal regulators. In *Drosophila*, APC2 is required for effective tethering of the mitotic spindle to the cortex, acting with Arm in this process (McCartney *et al.*, 2001). This prompted the hypothesis that it may help link the plus ends of astral microtubules to actin at the cortex. In cultured mammalian cells, APC localizes to kinetochores, and in the absence of functional APC, the fidelity of chromosome segregation is reduced (Fodde *et al.*, 2001; Kaplan *et al.*, 2001). Here, APC may help link the plus ends of spindle microtubules to chromosomes. Finally, APC2 plays a role in maintaining the cell–cell adherens junction complex in epithelial cells (Townsley and Bienz, 2000; Hamada and Bienz, 2002).

These roles for APC proteins in both Wnt signaling and Wnt-independent cytoskeletal regulation raises the possibility that APC proteins may mediate known effects of Wnt signaling on the cytoskeleton. Wnt signaling regulates the actin cytoskeleton during the establishment of planar cell polarity, a process whereby epithelial tissues polarize their cytoskeletons along organ or body axes. This influences processes as diverse as wing hair positioning and dorsal closure in *Drosophila* and convergent extension during vertebrate gastrulation (reviewed in McEwen and Peifer, 2000). Wnt signaling also regulates the positioning of the mitotic spindle in certain cells undergoing asymmetric cell divisions (Gho and Schweisguth, 1998; Rocheleau *et al.*, 1997; Thorpe *et al.*, 1997), and in at least some cases, this effect is direct, without a transcriptional intermediate (Schlesinger *et al.*, 1999).

We examined possible redundancy between APC family members and possible cytoskeletal roles, using the *Drosophila* larval brain as a model (Figs. 1A and 1B). In the brain, neural stem cells known as neuroblasts undergo a series of asymmetric divisions during larval development (Fig. 1C; Ceron *et al.*, 2001; Ito and Hotta, 1992). Each division produces a large daughter that remains a stem cell and a smaller daughter that becomes a ganglion mother cell (GMC), whose subsequent divisions produce neurons. In embryonic neuroblasts, the actin and microtubule cytoskeletons play important roles in the asymmetric localization of neural determinants and in asymmetric division. We previously found that APC2 and Arm localize asymmetrically in larval neuroblasts, accumulating at high levels on the side of the neuroblast where the daughter will be born (Figs. 1C–1F; McCartney *et al.*, 1999).

Here, we present an examination of the localization and function of APC family members in the larval brain. This

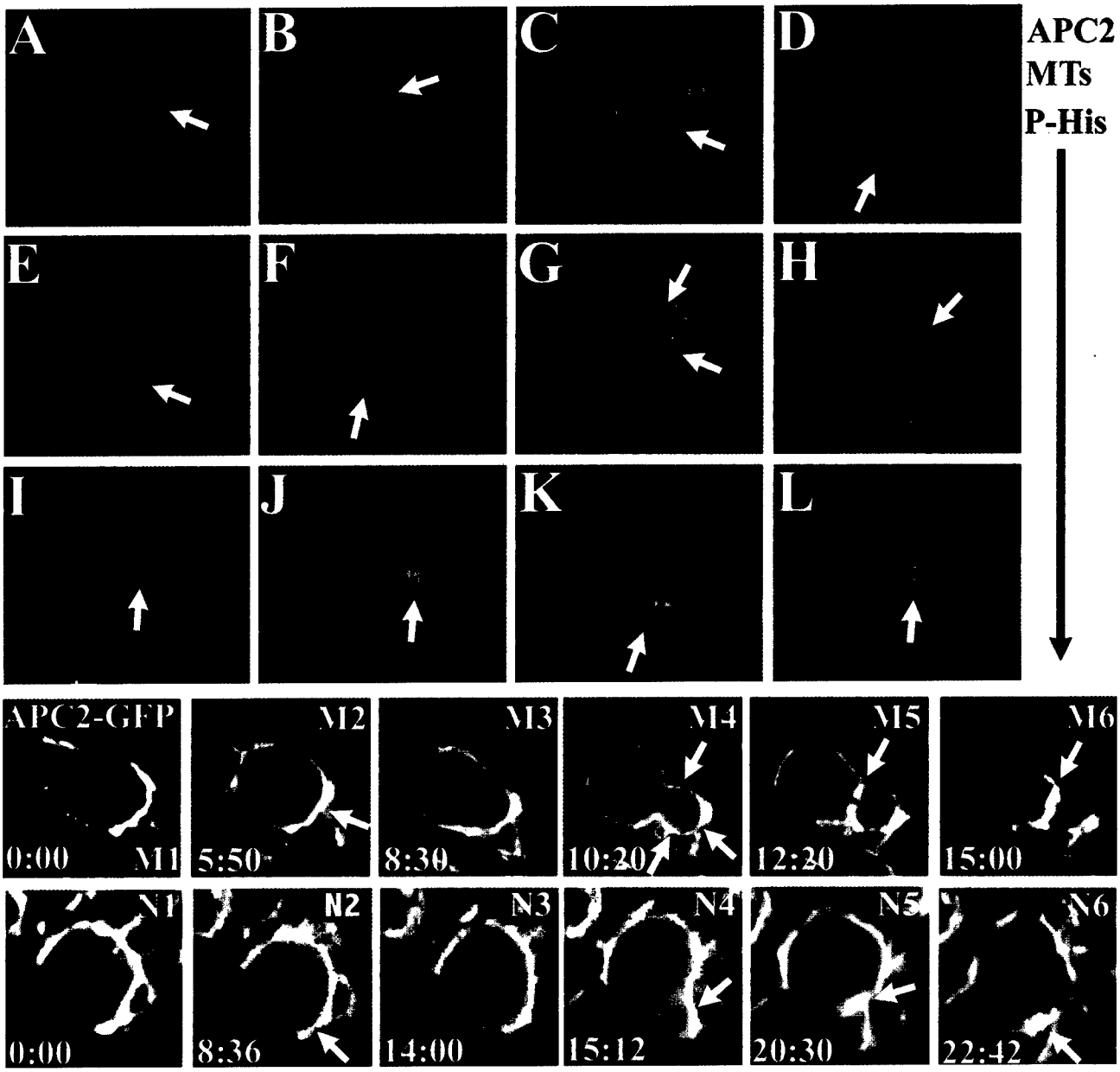

FIG. 2. APC2 accumulation during the cell cycle. (A–L) Triple-labeled third instar CB neuroblasts: APC2 (red), β-tubulin (green), mitotic chromosomes (anti-phosphohistone H3; blue). (A, B) Interphase. Arrows, APC2 crescent. (C, D) Prophase. (E, F) Metaphase. Arrows, spindle pole. (G, H) Anaphase. Arrows, APC2 accumulation on budding GMC daughter. (C, E, G) Divisions in which one spindle pole points toward the center of the APC2 crescent. (D, F, H) Divisions in which one spindle pole points toward the edge of the APC2 crescent. (I–K) Early to late telophase. (L) Neuroblast after cytokinesis. Arrows, APC2 accumulation at cleavage furrow and division site. (M, N) Stills from movies following APC2–GFP during mitosis (M, Movie 1; N, Movie 2). Times in minutes are indicated. (M) Neuroblast in which one spindle pole points toward the center of the APC2 crescent. M2 arrow, spindle pole. M4 arrows, APC2 accumulation all around the budding GMC. M5 and M6 arrows, APC2 accumulation at cleavage furrow. (N) Neuroblast in which one spindle pole points toward the edge of the APC2 crescent. N2 arrow, spindle pole. N4 arrow, APC2 accumulation along one side of budding GMC. N5 and N6 arrow, APC2 at cleavage furrow and division site.

revealed a dynamic localization of APC2 during the neuroblast cell cycle, relative to other neuroblast markers. We found that APC1 also accumulates at low levels in neuroblasts. Neither single mutant had noticeable effects on brain development or neuroblast asymmetric divisions. However, *APC2 APC1* double mutants have substantial

defects in brain development, suggesting functional redundancy between the two APCs. Our data suggest that this role may be Wnt-independent.

MATERIALS AND METHODS

Genetic and Phenotypic Analysis

Alleles used were: *APC2*$^{\Delta 5}$ (McCartney *et al.*, 1999), *APC2*^{d40} (McCartney *et al.*, 2001), and *APC1*^{Q8} (Ahmed *et al.*, 1998). *APC2*^{g10} and *APC2*^{f90} were generated in an EMS mutagenesis screen, identified by failure to complement *APC2*$^{\Delta 5}$ (unpublished data). Double mutant *APC2 APC1* chromosomes were generated by meiotic recombination. All stocks were kept at 25°C. Embryo first and second instar larvae collections were done at 27°C. Wandering third instar larvae collections were done at 25°C. Transgenic lines used for misexpression and overexpression studies were UAS–APC2–GFP (R. Rosin-Arbesfeld and M. Bienz), UAS-APC1 (E. Wieschaus), and UAS–Arm^{S10} (Pai *et al.*, 1997). Transgenes were expressed in specific tissues by crossing to Prospero–GAL4 (Ohshiro *et al.*, 2000) at 27°C. Canton S was the wild type, except when protein levels were compared by immunofluorescence, where controls were histone–GFP transgenics (R. Saint).

Immunolocalization and Time-Lapse Microscopy

Larval tissues were dissected in Schneider's *Drosophila* Medium (GIBCO) with 10% fetal bovine serum. Brains were fixed for 20 min in 4% paraformaldehyde or 3.7% formaldehyde in PBS/0.2% Triton X-100 with indistinguishable results. Embryos were fixed in 1:1 3.7% formaldehyde in PBS:heptane for 20 min. All were blocked in 1% normal goat serum/0.1% Triton X-100 in PBS for at least 2 h. Primary antibodies were as follows: rat polyclonal anti-APC2 (1:1000), mouse monoclonals anti-Arm N27A1 (DSHB, 1:200), anti-βtubulin E7 (DSHB, 1:500), anti-Prospero (DSHB, 1:4), anti-BP102 (DSHB, 1:100), anti-myc 9E10 (DSHB, 1:100), anti-BrdU (1:100, Becton-Dickinson), rabbit polyclonals anti-Miranda (1:2000, F. Matsuzaki), anti-Bazooka (1:1000, E. Knust), anti-Inscuteable (1:1000, W. Chia), anti-phospho-histone H3 (1:500, Upstate Biotechnology), anti-Armadillo N2 (1:200), and anti-APC1 (1:1000; E. Wieschaus), rat monoclonals anti-DE-cadherin (1:200, M. Takeichi) and anti-α-catenin (1:200, M. Takeichi). For movies, larval brains of genotype *UAS–APC2–GFP/Pros–GAL4* were dissected in Schneider's *Drosophila* Medium with 10% fetal bovine serum and mounted in halocarbon oil (Halocarbon Products) between a glass coverslip and a gas-permeable membrane (Petriperm; Sartorius). Images were collected on a Perkin-Elmer Wallac Ultraview Confocal Imaging System every 6–10 s for 1–2 h.

BrdU Incorporation

Newly hatched first instar larvae were fed Instant *Drosophila* Medium Blue (Carolina Biological Supply) with 0.5 mg/ml BrdU for 24–28 h at 27°C until the second instar molt.

RESULTS

APC2 Has a Dynamic, Asymmetric Localization during Neuroblast Divisions

We previously found that APC2 localizes asymmetrically in larval neuroblasts (Fig. 1; McCartney *et al.*, 1999). Here, we extend this observation, examining the dynamic behavior of APC2 during the cell cycle, and comparing its localization with other asymmetric markers and with cytoskeletal and adhesive proteins. We focused our attention on central brain neuroblasts, which are located medially to the proliferation centers of the optic lobes (Figs. 1A and 1B; Ito and Hotta, 1992). Neuroblast divisions are asymmetric in size and fate, with the larger daughter remaining a neuroblast (Figs. 1C, 1E, and 1F, white arrows) and the smaller daughter becoming a ganglion mother cell (GMC; Figs. 1C and 1E, arrowheads; Ceron *et al.*, 2001; Ito and Hotta, 1992). Each central brain neuroblast divides a series of times to produce a "cap" of GMCs (Fig. 1C) that remain joined to the mother, and divide mitotically themselves. Their progeny become ganglion cells and ultimately differentiate as neurons (Fig. 1E, green arrows).

To characterize APC2 dynamic localization during the cell cycle, we took two parallel approaches (Fig. 2; Movies 1 and 2). We used immunofluorescence and confocal microscopy to colocalize APC2, microtubules, and mitotic DNA (via the phosphohistone H3 epitope) in fixed tissue, and we used an APC2–GFP fusion (kindly provided by R. Rosin-Arbesfeld and M. Bienz) under the control of the GAL4–UAS system and driven in a subset of neuroblasts by prospero–GAL4 (pros–GAL4; Ohshiro *et al.*, 2000). The localization of APC2 revealed by these approaches is quite similar, though not identical. APC2–GFP accumulated somewhat more uniformly around the cortical circumference and was present at higher levels in GMCs; we suspect these differences reflect the elevated levels of APC2–GFP, although they could be due to localization differences between the GFP fusion and endogenous APC2. In collecting images, we attempted to select neuroblasts dividing parallel to the plane of focus; however neuroblasts and their GMC daughters are three-dimensional, and neuroblasts do not divide with a defined polarity relative to the brain surface. Thus, we might sometimes have looked at sections not precisely parallel to the plane of division.

During interphase, APC2 forms a strong asymmetric crescent (Fig. 1E, dashed lines; Fig. 2A, arrow), with APC2 accumulating at the border between the neuroblast and its previous daughters; this is where the next daughter will be born. The APC2 crescent remains strong through prophase, as the centrosomes separate and begin to set up the spindle (Figs. 2B–2D, 2M1, and 2N1). The crescent becomes less pronounced at metaphase (Figs. 2E and 2F). The orientation of the neuroblast spindle at metaphase determines where the GMC is born. We observed two different relationships between the cortical APC2 crescent and the mitotic spindle, which in our movies and our confocal images, were present in approximately equal numbers. In about half of the neuroblasts, the forming mitotic spindle was directed toward the center of the APC2 crescent (Figs. 2C, 2E, and 2M2, arrows). In the other neuroblasts, the forming mitotic spindle was directed toward one edge of the crescent (Figs. 2D, 2F, 2N2, arrows). The difference was first apparent during late prophase (Figs. 2B–2D), and continued through

metaphase (Figs. 2E, 2F, 2M2, and 2N2) and anaphase (Figs. 2G, 2H, 2M4, and 2N4). The reason for this difference in APC2 localization in different neuroblasts remains to be determined. One speculative possibility is that the relationship of GMC birth position to the APC2 crescent differs depending on how many GMCs have already been born. We have found that the new GMC daughter is usually born adjacent to one of the earlier daughters (see below). At early stages, when there are relatively few GMC daughters, the spindle may be directed toward the middle of the APC2 crescent. In later divisions, when there are more GMC daughters, the new GMC may be born at the edge of the APC2 crescent, which is found at the interface between the neuroblast and the cap of previous GMC daughters.

As neuroblasts enter anaphase, APC2 remains cortical. In neuroblasts where the spindle pointed toward the center of the APC2 crescent, APC2 surrounds the budding daughter (Figs. 2G and 2M4, arrows). In cells in which the spindle was directed toward the edge of the crescent, APC2 localizes along one side of the GMC (Figs. 2H and 2N4, arrows). As cytokinesis begins, APC2 localizes prominently to the cleavage furrow in all cases (Figs. 2I and 2M5, arrows). This enrichment is even more prominent at the end of cytokinesis (Figs. 2J and 2K, arrows); at times, the cleavage furrow localization resolved into an apparent double ring (Fig. 2N5, arrow). APC2 remains enriched at the division site after cytokinesis, marking the spot where the last daughter was born (Figs. 2L, 2M6, and 2N6, arrows), and it only gradually reexpands to the interface between the neuroblast and all of her GMC daughters.

Our live imaging of APC2–GFP also provided a glimpse of the timing of neuroblast cell cycles. We found that mitosis lasts ~15–20 min. In two cases, we observed a single neuroblast divide twice, allowing us to assess the minimum cell cycle length. In these cases, the two mitoses were completed in 106–120 min. This is comparable to the cell cycle length of embryonic neuroblasts (about 50 min; Foe *et al.*, 1993), and fits previous estimates of neuroblast cell cycle length from BrdU-labeling experiments (e.g., Ito and Hotta, 1992). Other neuroblasts within the same brain, however, divided only once, while still others did not divide at all during the ~2.5 h of the movie.

The Relationship between APC2 Localization and That of Other Asymmetric Proteins

One striking feature of the asymmetric localization of APC2 is that it is present throughout the cell cycle and is particularly strong during interphase. During embryonic neuroblast divisions, most asymmetric markers are only localized during mitosis (reviewed in Jan and Jan, 2001). However, we know less about their localization in larval neuroblasts. We thus examined several asymmetric markers in larval neuroblasts, extending previous work, and compared their localization with that of APC2. In embryonic neuroblasts, the transcription factor Prospero (Pros) and its mRNA are GMC determinants that are asymmetrically localized to the GMC daughter (reviewed in Jan and Jan, 2001). Pros protein then becomes nuclear and helps direct cell fate. In larval neuroblasts, we observed a similar localization. Pros is not detectable in interphase neuroblasts, when the cortical APC2 crescent is strongest (Fig. 1E, dashed line). A small amount of Pros transiently localizes to an asymmetric crescent during mitosis (Fig. 3A, dashed line). Pros is present at low levels in GMC nuclei (Fig. 1E, arrowheads) and at higher levels in the nuclei of ganglion cells (Fig. 1E, green arrows). Our results differ somewhat from those of Ceron *et al.* (2001) who did not detect Pros in GMCs.

We next examined Miranda (Mira), extending the earlier characterization by Ceron *et al.* (2001), and compared Mira with APC2. Mira is basally localized in embryonic neuroblasts, and required there for localization of Pros protein and mRNA (reviewed in Jan and Jan, 2001). We found that, in central brain neuroblasts, Mira is diffusely cytoplasmic during interphase (Fig. 3D), when the APC2 crescent is the strongest. As cells enter mitosis, Mira first becomes cortical (Fig. 3E) and then begins to accumulate asymmetrically on the side of the neuroblast where the daughter will be born (Figs. 3F and 3H, dashed line). By metaphase, Mira asymmetry is very pronounced (Fig. 3I, arrow; Figs. 3J–3L, dashed line). The center of the Mira crescent is always precisely aligned with one spindle pole. As a result, in cells with the spindle pointing toward the center of the APC2 crescent, the Mira and APC2 crescents substantially overlap (Figs. 3F–3H and 3J–3L), while in cells in which the spindle points to the edge of the APC2 crescent, the two crescents are

FIG. 3. The relationship of APC2 to other markers of asymmetric divisions. Third instar CB neuroblasts; in most, the GMC daughter will be born on the right-hand side. (A) Pros (green), mitotic chromosomes (anti-phosphohistone H3; red). Pros accumulates in a transient crescent where the GMC will be born (dashed line). (B–D, F–H, J–L, M, P, S, T) Triple-labeled neuroblasts: APC2 (red), Mira (green), microtubules (blue). (E, I, N, O, Q, R) Double-labeled neuroblasts: Mira (red), microtubules (green). (B–H) Prophase. (I–M) Metaphase. As cells enter prophase, cytoplasmic Mira is recruited uniformly to the cortex (D, E), and then reorganizes into a cortical crescent where the GMC will be born (F, H, dashed line). One spindle pole always points toward the Mira crescent. Arrowhead in (E, F, J): the opposite spindle pole. (F–H, J–L) In cells in which one spindle pole points toward the APC2 crescent, the Mira and APC2 crescents largely overlap (dashed lines). (M) In cells in which one spindle pole points toward the edge of the APC2 crescent, overlap between APC2 and Mira is only partial (red dashed line, APC2; green dashed line, Mira). (N–Q) Anaphase. (R–T) Telophase. Arrowhead, neuroblast. Mira is partitioned into the GMC (N–R, arrows). During anaphase, APC2 brackets the GMC (P), and during telophase it localizes to cleavage furrows (S, T, arrow).

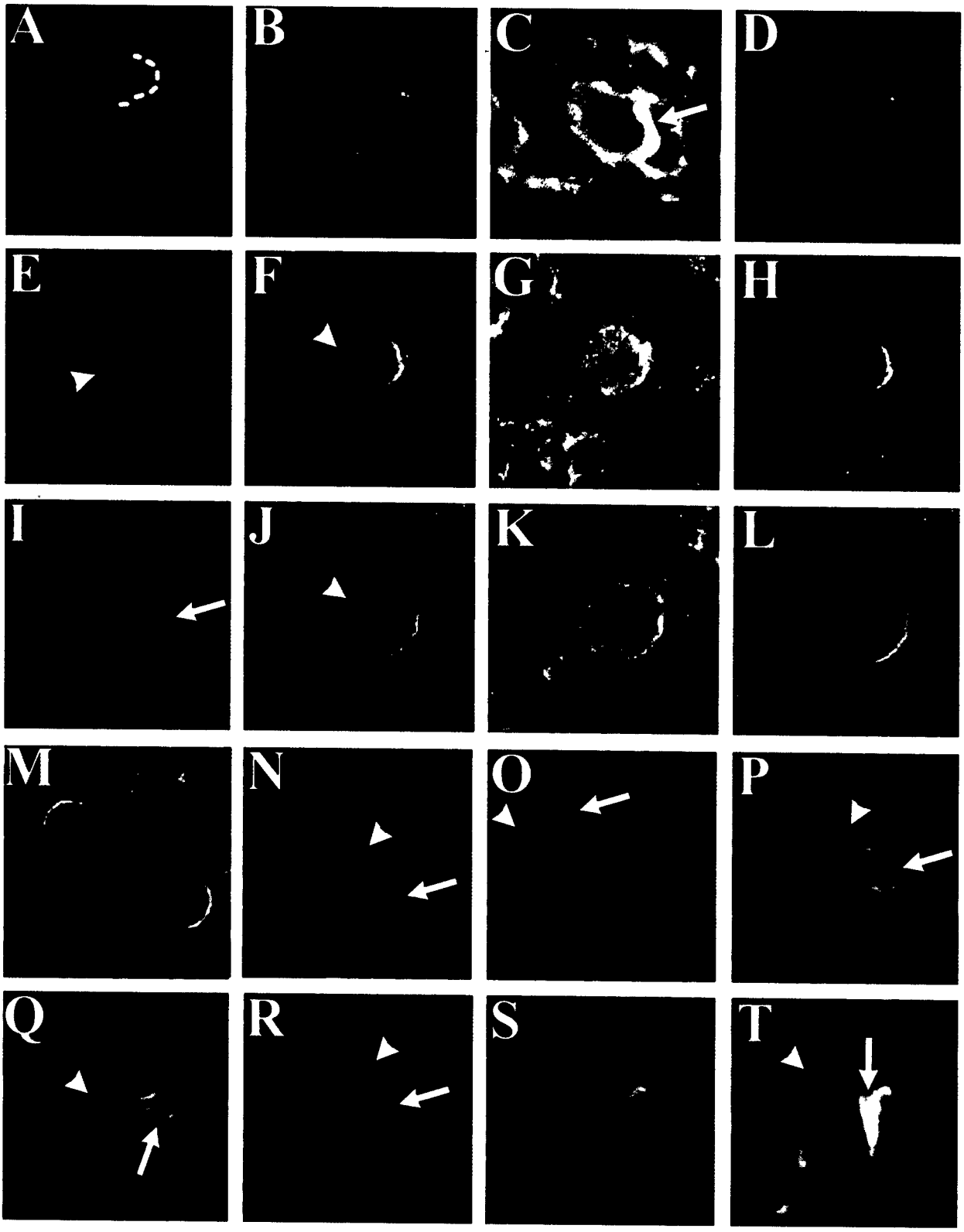

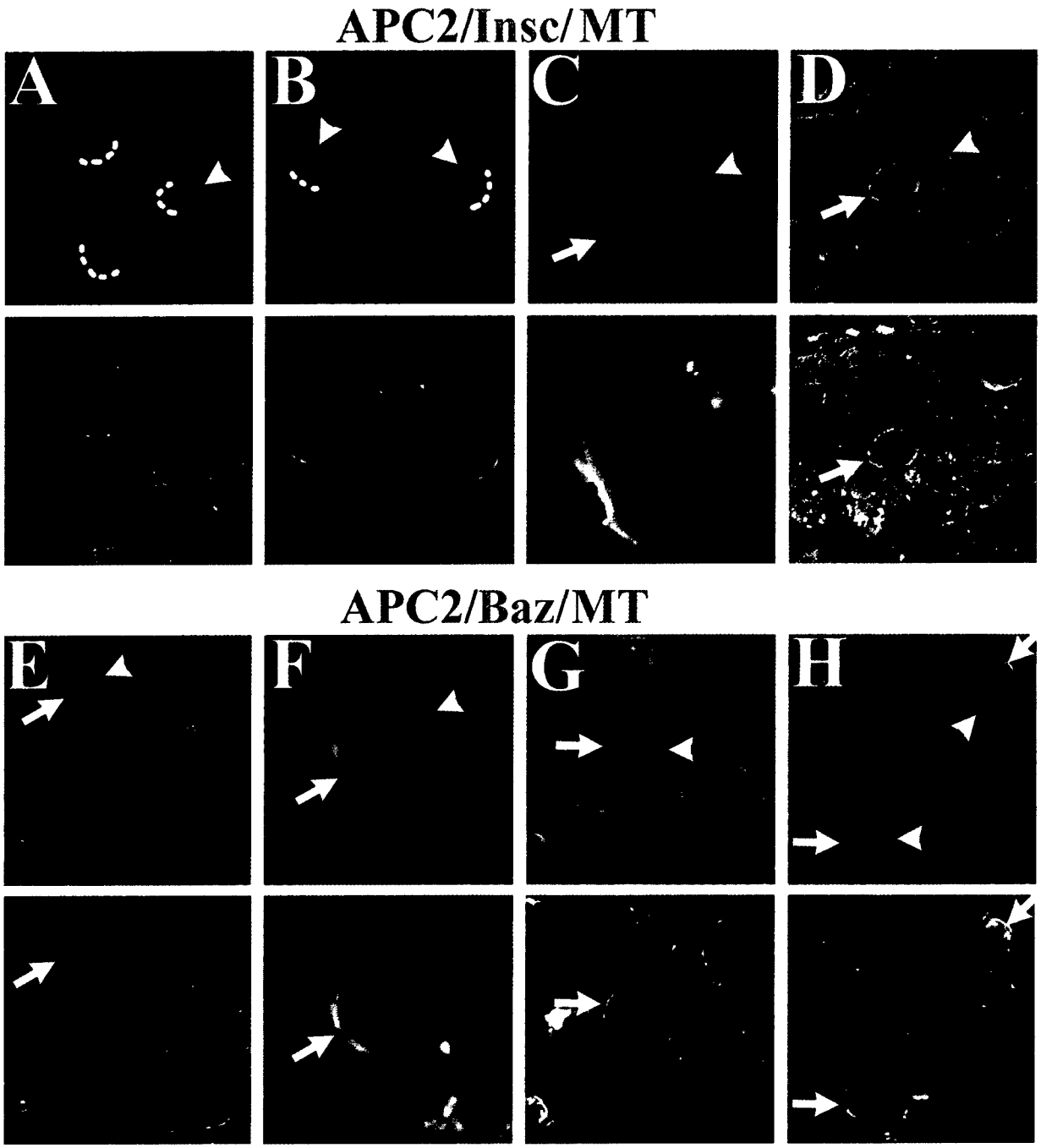

FIG. 4. APC2 localizes opposite Insc and Baz. Third instar CB neuroblasts. (A) Double-labeled: APC2 (red), Insc (green). (B–D) Triple-labeled: APC2 (red), Insc (green), microtubules (blue). Bottom row, Insc alone. (A) Interphase. A prominent APC2 crescent (arrowhead) localizes opposite a faint but detectable Insc crescent (dashed lines). (B) Prophase. The APC2 crescent becomes less pronounced (arrowheads) as the Insc crescent becomes more pronounced (dashed lines). (C) Metaphase. Insc localizes to the cell cortex (arrow) at the end of the spindle opposite where the GMC will be born, thus not overlapping APC2 (arrowhead). (D) Anaphase. Insc localizes to the neuroblast cortex (arrow in top panel, dashed line in bottom panel), while APC2 surrounds the neck of the GMC (arrowhead). (E–H) Triple-labeled: APC2 (red), Baz (green), microtubules (blue). Bottom row, Baz alone. (E) Interphase. In cells with a strong APC2 crescent (arrowhead), Baz is diffusely cytoplasmic (arrow). (F) Prophase. Baz localizes to a crescent at the end of the spindle (top-arrow, bottom-dashed line) opposite where the daughter will be born, and thus does not overlap APC2 (arrowhead). (G) Metaphase. Baz remains in a crescent (top-arrow, bottom-dashed line) opposite APC2 (arrowhead). (H) Anaphase onset. Baz remains localized to the cortex (top-arrow, bottom-dashed line) near the end of the spindle opposite where the daughter will be born and thus opposite APC2 (arrowhead).

offset (Fig. 3M). Mira is partitioned into the GMC during anaphase (Figs. 3N–3R, arrows), while APC2 relocalizes to the cleavage furrow (Figs. 3S and 3T, arrow). Mira could still be detected in some GMCs, which we suspect are those that were recently born (see below).

In contrast to Mira and Pros, Inscuteable (Insc) and Bazooka (Baz) localize to the apical sides of embryonic neuroblasts, where they play essential roles in asymmetric divisions (reviewed in Jan and Jan, 2001). Insc is asymmetrically localized in larval neuroblasts (Parmentier *et al.*, 2000; Ceron *et al.*, 2001). We found that Insc localizes to the side of the neuroblast opposite that of APC2 through much, if not all, of the cell cycle (Figs. 4A–4D, dashed lines and arrows). Interestingly, there is a weak Insc crescent during interphase (Fig. 4A), that became stronger through prophase and metaphase (Figs. 4B and 4C). During anaphase, Insc localized to the neuroblast cortex but not the GMC daughter (Fig. 4D). Baz localization was similar to that of Insc, though no cortical localization during interphase was detected (Fig. 4E, arrow). During prophase and metaphase, Baz localized to a crescent (Figs. 4F and 4G, dashed lines and arrows) opposite APC2 (Figs. 4F and 4G, arrowheads), and as the chromosomes began to separate, Baz localized to a tight cap opposite the future GMC (Fig. 4H). Together, these data confirm that larval and embryonic neuroblasts asymmetrically localize many of the same proteins, and that APC2 localizes on the GMC side of the neuroblast, overlapping Mira and opposite Baz and Insc.

Adherens Junction Proteins Localize Asymmetrically in Larval Neuroblasts

In our initial characterization of APC2, we found that Arm also localizes asymmetrically in neuroblasts (McCartney *et al.*, 1999). We extended this, examining the localization of Arm's adherens junction partners DE-cadherin and α-catenin. When central brain neuroblasts undergo a sequential series of asymmetric divisions, the GMCs remain associated with their neuroblast mother, resulting in a cap of GMCs in association with each neuroblast. APC2 localizes strongly to the boundary between the neuroblast and each GMC, and more weakly to the borders between the GMCs (Figs. 1E and 1F). APC2 is present at lower levels in ganglion cells and differentiating neurons (Figs. 1E and 1F). The adherens junction proteins DE–cadherin, Arm, and α-catenin all show a striking and asymmetric localization pattern in central brain neuroblasts (Figs. 5A–5H). All precisely colocalize both at the boundary between neuroblasts and GMCs (dashed lines) and at the boundaries between GMCs (arrowheads). DE–cadherin, Arm, and α-catenin are also all expressed in epithelial cells of the outer proliferation center (e.g., Fig. 5E, bracket).

The localization of DE–cadherin and the catenins is consistent with the idea that cadherin–catenin-based adhesion could help ensure that GMCs remain associated with each other, via association with their neuroblast mother. To further explore this, we examined how successive GMCs are positioned relative to their older GMC sisters, using two different approaches. We first used Mira (Fig. 5I, green; Figs. 5K and 5L green) to mark the newborn GMCs (arrowheads) and DE–cadherin (Fig. 5I, red; Figs. 5J and 5L, red) to mark the neuroblast (arrows) and all of her GMC daughters. Mira localizes to a crescent on the side of the neuroblast where the daughter will be born, and then is segregated into the daughter. We found that Mira persists for some time in newborn GMCs, and that it remains detectable in the other GMCs as well (Fig. 5K), thus allowing us to examine the position of newborn GMCs relative to their older sisters. In many cases, new GMCs are clearly born at the edge of the cluster of older GMCs. This is particularly striking in neuroblasts with many progeny (e.g., Fig. 5I, arrows). It is worth noting that the cluster of daughters is three-dimensional, comprising a "cap" of daughters in three dimensions rather than the two-dimensional line of daughters illustrated in Fig. 1. We thus suspect new daughters are born near the edge of this cap. We obtained further resolution by live imaging of dividing neuroblasts in brains expressing APC2–GFP (Movie 3 = M1, Movie 4 = M2). In the two cases when we followed a single neuroblast through two divisions, the orientation of the mitotic spindles were similar in each division, such that second daughter (M1b or M2b) was born very near the first (M1a or M2a).

These data suggest that neuroblasts and their GMC progeny remain closely associated. The GMCs then divide to form ganglion cells and ultimately neurons. Our data further suggest that these latter cells may also remain associated and send their axons together toward targets in the central brain. When we sectioned more deeply into the brain, below each cluster of neuroblasts and GMCs (Fig. 5N, arrowhead; Fig. 5O, arrow and arrowhead), we could detect structures that appear to be axons projecting from these groups of cells (Fig. 5N, arrows; Figs. 5P and 5Q, arrow and arrowheads). These axons label with Arm (Figs. 5N–5Q), DE–cadherin (Fig. 5N), APC2 (Figs. 5O–5Q), and APC1 (see below). Arm also localizes to the axons of the neuropil, while DE–cadherin (Fig. 5N, large arrow) and APC2 (Fig. 5Q, inset, arrow) are present at low levels or are absent from this structure.

APC2 Is Not Essential for Asymmetric Divisions

Given APC2's asymmetric localization and our previous observation that it plays a role in spindle attachment in syncytial embryos (McCartney *et al.*, 2001), we hypothesized that APC2 might play a role in spindle orientation and thus division asymmetry in larval neuroblasts. To test this, we examined neuroblast divisions in larvae homozygous, hemizygous, or trans-heterozygous for different *APC2* alleles. $APC2^{\Delta S}$ and $APC2^{d40}$ are strong hypomorphic alleles that disrupt cortical localization of APC2 (McCartney *et al.*, 1999, 2001). $APC2^{\Delta S}$ results from the deletion of a serine residue in the Arm repeat region, while $APC2^{d40}$ encodes a truncated protein lacking much of the Arm-binding region.

APC2^{g10} and *APC2*^{f90} are stronger alleles, as assessed by their maternal-effect embryonic phenotype (unpublished data). They may be null mutations, as they result from premature stop codons in the Arm repeat region (unpublished data) and thus do not produce a protein detectable with our antibody, which recognizes the C-terminal half of APC2.

All four *APC2* mutations are zygotically viable, suggesting that brain development was unlikely to be severely disrupted. We examined the brains of larvae mutant for three of these alleles, and found that the asymmetric divisions appeared unaffected, as assessed by Mira localization (Figs. 6A and 6B, arrows), its match with spindle position, and the size asymmetry between mother and daughter (Figs. 6A and 6B; data not shown). In the case of *APC2*$^{\Delta 5}$, we also examined Pros, Insc, and Baz, all of which were correctly localized (Fig. 6E, dashed line; Figs. 6F–6H, arrows). Finally, we examined the effect of loss of APC2 function on the levels and localization of Arm, as Arm levels are substantially elevated in embryonic ectodermal cells mutant for *APC2* (McCartney *et al.*, 1999). We saw no differences in either Arm levels or localization in the brains of *APC2* mutant larvae (Figs. 6I–6L). DE–cadherin localization also appeared normal (data not shown). To complete this analysis, we also examined whether a null mutation in the other fly *APC* gene, *APC1*^{Q8}, had any effect on asymmetric divisions. Once again, asymmetric divisions, as assessed by Mira localization (Figs. 6C and 6D, arrows), its match with spindle position, and the size asymmetry of mother and daughter, appeared normal (Figs. 6C and 6D).

APC1 and APC2 Differ in Their Cell Biological Properties

Thus, despite its striking localization, APC2 is not essential for brain development. One possible explanation is that APC1 is also expressed in larval neuroblasts and plays a redundant role there. We thus examined the localization and function of APC1 in brain development. In embryos, APC1 is expressed in primordial germ cells and in CNS axons (Hayashi *et al.*, 1997). We used anti-APC1 antibody to examine its expression in the larval brain, using the null allele *APC1*^{Q8} (Ahmed *et al.*, 1998) as a negative control. APC1 accumulates at apparently low levels throughout the brain. It is largely diffuse throughout the cell, with slight cortical enrichment (Figs. 7A and 7C). There was a small amount of residual staining in the *APC1* mutant (Figs. 7B and 7D), that we suspected might represent slight cross-reactivity with APC2 (cross-reactivity is detectable in immunoblotting; data not shown). To test this, we stained brains from *APC2*^{g10} mutants (Figs. 7F and 7H–7J), which lack detectable APC2, with anti-APC1. These brains exhibited only slightly reduced levels of staining compared to wild-type controls (Figs. 7E and 7G; cortical neuroblast staining was slightly reduced), suggesting that any cross-reaction with APC2 was weak. This experiment also highlighted the strong accumulation of APC1 in the axons emerging from clusters of neuroblast, GMCs, and their progeny (Figs. 7I and 7J, arrows). Together, these data indicate that low levels of APC1 accumulate in neuroblasts, GMCs, and their progeny, with higher levels found in axons projecting from these cells. Thus, APC1 could potentially compensate for loss of APC2 in the larval brain. We explore this further in the next section.

We next compared the cell biological properties of APC1 and APC2. The four known APC family members, two in flies (Hamada *et al.*, 1999; Hayashi *et al.*, 1997; McCartney *et al.*, 1999; Yu *et al.*, 1999) and two in mammals (Groden *et al.*, 1991; Nakagawa *et al.*, 1998; van Es *et al.*, 1999), share certain structural features but differ in others. All share a block of N-terminal Arm repeats, followed by a set of short repeated sequences that serve as binding sites for Arm/βcat and Axin. These regions comprise most of fly APC2, which is the shortest family member. Fly APC1 (Hayashi *et al.*, 1997) is significantly longer at its N and C termini. Its extended C-terminal region contains a sequence similar to the microtubule-binding domain of human APC. Given these structural differences between fly APC1 and APC2, we asked whether they would exhibit similar or distinct cell biological properties when both were expressed at equivalent levels. We used the GAL4–UAS system to overexpress each protein in the same cellular environments, and examined where each localized under these conditions.

We first expressed each protein in the larval brain, using pros–GAL4 (Ohshiro *et al.*, 2000), which drives expression in most but not all neuroblasts, as well as in the outer proliferation center. To determine the level of protein expression driven by pros–GAL4 relative to the levels of the endogenous protein, we drove APC2–GFP with pros–GAL4, visualizing both the endogenous plus the exogenous fusion protein using anti-APC2 antibody. In the same experiment, we stained wild-type brains that did not mis-express APC2. When we imaged these brains at the same confocal settings, we found that pros–GAL4 drives expression at levels substantially above that of the endogenous protein. The endogenous protein in wild-type brains (Fig. 8B) was barely visible at settings where the GAL4-driven protein was easily visible (Fig. 8A). However; when we turned up the brightness setting, we could easily visualize the endogenous protein in the wild-type brain (Fig. 8C). Overexpression with pros–GAL4 of APC2-GFP, APC1, or both had no effects on adult viability or on overall brain morphology.

When we overexpressed APC2–GFP (Figs. 8A and 8D; see also Figs. 2M and 2N), it localized asymmetrically to the cortex of the larval neuroblasts (Figs. 8A and 8D, arrows), as well as to the junctions between the GMCs (Fig. 8D, bracket) and thus paralleled the localization of endogenous APC2 (Fig. 8C, arrow). In contrast, when we overexpressed APC1 (Figs. 8E–8M), it had a strikingly different localization. APC1 localized very strongly to the centrosome and the microtubules emanating from it (Figs. 8E–8M, white arrowheads). It also localized to interphase microtubule arrays in cells of the inner proliferation center (e.g., Figs. 8K

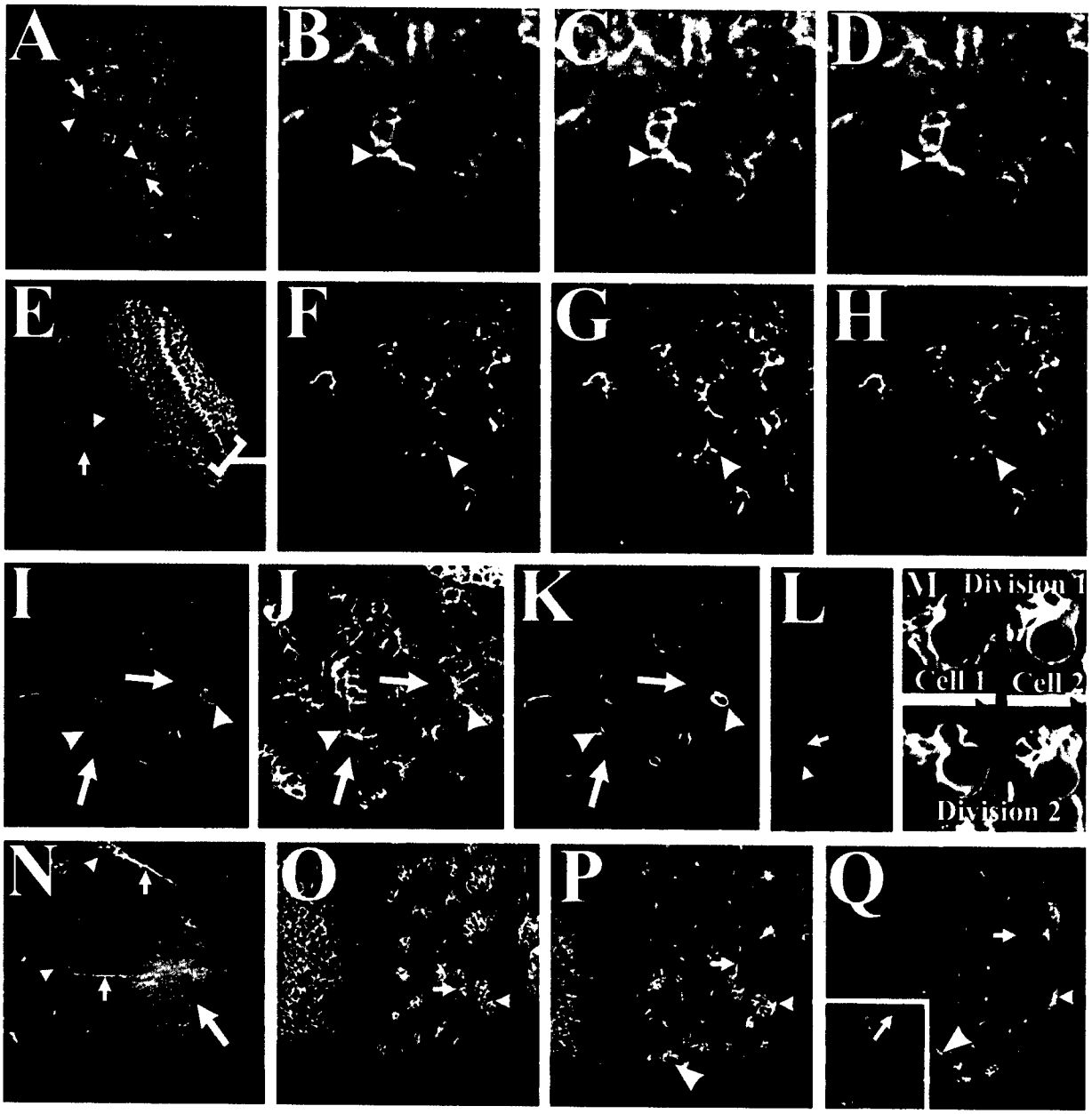

FIG. 5. Adherens junction proteins are asymmetrically localized in neuroblasts. Third instar brains or CB neuroblasts. (A–D) Double-labeled: Arm (green), α-catenin (red). Both precisely colocalize (A). (B–D) They localize to junctions between the neuroblast and the GMCs (dashed line) and junctions between GMCs (arrowhead), and are present at lower levels in ganglion cells. (E–H) Double-labeled: Arm (green), DE–cadherin (red). (E) Both precisely colocalize in most regions of the brain (E), including neuroblast (arrow)–GMC (arrowhead) clusters, and the epithelial cells of the proliferative centers (bracket). (F, H) Close-up showing colocalization to junctions between neuroblast and GMCs (e.g., dashed line) and junctions between GMCs (e.g., arrowhead). (I–L) Double-labeled CB neuroblasts (e.g., arrows): Mira (green), DE–cadherin (red). Mira localizes to a crescent during mitosis, and is concentrated in GMCs, where it remains at detectable levels for some time (K). New GMCs (e.g., I, L, arrowheads) are often born at the edge of the cluster of previous GMCs. (M) Still images from APC2–GFP movies of two different neuroblasts (cell 1 = movie 3; cell 2 = movie 4), which were filmed through two successive mitoses, showing each cell in anaphase of division 1 and division 2. Spindle orientation remained similar for the second division, and thus the second GMC was born near to the spot on the neuroblast cortex where the first GMC was born. Green arrowhead in division 2, approximate location of the earlier daughter. (N–Q) Axons emerging from the progeny of individual neuroblast–GMC clusters accumulate DE–cad, Arm, and APC2. (N) Double-labeled brain: Arm (green), DE–cadherin (red). Arrowheads, two neuroblast/GMC/neuron clusters. Small arrows, two nerves emerging from these clusters, which express both proteins. Large arrow, the neuropil, which is enriched for Arm but not DE-cadherin. (O–Q) Successive sections of double-labeled brain: Arm (green), APC2 (red). Arrowhead, arrow in (O), large arrowhead in (P), neuroblast/GMC clusters. Arrowheads and small arrows in (P) and (Q) follow putative axons emerging from these clusters through successively deeper sections. The neuropil (Q, inset, arrow) is enriched for Arm but not APC2.

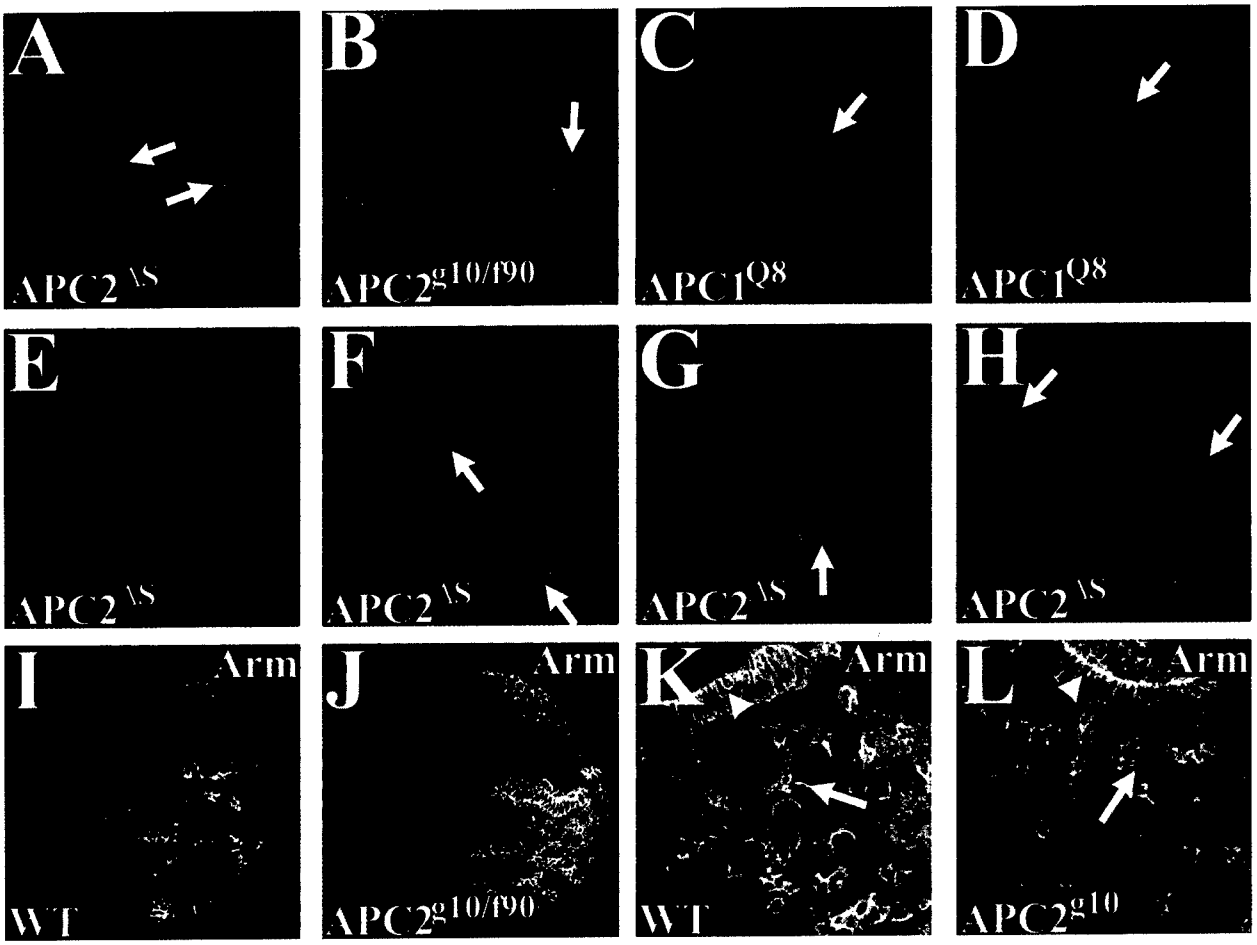

FIG. 6. Asymmetric divisions occur normally in *APC2* and *APC1* single mutants. Third instar brains or CB neuroblasts. (A) Triple-labeled $APC2^{\Delta S}$ mutant neuroblasts: APC2 (red), Mira (green), microtubules (blue). Mutant APC2 protein is no longer cortical, but asymmetric Mira localization during metaphase (A, arrows) is normal. (B–D) Double-labeled $APC2^{g10}/APC2^{f90}$ mutant neuroblasts (B) or $APC1^{Q8}$ mutant neuroblasts (C, D): Mira (red), microtubules (green). Mira localization is normal (arrows). (E–H) $APC2^{\Delta S}$ mutant neuroblasts. (E) Double-labeled: APC2 (red), Pros (green). Pros accumulates in transient crescents (dashed lines) as in wild-type. (F, G) Triple-labeled: APC2 (red), Insc (green), microtubules (blue). (H) Triple-labeled: APC2 (red), Baz (green), microtubules (blue). Insc and Baz localize normally (arrows). (I–L) Wild-type (identified using histone-GFP) and $APC2^{g10}$ mutant brains simultaneously labeled to visualize Arm and imaged under the same confocal conditions. Arm levels and localization were normal in the brain lobes (I, J), the neuroblast–GMC clusters (K, L, arrows) and the epithelial cells of the inner proliferation center (arrowhead).

and 8L, bracket). It did not strongly colocalize with all microtubule-based structures; however, for example, it was only marginally enriched in the spindle at metaphase (Fig. 8K, inset). In parallel, we carried out similar localization experiments after mis-expression in the embryonic epidermis, with similar results; APC2 localizes to the cell cortex, while APC1 localizes to centrosomes and microtubules (see accompanying paper). Together, the data from brains and embryos suggest that sequence differences between APC1 and APC2 direct them to quite different intracellular locations, despite their strong similarity in the core region of the protein.

Mammalian APC protein can oligomerize (Day and Alber, 2000), and we thus wondered whether fly APC1 and APC2 proteins might interact. To begin to examine this, we examined the effect of APC1 overexpression on the localization of endogenous and overexpressed APC2. Pros–GAL4 is not expressed in all neuroblasts (e.g., Figs. 8F and 8G, green arrowheads), allowing cells not overexpressing APC1 to serve as an internal control. Overexpression of APC1 in neuroblasts had a striking effect on APC2: its localization to cortical crescents was substantially diminished in neuroblasts overexpressing APC1 (e.g., Figs. 8F, 8G, and 8K–8M, white arrowheads), but not in those that did not (e.g., Figs. 8F and 8G, green arrowheads; Figs. 8H–8J, white arrow). Further, endogenous APC2 now localized to centrosomes (e.g., Figs. 8F, 8G, and 8K–8M, white arrowheads), though less strikingly than APC1. This suggests that APC1

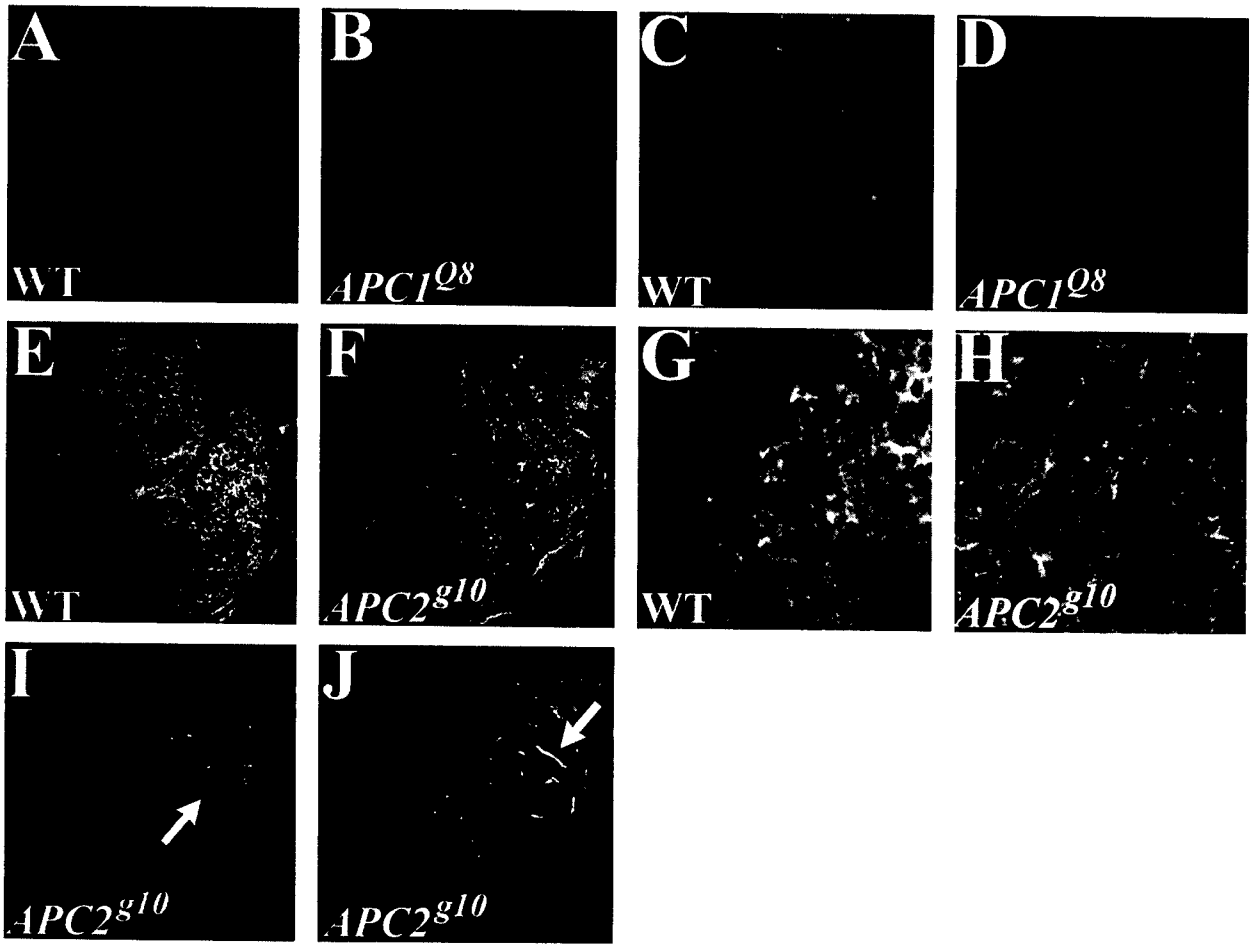

FIG. 7. APC1 localization in the larval brain. Third instar brains stained to reveal APC1. (A–D) Wild-type (A, C, expressing Histone-GFP to allow identification) and $APC1^{Q8}$ (protein null) mutant brains labeled and visualized together, to allow comparison of signal level. (E–H) Wild-type (E, G, expressing Histone–GFP to allow identification) and $APC2^{g10}$ (null for reactivity with APC2 antibody) mutant brains labeled and visualized together, to allow comparison of signal level. In wild-type, APC1 antibody stains the cytoplasm of all cells in the brain, and is cortically enriched in many cells. The level of labeling is substantially reduced in the $APC1^{Q8}$ mutants (A vs B, C vs D), suggesting that the antibody recognizes APC1 specifically. The slight residual cortical staining may reflect slight cross-reaction with APC2, as it was slightly reduced in an *APC2* mutant (G vs H). (I, J) Successive sections through an $APC2^{g10}$ mutant brain. APC1 accumulates at high levels in axons emerging from the progeny of neuroblast–GMC clusters (arrows).

and APC2 may interact, either directly or indirectly, allowing APC1 to recruit APC2 to a new location.

We further examined this issue by coexpressing APC1 and APC2–GFP in the same neuroblasts, using Pros–GAL4 to drive both simultaneously (Figs. 8N–8S). When we did so, APC2–GFP localized both to its normal cortical site (e.g., Figs. 8N–8S, green arrowheads) and, more weakly, to centrosomes and microtubules with APC1 (Figs. 8N–8S, white arrowheads). We also looked at the effects of APC2 overexpression on APC1. APC1 localized most prominently to centrosomes and their associated microtubules (e.g., Figs. 8N–8S, white arrowheads), but we now saw APC1 accumulation at the cortex (Figs. 8N–8S, green arrowheads); this was less prominent when APC1 was singly overexpressed (Figs. 8E–8M). These data suggest that APC2 may recruit APC1 to the cell cortex; however, this is subject to the caveat that the APC1 antibody may weakly cross-react with APC2.

APC1 and APC2 Play Functionally Redundant Roles in Brain Development

Given the striking localization of APC2 in the brain, we were surprised that *APC2* mutants had no apparent brain defects. The brain is only one of several tissues where neither single mutant had any apparent phenotype (Ahmed *et al.*, 1998; McCartney *et al.*, 1999); this was surprising as Wg signaling plays an important role in several of these tissues. The realization that APC1 is also expressed in the brain (Fig. 7) raised the possibility that it might play a

partially redundant role in this tissue. To test this, we examined the phenotype of animals mutant for both *APC1* and *APC2*.

APC1 and *APC2* single mutants are both zygotically viable to adulthood (Ahmed *et al.*, 1998; McCartney *et al.*, 1999). The only known problem in *APC1* mutants are morphological defects and inappropriate apoptosis in the photoreceptors of the eye (Ahmed *et al.*, 1998), while *APC2* zygotic mutants are morphologically wild type, with a phenotype only emerging in embryos maternally and zygotically mutant (McCartney *et al.*, 1999). In contrast, we found that *APC2 APC1* double mutants are zygotically lethal. Two allelic combinations, $APC2^{\Delta S}$ $APC1^{Q8}$ and $APC2^{g10}$ $APC1^{Q8}$, die as second instar larvae, while the third, $APC2^{d40}$ $APC1^{Q8}$, dies primarily during the first larval instar. None of the double mutants had any apparent defects in segment polarity as first instar larvae (data not shown). Mitotic activity during larval stages is restricted to the imaginal tissues and the brain, and imaginal discs are dispensable for larval development. Given this and the observed expression pattern of APC2 and APC1 in the CNS, we examined brain development in double mutant larvae.

During normal brain development, most embryonic neuroblasts exit the cell cycle during late embryogenesis. Immediately after hatching, the only mitotically active neuroblasts are the so-called mushroom-body neuroblasts, which are at a ventrolateral position (Ito and Hotta, 1992). Eight hours after hatching, other neuroblasts become mitotically active, such that by 20 h after hatching, 20–30 central brain neuroblasts per hemisphere are dividing. During the early first instar, the cells of the optic anlage become epithelially arranged and also begin dividing. The number of proliferating neuroblasts continues to increase, plateauing 20–50 h after egg laying.

$APC2^{\Delta S}$ $APC1^{Q8}$ zygotic double mutants die during the second larval instar. We thus compared wild-type and double mutant animals immediately after they completed the second instar larval molt. Double mutant brains were essentially normal in size, and the optic anlage had become epithelial (data not shown). However, double mutants had a strikingly different pattern of neuroblast proliferation than wild type. While presumptive mushroom body neuroblasts continued to proliferate (Figs. 9B, 9D, 9F, and 9H, arrowheads), the number of other mitotic neuroblasts was drastically reduced relative to wild type (Figs. 9A, 9C, 9E, and 9G), as assessed both by phosphohistone H3-labeling (Figs. 9A–9D) and by Mira and Pros staining (Figs. 9E–9I). We saw a similar, though less drastic, block in mitotic activity in $APC2^{g10}$ $APC1^{Q8}$ (Fig. 9I, arrowheads). To determine whether DNA synthesis was initiated but mitosis blocked, we labeled larvae with BrdU throughout the first instar, identifying cells that replicated their DNA during this period. The results were similar to those seen with mitotic markers. $APC2^{\Delta S}$ $APC1^{Q8}$ double mutants had drastically reduced numbers of BrdU-labeled cells; most labeled cells remaining appeared to be mushroom-body neuroblasts (Figs. 9J and 9K, arrowheads). We next examined whether embryonic CNS development was altered, by examining the axonal scaffold produced by progeny of the embryonic neuroblasts, using the marker BP102 that labels all axons (Fig. 9L). Zygotic double mutants were distinguished from wild-type siblings by the presence (Fig. 9N) or absence (Fig. 9O) of APC1 in the CNS. The axonal scaffold was unaltered in $APC2^{\Delta S}$ $APC1^{Q8}$ double mutants (Fig. 9M), suggesting that embryonic neuroblast proliferation is at least roughly normal. Finally, we examined whether we could detect defects in asymmetric divisions in double mutants, as assessed by examining asymmetric localization of Mira. In

FIG. 8. APC1 and APC2 localize differently when overexpressed in the larval brain. Third instar brains. (A–D) APC2–GFP localizes to the cortex even when highly overexpressed. (A, B) APC2–GFP is expressed at levels much higher than endogenous APC2. (A) Brain lobes overexpressing UAS–APC2–GFP under control of *pros*–GAL4. (B) Wild-type control brain. (A) and (B) were imaged by using the same confocal settings, visualizing both APC2 and APC2–GFP with anti-APC2. Levels of APC2 expression driven by *pros*–GAL4 (A) are much higher than those of endogenous APC2 (B). (C) Same brain as (B), with brightness turned up to show endogenous APC2. (A, C) Arrows, neuroblast GMC clusters. Brackets, outer proliferation center. (D) APC2–GFP driven by *pros*–GAL4 localizes like endogenous APC2, accumulating in neuroblast cortical crescents (e.g., arrow) and junctions between GMCs (e.g., bracket). APC2–GFP also accumulates in ganglion cells, neurons and their nerves (e.g., arrowheads). (E–M) APC1 overexpressed with *pros*–GAL4 localizes to centrosomes and microtubules, and recruits endogenous APC2 to these structures. (E) APC1 localizes to centrosomes and associated microtubules (white arrowheads; green arrowheads show cells with separated centrosomes), as well as to interphase microtubules in the outer proliferation center (arrow). (F, G) Double-labeled brain lobe: APC1 (F, green), endogenous APC2 (F, red; G). In neuroblasts that do not express APC1, APC2 remains in cortical crescents (green arrowheads). In neuroblasts overexpressing APC1 (white arrowheads), APC1 localizes to centrosomes, while endogenous APC2 cortical localization is reduced and it relocalizes to centrosomes. (H–J) Triple-labeled CB neuroblasts: APC1 (H, green; I), APC2 (H, red), microtubules (H, blue; J). (K–M) Double-labeled CB neuroblasts: APC1 (K, green; L), APC2 (K, red; M). APC1 localizes to centrosomes and microtubules, and endogenous APC2 is recruited into these structures (white arrowheads; H-J green arrowheads, cell with separated centrosomes). In neuroblasts that do not misexpress APC1, APC2 remains cortical (arrows). During metaphase, both APC1 and APC2 weakly label spindles (K, inset). In the outer proliferation center, APC1 accumulates along interphase microtubules (K–M, bracket), while APC1 and APC2 colocalize in cortical spots (K–M, green arrowheads). (N–S) Neuroblasts mis-expressing both APC1 (N, green; P; Q, green; R) and APC2–GFP (N, red; O; Q, red; S) under the control of *pros*–GAL4. APC1 localizes to centrosomes (white arrowheads) and to the cortex (green arrowheads). APC2 strongly labels the cortex (green arrowheads) and localizes more weakly to centrosomes (white arrowheads).

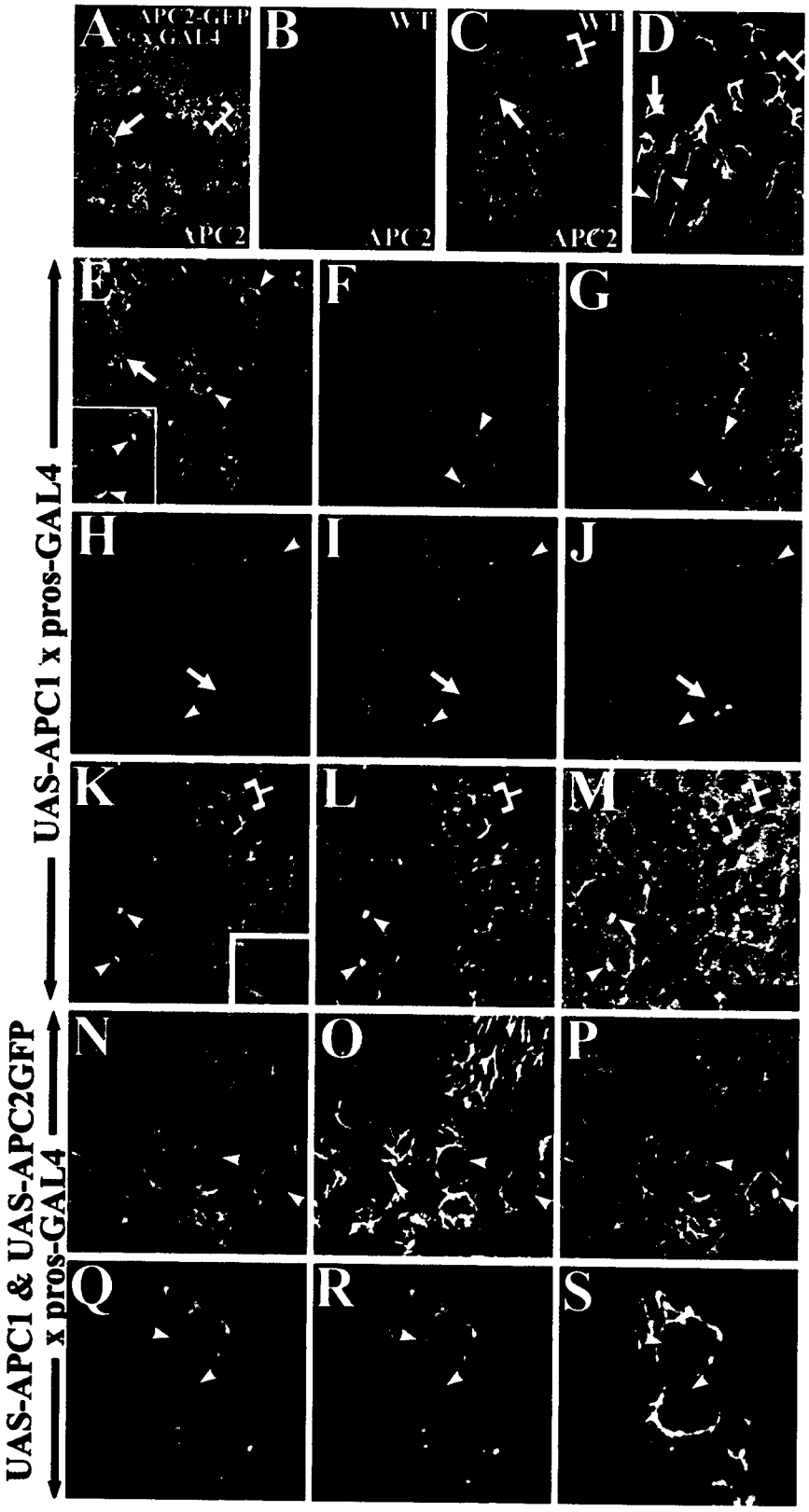

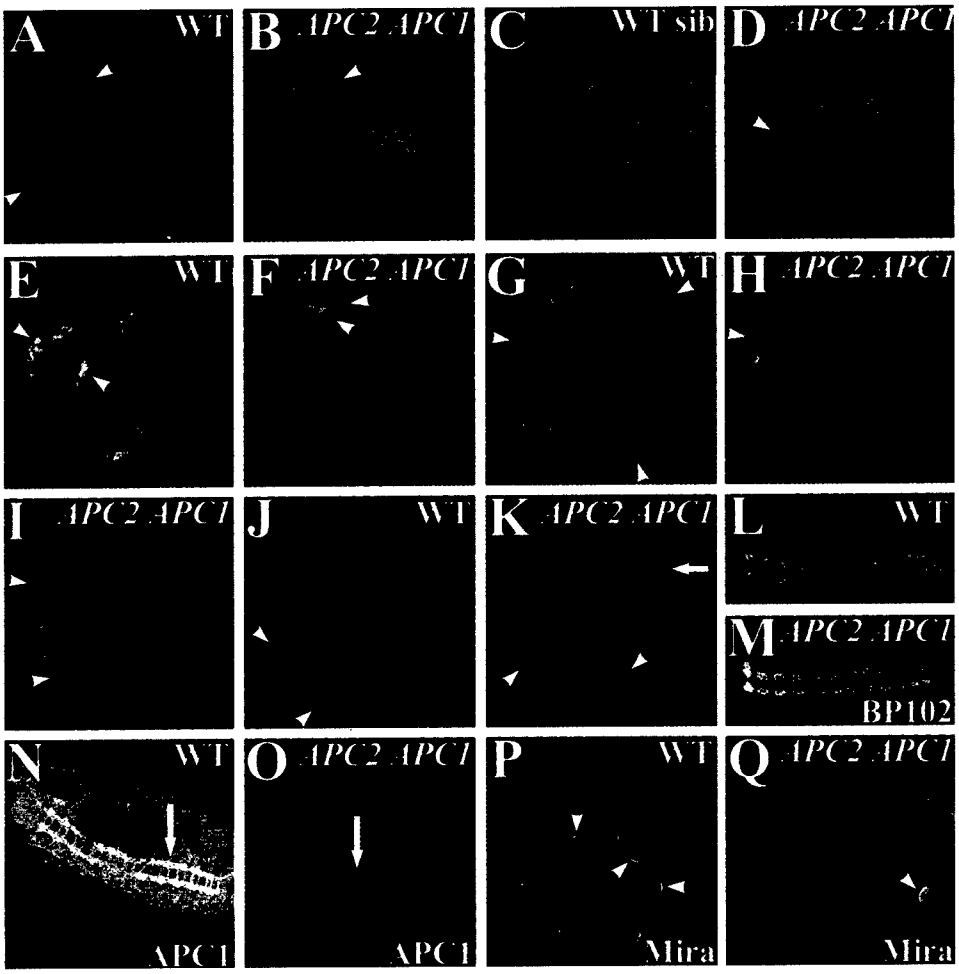

9

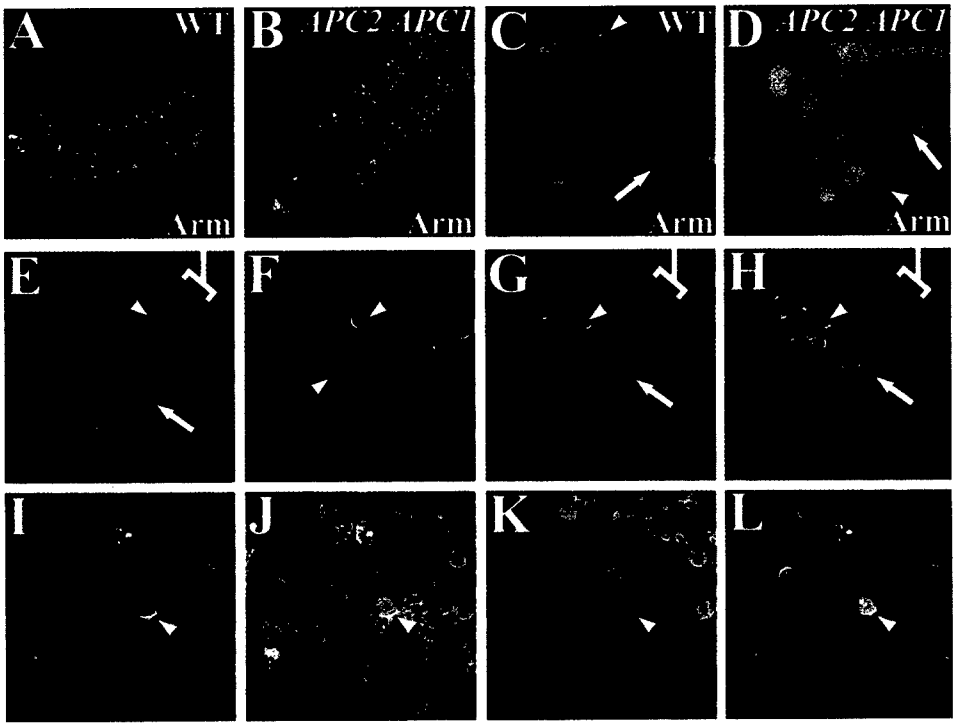

10

the wild-type first and second instar brain, the localization of Miranda is less strikingly asymmetric, with reasonably high levels in the cytoplasm (Fig. 9G). However, we could detect crescents of Mira and see it localize to smaller daughters (Fig. 9P). In double mutants, many fewer Mira-positive neuroblasts were seen, but we could find neuroblasts with Mira crescents or Mira segregated to smaller daughters (Fig. 9Q). In addition, Prospero-positive daughters are found in the double mutants, though in reduced numbers. These data thus suggest that asymmetric divisions still can occur, though it remains possible that they are not entirely normal or occasionally fail. Together, these data suggest that most likely explanation for the mutant phenotype is that double mutant embryonic neuroblasts do not reenter the cell cycle during the first larval instar.

APC1 and APC2 regulate Wg signaling, and thus one mechanism that could underlie the zygotic double mutant phenotype is the failure to properly regulate Arm levels. To test this, we first examined Arm accumulation in zygotic double mutant embryos. We identified stage 16 double mutants by the absence of APC1 accumulation in the CNS, and examined the level of Arm accumulation relative to wild-type embryos. Arm accumulation appeared completely normal in the epidermis of $APC2^{s10}$ $APC1^{Q8}$ double mutant embryos (Fig. 10B) relative to wild-type controls (Fig. 10A), suggesting that maternally contributed protein from the two loci is sufficient for normal Arm regulation in the embryo.

We next looked at Arm accumulation in the brains of midfirst instar larvae. Figures 10C and 10D display projections of optical sections through the entire brain. In the wild-type brain, Arm accumulates heavily in axons of the ventral nerve cord and neuropil (Fig. 10C, arrow). Arm accumulation in the cellular portion of the first instar brain is much lower. In the brain lobes, we found weak cortical staining of most cells. The only significant Arm accumulation outside the neuropil was in cells that we believe are epithelial cells of the developing optic lobe (Fig. 10C, arrowhead). The accumulation of Arm in zygotic double mutant brains is not substantially elevated from that of wild-type. Arm levels in the neuroblasts and cell bodies are unchanged (Fig. 10D, arrowhead), while Arm levels in axons are similar or only slightly elevated (Fig. 10D, arrow). These data thus do not support the hypothesis that elevated Arm levels cause the phenotype.

As a second test for the hypothesis that the double mutant phenotype results from deregulated Arm levels, we attempted to mimic it by misexpressing in neuroblasts

FIG. 9. *APC2 APC1* double mutants have defects in larval neuroblast proliferation. (A–D) Wild-type (A, C) and $APC2^{\Delta 5}$ $APC1^{Q8}$ (B, D) double mutant second instar larval brains. Double-labeled: phosphotyrosine (green, marks cell junctions and axons), mitotic cells (red, phosphohistone H3). (A, C) In wild-type brains (A) or brains of wild-type siblings of double mutants (C, identified using a GFP-marked Balancer chromosome), many mitotic neuroblasts (red) are seen in any section through the brain lobes (A, arrowhead). Mitotic cells are found all around the circumference (C). (B, D) In double mutants, the number of mitotic cells is strongly reduced, and those remaining are often in the position of the mushroom-body neuroblasts (arrowheads). (E–I) Wild-type (E, G), $APC2^{\Delta 5}$ $APC1^{Q8}$ (F, H) double mutant, or $APC2^{s10}$ $APC1^{Q8}$ (I) double mutant second instar brains. Double-labeled: Mira (red, labels neuroblasts), and Pros (green, labels GMCs, ganglion cells and neurons). (E, G) Wild-type. Neuroblasts (red) are found all around the circumference of the brain (arrowheads), and they have given rise to many differentiating progeny (green). (F, H, I) Double mutants. The number of neuroblasts (red) and differentiating progeny (green) is reduced, with the most severe reduction in $APC2^{\Delta 5}$ $APC1^{Q8}$ (E, H). Neuroblasts remaining (arrowheads) are often in the position of the mushroom-body neuroblasts. (J, K) Wild-type (J), and $APC2^{\Delta 5}$ $APC1^{Q8}$ (K) double mutant second instar brains labeled with BrdU to visualize cells that have replicated their DNA. (J) Wild-type. Many cells in the brain lobes have replicated DNA during the labeling period (arrowheads). (K) Double mutant. The number of labeled cells is substantially reduced (arrowhead). Arrow, polyploid cells from another tissue. (L–O) Stage 15 wild-type (sibling of a double mutant; L, N) and $APC2^{\Delta 5}$ $APC1^{Q8}$ zygotic double mutant (M, O) embryos. Double-labeled: axonal scaffold (using BP102 antibody; L, M), APC1 (accumulates in axons; N, arrow; O; note lack of APC1). The axonal scaffold appears normal. (P, Q) Wild-type (P) and $APC2^{\Delta 5}$ $APC1^{Q8}$ double mutant (Q) second instar brains, labeled to visualize Mira. In wild-type neuroblasts of this stage (P), Mira labels both the cytoplasm and accumulates in cortical crescents (arrowheads). While double mutant brains have far fewer Mira-positive neuroblasts (Q), seemingly normal cortical crescents of Mira are detected (arrowhead).

FIG. 10. The *APC2 APC1* double mutant phenotype does not result from elevated Arm levels. (A, B) Epidermal Arm levels in stage 16 $APC2^{s10}$ $APC1^{Q8}$ double mutant embryos (B) and wild-type siblings (A) are indistinguishable. Double-labeled to visualize Arm and APC1 (not shown), which we used to distinguish double mutants from wild-type siblings. (C, D) Arm levels in the ventral nerve cord (arrows) and brain lobes (arrowheads) of mid-first instar wild-type (C) or $APC2^{\Delta 5}$ $APC1^{Q8}$ zygotic double mutants (D) are indistinguishable. Double mutant larvae, identified using a GFP-Balancer, were stained and imaged together with wild-types (marked with Histone–GFP). (C, D) Projections of sections through the entire brain. In both genotypes, high levels of Arm are found in the neuropil—other cells show only weak cortical staining—with somewhat elevated levels in a few cells that we believe are epithelial cells of the developing optic lobes (arrowheads). (E, F) Double-labeled wild-type third instar brains: APC2 (E, F, red), Mira (E, F, green). Arrowheads show neuroblasts with typical cortical APC2, while the bracket and arrow illustrate the cortical localization of APC2 in the cells of the outer and inner proliferation center, respectively. (G–L) Third instar brains in which Arm^{S10} was mis-expressed by using pros–GAL4. Triple-labeled: APC2 (G, I red; H, J), Mira (G, I, green; L), Arm^{S10} (via myc-epitope; G, I, blue; K). The brains are normal in all aspects except one. In neuroblasts expressing Arm^{S10}, APC2 is diffusely cytoplasmic (green arrowheads), while in neuroblasts not expressing Arm^{S10}, APC2 remains cortical (white arrowheads). Cortical APC2 localization is also lost in the outer proliferation center (bracket), that expresses Arm^{S10}, but not in the inner proliferation center (arrow), that does not. Asymmetric divisions are normal.

Arm^{S10}, a mutant form of Arm that cannot be targeted for destruction (Pai *et al.*, 1997). Mis-expression of Arm^{S10} mimics the *APC2* single mutant in the embryonic epidermis (McCartney *et al.*, 1999) and the *APC1* single mutant in the photoreceptors (Ahmed *et al.*, 1998), as both result from deregulated Wg signaling. We thus used Pros-GAL4 to express myc-tagged Arm^{S10} in neuroblasts, and verified expression by staining with antibodies to myc. To our surprise, these animals survived larval development and emerged as viable adults, suggesting that deregulation of Arm destruction does not disrupt neuroblast development.

We also examined the consequences of Arm^{S10} expression on third instar brains directly to look for more subtle effects on neuroblast proliferation or asymmetric divisions. Animals expressing Arm^{S10} had brains of normal morphology, with normal numbers of neuroblasts that were mitotically active and exhibited normal asymmetric cell divisions (Figs. 10E and 10F vs 10G–10L). We did see one striking effect of Arm^{S10}, however. In neuroblasts expressing Arm^{S10}, the amount of cortical APC2 was strongly reduced (Figs. 10G–10L, green arrowheads), perhaps because the excess Arm protein in these neuroblasts competed for APC2 binding, preventing it from associating with its cortical binding partners. Neuroblasts not expressing pros–GAL4 were an internal control; they retained normal cortical APC2 (Figs. 10G–10L, white arrowheads). We saw a similar reduction in cortical APC2 in the outer proliferation center (Figs. 10G and 10H, bracket), which expressed Arm^{S10}, relative to cells of the inner proliferation center (Figs. 10G and 10H, arrow), that did not. Together, these results suggest that the larval brain phenotypes of *APC2 APC1* double mutants do not result from elevated levels of Arm or activation of Wg signaling.

DISCUSSION

APC was first identified because loss-of-function mutations result in colon tumors. In this context, it functions as a negative regulator of Wnt signaling, via its role in the Arm/βcat destruction complex (reviewed in Polakis, 2000). The role in tumors reflects a normal role for APC proteins in Wnt regulation, as demonstrated by the phenotype of loss-of-function mutations in *Drosophila APC1* and *APC2* (Ahmed *et al.*, 1998; McCartney *et al.*, 1999; Yu *et al.*, 1999). However, this relatively simple picture recently became more complex. First, APC proteins have novel abilities that appear separate from their role in the destruction complex. These include interactions with cytoskeletal proteins, by which APC family members influence Wnt-independent cytoskeletal events (see Introduction). Second, both mammals and flies have two APC family members, which share common structural elements but also have structural differences. These new data raise new questions about the functions of APC family members, which we have begun to address with the work presented here.

Possible Roles for APC1 and APC2 in Brain Development

Our data demonstrate that APC1 and APC2 play redundant roles in larval brain development. Further, our data suggest that this role is Wg-independent, as it is not mimicked by elevating Arm levels. This contrasts with what we and others observed in embryos and imaginal discs, where the two proteins also have overlapping functions but where these clearly involve Wg signaling (see accompanying paper; Ahmed *et al.*, 2002). Hamada and Bienz (2002) recently found that APC1 and APC2 also play redundant roles in cell adhesion during oogenesis. Maternal contribution of the two proteins appears sufficient for many if not all aspects of embryogenesis, as double mutant embryos hatch with a normal cuticle pattern and an apparently normal brain. However, we saw striking differences between the larval brains of wild-type and double mutant animals. During wild-type development, most neuroblasts become quiescent during late embryogenesis, with only the mushroom body neuroblasts mitotically active upon hatching (Ito and Hotta, 1992). In the middle of the first instar, however, other embryonic neuroblasts reenter the cell cycle and proliferate. In the *APC2 APC1* double mutant, this appears not to occur, as we see far fewer total neuroblasts, and the number of brain cells in mitosis and the number that have gone through S-phase is substantially reduced.

There are several possible interpretations of these data, which now must be tested. First, double mutant neuroblasts may be driven into apoptosis, as occurs in *APC1* mutant photoreceptors (Ahmed *et al.*, 1998). However, we think this is less likely, as overall brain size is not substantially reduced in the double mutants, and expression of activated Arm in neuroblasts does not mimic the phenotype as it did in the photoreceptors. However, this possibility must now be rigorously tested. Second, it is possible that there are defects in asymmetric cell divisions, which, if they resulted in symmetric divisions producing two GMC daughters, would rapidly deplete the pool of stem cells. We observed Mira crescents in the subset of double mutant neuroblasts that continue to divide, however, suggesting that at least some cells can undergo asymmetric divisions. This does not rule out a more subtle defect in asymmetric divisions; we must further test this by generating clones of double mutant cells in the brain of third instar larvae, when asymmetric divisions are easier to visualize. We think the most likely model is that neuroblasts simply remain quiescent. This could be due to intrinsic problems in reactivating the cell cycle in the brain, or could be due to defects in signaling from other tissues; ecdysone regulates cell cycle reactivation and this influences a similar brain phenotype seen in *trol* mutants (Datta, 1995, 1999). We need to test this possibility by trying to rescue the double mutant phenotype by expressing APC1 or APC2 specifically in the brain.

Regardless of which theory is correct, we must determine the mechanism by which defects arise. Earlier studies

suggested two possibilities. First, loss of both APC proteins may elevate Arm levels, triggering the phenotype by activating a program of gene expression. We did two experiments to test this possibility, both of which suggest that this mechanism is less likely. First, expression of activated Arm in neuroblasts does not disrupt brain development. Second, Arm levels are not substantially elevated in zygotic double mutant embryos or larval brains. Other possible mechanisms are cytoskeletal or adhesive ones. If the two APCs have overlapping functions in cytoskeletal regulation and/or cell adhesion, defects in these might affect cell cycle progression or asymmetric divisions.

APC2 and the Cadherin–Catenin Complex in the Larval Brain

The larval brain provides an opportunity to examine potential roles for APC proteins in asymmetric cell divisions. The embryonic neuroblasts in *Drosophila* are one of the best-characterized examples of this process, with many proteins required for asymmetric divisions identified (reviewed in Jan and Jan, 2001). Some of these are widely used in different asymmetric divisions in the fly. The process that triggers asymmetry can differ from cell to cell, however, with apical–basal cues used in embryonic neuroblasts (reviewed in Jan and Jan, 2001), adherens junction proteins helping orient the asymmetric divisions of certain adult sense organ precursors (Le Borgne *et al.*, 2002), and Fz signaling orienting the division in other adult sense organ precursors (Gho and Schweisguth, 1998).

Larval neuroblasts are less well characterized than their embryonic progenitors. We thus examined APC2 localization in these cells through the cell cycle, and compared its localization with those of proteins involved in embryonic asymmetric divisions. APC2 has a dynamic localization. Its asymmetry is strongest during interphase, when most asymmetric proteins are either not present or not localized (although we saw weak asymmetry of Insc during interphase, differing from what occurs in embryos). The APC2 crescent diminishes as the cell enters metaphase, but remains asymmetric throughout mitosis. As cytokinesis commences, APC2 localizes very strongly to the cleavage furrow, continuing to mark the division site after cytokinesis is complete. The APC2 crescent overlaps those of Pros, Mira, and is complementary to those of Insc and Baz.

The striking asymmetric localization of APC2 in neuroblasts prompted us to examine its role there. As neither single mutant has an effect on brain development, if there is a role for APC proteins in asymmetric divisions, both APC family members must be able to carry it out. We have several hypotheses to explain the asymmetric APC2 localization. Our favorite hypothesis stems from the observation that the interphase crescent of APC2 overlaps a similar crescent formed by the cadherin–catenin complex. This prompted us to consider the relationship between the neuroblast, its GMC daughters, and the ganglion cells and neurons derived from them. In the central brain, GMCs remain tightly associated with their neuroblast mother, an event potentially mediated by cadherin-based cell–cell adhesion. Our APC2–GFP data suggest that ganglion cell and neuronal progeny also remain in the immediate vicinity, and that each group of neurons so formed sends out axons that join to form a common nerve. These nerves express DE–cadherin, Arm, and both APCs. One possible hypothesis to explain these data is that the daughters of a single neuroblast form a structural unit, as a part of the larger scale brain architecture. If these units are functional entities, maintaining the association of the neuroblast and its daughters and granddaughters may be important. The cadherin–catenin system could mediate selective adhesion between these cells, and APC2/APC1 could work with them in adhesion, as they do in the ovary (Townsley and Bienz, 2000; Hamada and Bienz, 2002).

It is also possible that APC2/APC1 and the cadherin–catenin system work together to orient the plane of division of the neuroblast, as the cadherin–catenin complex does in the peripheral nervous system (Le Borgne *et al.*, 2002). Our data suggest that newborn GMC daughters are not positioned randomly, but instead are born adjacent to the cluster of previous GMCs. This division pattern would help maintain a compact cluster of daughters and granddaughters. Further experiments are needed to test this hypothesis. First, we will need to generate mosaic brains in which small groups of cells lack cadherin or catenin function. Second, we will need to get around the early role for APC proteins in brain development by generating clones of *APC2 APC1* double mutant cells.

An alternate possibility is that APC2 and APC1 work independently of the cadherin–catenin system to mediate asymmetric division, helping to position the spindle, perhaps by mechanisms analogous to the role APC2 appears to play in spindle anchoring in the early syncytial fly embryo. However, if such a role exists, it must act in two different modes, allowing some neuroblasts to point their spindles at the center of the APC2 crescent and others to point one spindle pole toward the edge of the crescent, the two patterns we observe *in vivo*. Finally, it is possible that asymmetric localization of APC2 is not critical in the asymmetric divisions at all; instead, the asymmetry may reflect the fact that APC2 interacts with other asymmetrically localized proteins, such as actin or the catenins.

ACKNOWLEDGMENTS

We thank E. Wieschaus and Y. Ahmed for sharing information and reagents before publication, and R. Rosin-Arbesfeld and M. Bienz for sharing the APC2–GFP fusion before publication. We also thank W. Chia, E. Knust, F. Matsuzaki, R. Saint, M. Takeichi, the Bloomington *Drosophila* Stock Center, and the Developmental Studies Hybridoma Bank for flies and antibodies, B. Duronio and S. Selleck for helpful discussions, and S. Whitfield for help with the figures. This work was supported by grants to M.P. from the HFSP and the NIH (GM47857). B.M. was supported by a Leukemia and Lymphoma Society Senior Fellowship

and M.P. was supported in part by a CDA from the U.S. Army Breast Cancer Research Program.

REFERENCES

Ahmed, Y., Hayashi, S., Levine, A., and Wieschaus, E. (1998). Regulation of armadillo by a *Drosophila* APC inhibits neuronal apoptosis during retinal development. *Cell* **93,** 1171–1182.

Ahmed, Y., Nouri, A., and Wieschaus, E. (2002). Drosophila Apc1 and Apc2 regulate Wingless transduction throughout development. *Development* **129,** 1751–1762.

Ceron, J., Gonzalez, C., and Tejedor, F. J. (2001). Patterns of cell division and expression of asymmetric cell fate determinants in postembryonic neuroblast lineages of Drosophila. *Dev. Biol.* **230,** 125–138.

Datta, S. (1995). Control of proliferation activation in quiescent neuroblasts of the Drosophila central nervous system. *Development* **121,** 1173–1182.

Datta, S. (1999). Activation of neuroblast proliferation in explant culture of the Drosophila larval CNS. *Brain Res.* **818,** 77–83.

Day, C. L., and Alber, T. (2000). Crystal structure of the amino-terminal coiled-coil domain of the APC tumor suppressor. *J. Mol. Biol.* **301,** 147–156.

Fodde, R., Kuipers, J., Rosenberg, C., Smits, R., Kielman, M., Gaspar, C., van Es, J. H., Breukel, C., Wiegant, J., Giles, R. H., and Clevers, H. (2001). Mutations in the APC tumour suppressor gene cause chromosomal instability. *Nat. Cell Biol.* **3,** 433–438.

Foe, V. E., Odell, G. M., and Edgar, B. A. (1993). Mitosis and morphogenesis in the *Drosophila* embryo: Point and counterpoint. In "The Development of *Drosophila* " (M. Bate and A. Martinez-Arias, Eds.), Vol. I, pp. 149–300. Cold Spring Harbor Laboratory Press, Cold Spring Harbor, NY.

Gho, M., and Schweisguth, F. (1998). Frizzled signalling controls orientation of asymmetric sense organ precursor cell divisions in *Drosophila*. *Nature* **393,** 178–181.

Groden, J., Thliveris, A., Samowitz, W., Carlson, M., Gelbart, L., Albertson, H., Josyln, G., Stevens, J., Spirio, L., Robertson, M., Sargeant, L., Krapcho, K., Wolff, E., Burt, R., Hughes, J. P., Warrington, J., McPherson, J., Wasmuth, J., Paslier, D. L., Abderrahim, H., Cohen, D., Leppert, M., and White, R. (1991). Identification and characterization of the familial adenomatous polyposis coli gene. *Cell* **66,** 589–600.

Hamada, F., Murata, Y., Nishida, A., Fujita, F., Tomoyasu, Y., Nakamura, M., Toyoshima, K., Tabata, T., Ueno, N., and Akiyama, T. (1999). Identification and characterization of E-APC, a novel Drosophila homologue of the tumour suppressor APC. *Genes Cells* **4,** 465–474.

Hamada, F., and Bienz, M. (2002). A Drosophila APC tumour suppressor homologue functions in cellular adhesion. *Nat. Cell Biol.* **4,** 208–213.

Hayashi, S., Rubinfeld, B., Souza, B., Polakis, P., Wieschaus, E., and Levine, A. (1997). A *Drosophila* homolog of the tumor suppressor gene adenomatous polyposis coli down-regulates β-catenin but its zygotic expression is not essential for the regulation of Armadillo. *Proc. Natl. Acad. Sci. USA* **94,** 242–247.

Ito, K., and Hotta, Y. (1992). Proliferation pattern of postembryonic neuroblasts in the brain of *Drosophila melanogaster*. *Dev. Biol.* **149,** 134–148.

Jan, Y. N., and Jan, L. Y. (2001). Asymmetric cell division in the Drosophila nervous system. *Nat. Rev. Neurosci.* **2,** 772–779.

Kaplan, K. B., Burds, A. A., Swedlow, J. R., Bekir, S. S., Sorger, P. K., and Nathke, I. S. (2001). A role for the Adenomatous Polyposis Coli protein in chromosome segregation. *Nat. Cell Biol.* **3,** 429–432.

Le Borgne, R., Bellaiche, Y., and Schweisguth, F. (2002). Drosophila E-cadherin regulates the orientation of asymmetric cell division in the sensory organ lineage. *Curr. Biol.* **12,** 95–104.

McCartney, B. M., Dierick, H. A., Kirkpatrick, C., Moline, M. M., Baas, A., Peifer, M., and Bejsovec, A. (1999). *Drosophila* APC2 is a cytoskeletally-associated protein that regulates Wingless signaling in the embryonic epidermis. *J. Cell Biol.* **146,** 1303–1318.

McCartney, B. M., McEwen, D. G., Grevengoed, E., Maddox, P., Bejsovec, A., and Peifer, M. (2001). *Drosophila* APC2 and Armadillo participate in tethering mitotic spindles to cortical actin. *Nat. Cell Biol.* **3,** 933–938.

McEwen, D. G., and Peifer, M. (2000). Wnt signaling: Moving in a new direction. *Curr. Biol.* **10,** R562–R564.

Mimori-Kiyosue, Y., Shiina, N., and Tsukita, S. (2000). Adenomatous polyposis coli (APC) protein moves along microtubules and concentrates at their growing ends in epithelial cells. *J. Cell Biol.* **148,** 505–518.

Munemitsu, S., Souza, B., Müller, O., Albert, I., Rubinfeld, B., and Polakis, P. (1994). The APC gene product associates with microtubules *in vivo* and promotes their assembly *in vitro*. *Cancer Res.* **54,** 3676–3681.

Nakagawa, H., Murata, Y., Koyama, K., Fujiyama, A., Miyoshi, Y., Monden, M., Akiyama, T., and Nakamura, Y. (1998). Identification of a brain-specific APC homologue, APCL, and its interaction with beta-catenin. *Cancer Res.* **58,** 5176–5181.

Näthke, I. S., Adams, C. L., Polakis, P., Sellin, J. H., and Nelson, W. J. (1996). The Adenomatous Polyposis Coli (APC) tumor suppressor protein localizes to plasma membrane sites involved in active cell migration. *J. Cell Biol.* **134,** 165–180.

Ohshiro, T., Yagami, T., Zhang, C., and Matsuzaki, F. (2000). Role of cortical tumour-suppressor proteins in asymmetric division of Drosophila neuroblast. *Nature* **408,** 593–596.

Pai, L.-M., Orsulic, S., Bejsovec, A., and Peifer, M. (1997). Negative regulation of Armadillo, a Wingless effector in *Drosophila*. *Development* **124,** 2255–2266.

Parmentier, M. L., Woods, D., Greig, S., Phan, P. G., Radovic, A., Bryant, P., and O'Kane, C. J. (2000). Rapsynoid/Partner of inscuteable controls asymmetric division of larval neuroblasts in drosophila. *J. Neurosci.* **20,** RC84.

Polakis, P. (2000). Wnt signaling and cancer. *Genes Dev.* **14,** 1837–1851.

Rocheleau, C. E., Downs, W. D., Lin, R., Wittmann, C., Bei, Y., Cha, Y.-H., Ali, M., Priess, J. R., and Mello, C. C. (1997). Wnt signaling and an APC-related gene specify endoderm in early *C. elegans* embryos. *Cell* **90,** 707–716.

Schlesinger, A., Shelton, C. A., Maloof, J. N., Meneghini, M., and Bowerman, B. (1999). Wnt pathway components orient a mitotic spindle in the early *C. elegans* embryo without requiring gene transcription in the responding cell. *Genes Dev.* **13,** 2028–2038.

Smith, K. J., Levy, D. B., Maupin, P., Pollard, T. D., Vogelstein, B., and Kinzler, K. W. (1994). Wild-type but not mutant APC associates with the microtubule cytoskeleton. *Cancer Res.* **54,** 3672–3675.

Thorpe, C. J., Schlesinger, A., Carter, J. C., and Bowerman, B. (1997). Wnt signaling polarizes an early *C. elegans* blastomere to distinguish endoderm from mesoderm. *Cell* **90,** 695–705.

Townsley, F. M., and Bienz, M. (2000). Actin-dependent membrane association of a Drosophila epithelial APC protein and its effect on junctional armadillo. *Curr. Biol.* **10,** 1339–1348.

van Es, J. H., Kirkpatrick, C., van de Wetering, M., Molenaar, M., Miles, A., Kuipers, J., Destrée, O., Peifer, M., and Clevers, H. (1999). Identification of APC2, a homologue of the adenomatous polyposis coli tumour suppressor. *Curr. Biol.* **9,** 105–108.

Yu, X., and Bienz, M. (1999). Ubiquitous expression of a Drosophila adenomatous polyposis coli homolog and its localization in cortical actin caps. *Mech. Dev.* **84,** 69–73.

Yu, X., Waltzer, L., and Bienz, M. (1999). A new Drosophila APC homologue associated with adhesive zones of epithelial cells. *Nat. Cell Biol.* **1,** 144–151.

Zumbrunn, J., Kinoshita, K., Hyman, A. A., and Näthke, I. S. (2001). Binding of the adenomatous polyposis coli protein to microtubules increases microtubule stability and is regulated by GSK3 beta phosphorylation. *Curr. Biol.* **11,** 44–49.

Received for publication May 13, 2002
Revised June 26, 2002
Accepted June 27, 2002
Published online August 26, 2002